



Cite this: *Chem. Soc. Rev.*, 2021, 50, 1305

## Site-selective modification strategies in antibody–drug conjugates

Stephen J. Walsh, †<sup>ab</sup> Jonathan D. Bargh, †<sup>a</sup> Friederike M. Dannheim, †<sup>a</sup> Abigail R. Hanby, †<sup>a</sup> Hikaru Seki, †<sup>a</sup> Andrew J. Counsell, †<sup>a</sup> Xiaoxu Ou, †<sup>a</sup> Elaine Fowler, †<sup>a</sup> Nicola Ashman, †<sup>a</sup> Yuri Takada, †<sup>a</sup> Albert Isidro-Llobet, <sup>c</sup> Jeremy S. Parker, <sup>d</sup> Jason S. Carroll <sup>b</sup> and David R. Spring \*<sup>a</sup>

Antibody–drug conjugates (ADCs) harness the highly specific targeting capabilities of an antibody to deliver a cytotoxic payload to specific cell types. They have garnered widespread interest in drug discovery, particularly in oncology, as discrimination between healthy and malignant tissues or cells can be achieved. Nine ADCs have received approval from the US Food and Drug Administration and more than 80 others are currently undergoing clinical investigations for a range of solid tumours and haematological malignancies. Extensive research over the past decade has highlighted the critical nature of the linkage strategy adopted to attach the payload to the antibody. Whilst early generation ADCs were primarily synthesised as heterogeneous mixtures, these were found to have sub-optimal pharmacokinetics, stability, tolerability and/or efficacy. Efforts have now shifted towards generating homogeneous constructs with precise drug loading and predetermined, controlled sites of attachment. Homogeneous ADCs have repeatedly demonstrated superior overall pharmacological profiles compared to their heterogeneous counterparts. A wide range of methods have been developed in the pursuit of homogeneity, comprising chemical or enzymatic methods or a combination thereof to afford precise modification of specific amino acid or sugar residues. In this review, we discuss advances in chemical and enzymatic methods for site-specific antibody modification that result in the generation of homogeneous ADCs.

Received 29th August 2020

DOI: 10.1039/d0cs00310g

[rsc.li/chem-soc-rev](http://rsc.li/chem-soc-rev)

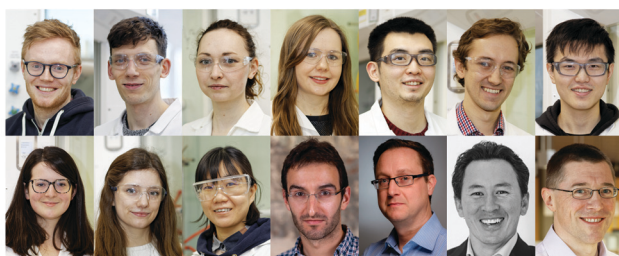
<sup>a</sup> Department of Chemistry, University of Cambridge, Lensfield Road, Cambridge, CB2 1EW, UK. E-mail: spring@ch.cam.ac.uk

<sup>b</sup> Cancer Research UK Cambridge Institute, University of Cambridge, Robinson Way, Cambridge, CB2 0RE, UK

<sup>c</sup> GSK, Gunnels Wood Road, Stevenage, SG1 2NY, UK

<sup>d</sup> Early Chemical Development, Pharmaceutical Development, R&D, AstraZeneca, Macclesfield, UK

† These authors contributed equally to this work.



David Spring is currently Professor of Chemistry and Chemical Biology at the University of Cambridge within the Chemistry Department. Jason Carroll is Professor of Molecular Oncology at the University of Cambridge and a Senior Group Leader at the Cancer Research UK Cambridge Institute. Jeremy Parker is Senior Director and Head of Early Chemical Development at AstraZeneca in Macclesfield. Albert Isidro-Llobet is an Investigator and Associate Fellow at GSK in Stevenage. Stephen Walsh, Jonathan Bargh, Friederike Dannheim, Abigail Hanby, Hikaru Seki, Andrew Counsell, Xiaoxu Ou, Elaine Fowler, Nicola Ashman and Yuri Takada are members of the Spring lab in the University of Cambridge Department of Chemistry. Stephen Walsh is also a postdoctoral research associate in the Carroll lab in the Cancer Research UK Cambridge Institute. Photos are in order of the author list (left to right, top to bottom).



# 1 Introduction

Antibody-drug conjugates (ADCs) are a class of targeted therapeutics, typically developed for the treatment of cancer. By harnessing the cell selectivity of monoclonal antibodies (mAbs) and the cytotoxicity of small molecule toxins, malignant cells can be selectively destroyed whilst sparing healthy tissue.<sup>1,2</sup> Critical to the success of this strategy is a covalent linker between the two therapeutic components, which facilitates the ADC's mechanism of action.<sup>3</sup> This marriage of macromolecular biology and small molecule chemistry is at the heart of the clinical success of ADCs. Indeed, the field has enjoyed significant clinical and commercial success in recent years, with nine ADCs receiving approval from the US Food and Drug Administration and >80 others in clinical development (Fig. 1).<sup>4–13</sup>

The antibody portion of the ADC targets and binds surface receptors that are expressed at discernibly higher levels on cancer cells compared to healthy tissue, thereby allowing selective targeting.<sup>1</sup> Once bound, the ADC–antigen complex is usually internalised into the malignant cell and trafficked through the endosomes and lysosomes. At this point the drug can be liberated from the antibody, thus enabling its cytotoxic function. In the case of a 'non-cleavable' linker the release of the cytotoxic metabolite occurs by lysosomal degradation of the

antibody into its constituent amino acids, releasing the payload with the linker and amino acid appendage.<sup>14–16</sup> More commonly, a 'cleavable' linker is employed, in which a chemical- (e.g. low pH<sup>17</sup> or glutathione<sup>18,19</sup>) or enzyme- (e.g. protease,<sup>20</sup> phosphatase,<sup>21,22</sup> glycosidase<sup>23,24</sup> or sulfatase<sup>25</sup>) sensitive trigger is incorporated.<sup>26</sup> Cleavable linker technology therefore enables the selective release of an unmodified payload at the target cell. Whilst an important ADC component, cleavable linker technologies have been discussed elsewhere and will not be the focus of this review, which focuses on linker-antibody attachment chemistry.<sup>26</sup>

Currently, all ADCs in clinical and preclinical development incorporate antibodies of the immunoglobulin G (IgG) isotype. IgGs can be divided into four subclasses: IgG1, IgG2, IgG3 and IgG4. The four subclasses have approximately 90% sequence homology, but vary in serum stability, number of interchain disulfide bonds, and their ability to activate the immune system *via* antibody-dependent cellular cytotoxicity (ADCC) or the complement pathway (Fig. 2).<sup>27</sup> Traditionally, IgG1 has been utilised the most in ADC development, due to its favourable balance of long serum half-life and moderate to strong immune activation. However, IgG4 has also been employed in cases where less immune activation is desirable.<sup>28</sup> Both IgG1 and IgG4 contain a total of 16 disulfide bonds per antibody. Of these, 12 are intrachain bonds and 4 are interchain bonds.

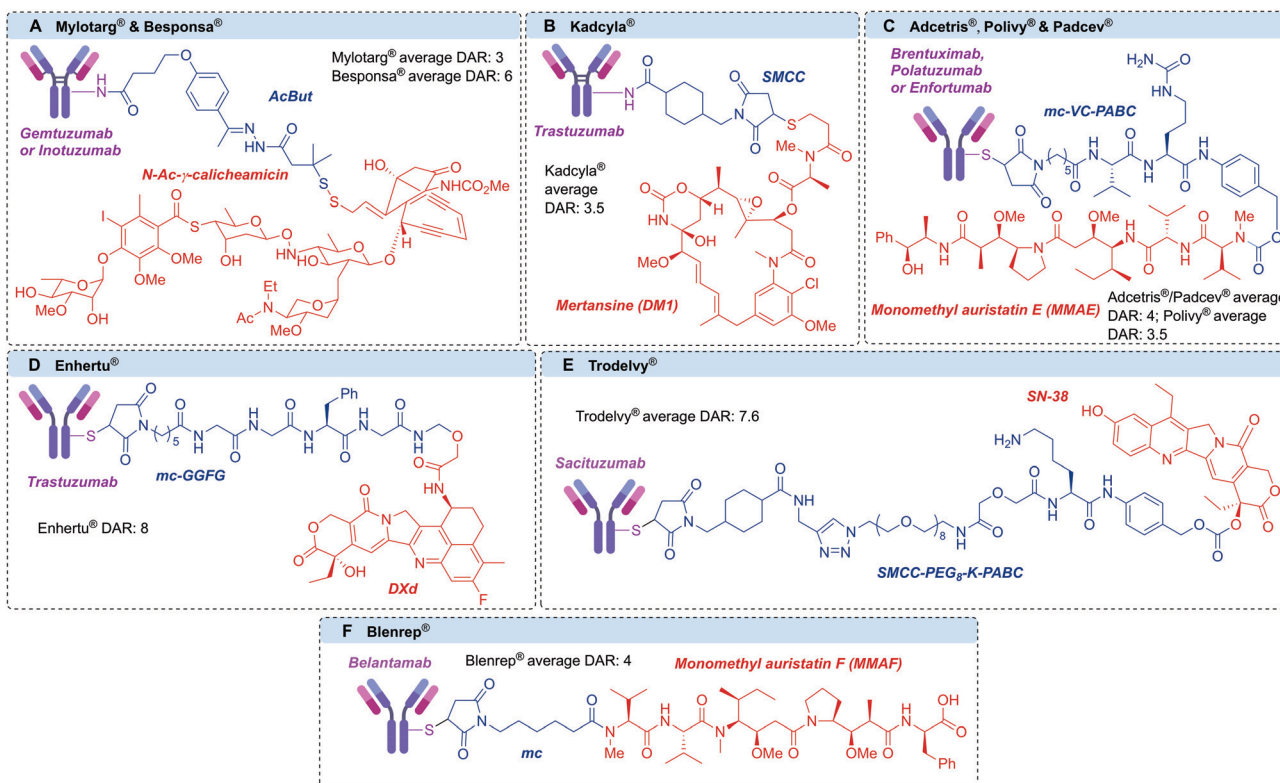


**Fig. 1** Structures of the clinically-approved ADCs, with linkers in blue and payloads in red. (A) Gemtuzumab ozogamicin (Mylotarg<sup>®</sup>) and inotuzumab ozogamicin (Besponsa<sup>®</sup>); (B) trastuzumab emtansine (Kadcyla<sup>®</sup>); (C) brentuximab vedotin (Adcetris<sup>®</sup>); polatuzumab vedotin (Polivy<sup>®</sup>) and enfurteumab vedotin (Padcev<sup>®</sup>); (D) trastuzumab deruxtecan (Entheru<sup>®</sup>); (E) sacituzumab govitecan (Trodelvy<sup>®</sup>); (F) belantamab mafodotin (Blenrep<sup>®</sup>). AcBut = 4-(4-acetylphenoxy)butanoic acid, SMCC = succinimidyl 4-(N-maleimidomethyl)cyclohexane-1-carboxylate, MC = maleimidocaproyl, PABC = p-aminobenzoyloxycarbonyl.



| Overview of IgG subclasses for potential use in ADCs |   |          |         |  |
|--|---|----------|---------|--|
|  | IgG1  | IgG2     | IgG3    | IgG4   |
| <b>Relative natural abundance</b>                    | 60%   | 32%      | 4%      | 4%   |
| <b># of interchain disulfide bonds</b>               | 4   | 6        | 13      | 4 <sup>a</sup>                                     |
| <b>Serum half-life</b>                               | ~21 days  | ~21 days | ~7 days | ~21 days   |
| <b>Immune activation</b>                             |   |          |         |  |
| <b>via C1q binding</b>                               | ++  | +        | +++     | -  |
| <b>via Fc<sub>γ</sub>R binding</b>                   | +++   | +        | ++++    | ++   |
| <b>Use in clinically-approved ADCs</b>               | Kadcyla <sup>®</sup> , Entheru <sup>®</sup> ,<br>Trodelvy <sup>®</sup> , Blenrep <sup>®</sup> ,<br>Adcetris <sup>®</sup> , Polivy <sup>®</sup> ,<br>Padcev <sup>®</sup> | -        | -       | Mylotarg <sup>®b</sup> ,<br>Besponsa <sup>®b</sup> |

Fig. 2 Overview of IgG subclasses for potential use in ADCs; <sup>a</sup>Hinge region disulfides are labile, enabling spontaneous Fab arm exchange with other IgG4 antibodies *in vivo* <sup>b</sup>Fab arm exchange is prevented through S228P mutation in the hinge region.

While interchain bonds are highly solvent exposed and may easily be reduced and/or modified by chemical methods, the intrachain bonds are buried within the globular fold of the protein and are therefore unreactive to chemical modification unless harsh denaturing conditions are applied.<sup>29</sup> In contrast to IgG1, native IgG4 molecules can undergo dynamic Fab arm exchange which may reduce their efficacy *in vivo* and lead to undesired off-target effects. However, this can be prevented through a S228P mutation in the hinge region of the heavy chain, as in the case of clinically approved ADCs Mylotarg<sup>®</sup> and Besponsa<sup>®</sup>.<sup>30,31</sup> Currently, all other approved ADCs utilise IgG1 antibodies.

### 1.1 ADC requirements

ADC research has progressed significantly over the past 30 years.<sup>32</sup> A wealth of knowledge now exists on the specific requirements for the three individual ADC components; the antibody, the cytotoxic drug and the linker. Whilst the natures of the target antigen, antibody,<sup>1,28,33</sup> linker-drug attachment<sup>16,26</sup> and payload<sup>34–36</sup> are all crucial to the pharmacology of an ADC, this review will focus on the developments in conjugation technology.

Early ADC research focused on the properties of the eponymous antibody and drug components, with little emphasis on the linker.<sup>32,37</sup> However, extensive research has revealed the importance of bioconjugation and the resulting linker-antibody attachments. To maximise the ADC's anti-tumour efficacy and safety, a number of key linker-antibody attachment attributes have been identified: (1) the attachment motif must be highly stable in circulation to avoid premature drug release, which can lower ADC efficacy and cause toxicity in healthy tissue;<sup>38,39</sup> (2) the number of linker-payloads per antibody should be

optimised for potency without compromising safety;<sup>40</sup> (3) the location of attachment on the antibody should not interfere with the antibody's function; and (4) the conjugation reaction should efficiently and selectively facilitate modification of the antibody in a controlled and consistent manner.<sup>41</sup>

### 1.2 Drug-to-antibody ratio and conjugation site

The stoichiometry of the linker-payloads on the antibody is referred to as the drug-to-antibody ratio (DAR). Given the limited number of ADCs that each target cell can internalise, it is desirable to maximise the DAR to increase potency (Fig. 3A).<sup>42</sup> However, the cytotoxins used in ADC research to achieve the desired potency tend to be large, lipophilic species. As such, increasing the DAR extensively can cause an increase in protein aggregation and an associated increase in ADC clearance, in turn returning diminished efficacy and safety.<sup>40,43</sup> A fine balance must be achieved to obtain the desired activity without eradicating the pharmacokinetic properties of the antibody. The optimal DAR is highly dependent on the nature of the linker and payload, but for most commonly used linker-payloads it is *ca.* 2–4.<sup>40</sup> However, in a handful of cases a DAR as high as 8 has safely been achieved through the use of hydrophilic linker-payloads, as exemplified with the clinically approved Entheru<sup>®</sup> and Trodelvy<sup>®</sup>.<sup>12,42,44–46</sup> It is also important to note that although an ADC synthesised *via* heterogeneous conjugation methods may have an average DAR of 2–4, there will be a distribution within this where some antibody molecules will be loaded with significantly higher or lower numbers of payloads relative to the reported average DAR.

As well as the drug loading, the attachment site of the linker-payload to the antibody is also an essential consideration (Fig. 3B).<sup>38,39</sup> It is critical that the attachment should be distal

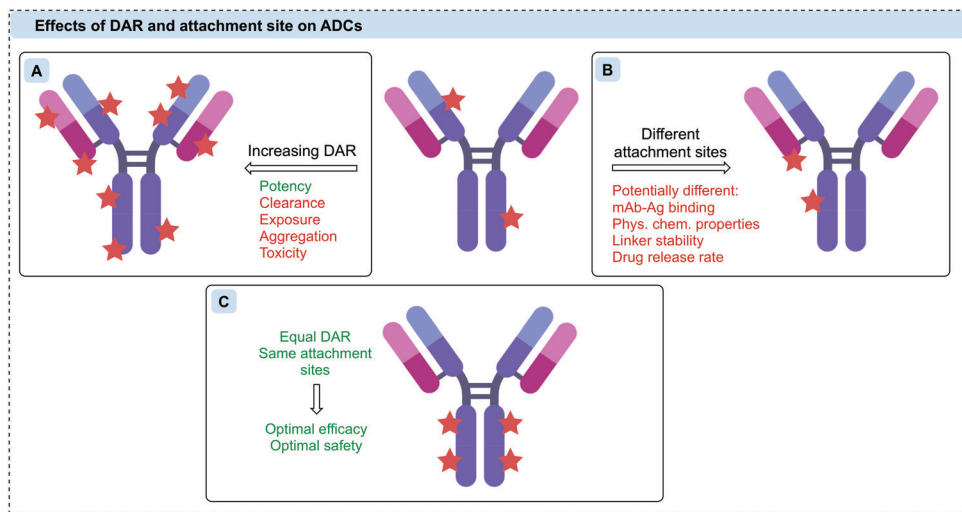


Fig. 3 The therapeutic effects of (A) increasing DAR, (B) different attachment sites, and (C) optimal DAR and conjugation sites on ADCs.

to the antigen-binding region, leaving antibody binding and internalisation unaffected. Furthermore, the attachment site can also have a dramatic effect on linker stability, which determines the rate of drug release both in circulation and at the tumour site.<sup>38,39</sup>

Many of the issues with early generation ADCs were attributed to the conjugation strategies that were employed, which led to heterogeneous and often unstable bioconjugates. To achieve optimal efficacy and safety, it is now widely accepted that ADCs with homogeneous DAR and attachment sites can generate superior therapeutics (Fig. 3C).<sup>47</sup> Given the huge number of reactive residues in an IgG, ADCs thus represent one of the most challenging applications of protein bioconjugation.<sup>48</sup> Advances in site-selective protein modification have enabled the development of a new generation of ADCs that fulfil these homogeneity requirements. Site-selective modification can be defined as chemo- and regio-selective protein modification and will be referred to as such hereafter.

In this review, we will discuss strategies for the construction of homogeneous ADCs including the most recent advances in the field. First, both chemical and enzymatic methods that facilitate amino acid modification will be discussed. This will be followed by a discussion of the developments made in the modification of the carbohydrate moiety of antibodies.

## 2 Amino acid modification – chemical methods

### 2.1 Stochastic conjugation with naturally occurring amino acids

Proteins can be considered meta-stable molecules. Thus, bioconjugation reactions between proteins and small molecules must meet a strict set of requirements to maintain protein structure and function. It is imperative that these reactions proceed in aqueous buffer under mild conditions (temperatures *ca.* 37 °C, pH 5–9, <15% organic co-solvent, low ( $\mu$ M)

protein concentration, <500 equivalents reagent).<sup>49–53</sup> While extensive work over recent decades has resulted in the generation of a toolbox of bioorthogonal reactions (reactions that can occur in living systems without affecting that system), such as the copper-catalysed azide–alkyne cycloaddition (CuAAC), the strain-promoted azide–alkyne cycloaddition (SPAAC) and the inverse electron demand Diels–Alder (iEDDA),<sup>54–56</sup> the natural reactivity of canonical amino acids such as lysine or cysteine has classically been exploited for the creation of protein conjugates. Indeed, all nine of the currently approved ADCs are synthesised *via* modification of either of these amino acids. Furthermore, other applications requiring modified antibodies, such as antibody–enzyme conjugates (for antibody-directed enzyme prodrug therapy [ADEPT]<sup>57,58</sup> or enzyme-linked immunosorbent assay [ELISA]),<sup>59</sup> as well as antibody–radioisotope<sup>60</sup> conjugates have generally employed stochastic lysine/cysteine modification techniques.

Lysine residues offer a facile method for bioconjugation due to their high natural abundance, surface accessibility and the nucleophilicity of the  $\epsilon$ -amino side chain. IgG1 antibodies contain approximately 85 lysine residues, of which more than 40 are typically modifiable.<sup>61</sup> Although the average DAR can be guided by reagent stoichiometry and reaction conditions, control of the conjugation site is essentially impossible and millions of different species can be generated in every synthetic batch (Fig. 4A).<sup>61</sup> Moreover, lysine residues decorate the entire surface of an antibody; therefore, their modification can impede antigen recognition, thus limiting the efficacy. Despite these shortcomings, Mylotarg<sup>®</sup>, Kadlec<sup>®</sup> and Besponsa<sup>®</sup> all employ lysine bioconjugation and are therefore administered as a heterogeneous mixture of products. Remarkably, in the case of Mylotarg<sup>®</sup>, 50% of the mAbs are unconjugated (DAR = 0), with the remaining species averaging DAR = 6, affording an overall average DAR  $\sim$  3.<sup>62</sup>

A range of lysine-selective reagents have been developed (Fig. 4B). *N*-Hydroxysuccinimide (NHS) esters (and their more soluble 3-sulfonated analogues) are by far the most commonly



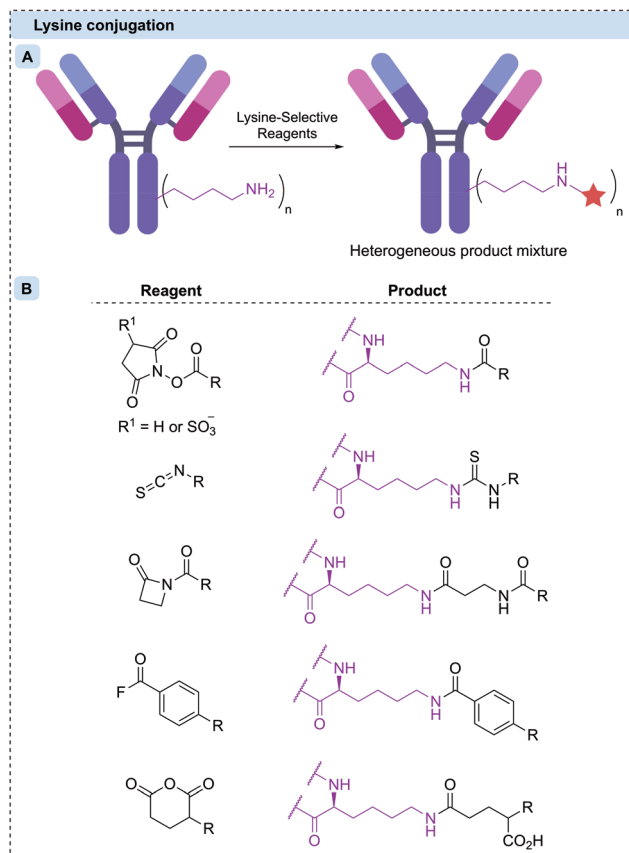


Fig. 4 (A) Stochastic reaction with surface-exposed lysine residues results in a heterogeneous product; (B) structures of lysine-selective reagents and their products upon conjugation.

used, due to their rapid lysine reactivity and the stability of the amide product. However, other amino acids such as cysteine and tyrosine, can also be modified during NHS ester reactions, forming less stable linkages.<sup>63–66</sup> These less stable linkages can release the linker-payload prematurely, potentially causing toxicity and lowering efficacy.<sup>63</sup> Other lysine-selective reagents that have successfully been used to construct ADCs include isothiocyanates,<sup>67</sup>  $\beta$ -lactams,<sup>68</sup> acyl fluorides,<sup>69</sup> and mixed anhydrides<sup>70</sup> (Fig. 4B).

Cysteine residues offer a particularly attractive target for protein bioconjugation due to their low natural abundance and the exceptionally high nucleophilicity of the deprotonated thiolate side chain. For IgG1 modification, naturally occurring cysteine residues can be unmasked by reduction of the four interchain disulfide bonds, revealing up to eight reactive thiol residues.<sup>71</sup> Subsequent reaction with soft electrophiles affords selective bioconjugation at the eight different sites (Fig. 5A). In some cases, including the approved ADCs Entheru<sup>®</sup> and Trodelvy<sup>®</sup>, a resulting DAR 8 conjugate has been achieved with high homogeneity, efficacy and safety. However, a DAR of 8 is not suitable for many linker-payloads.<sup>72</sup> Creation of ADCs with an average DAR of 2–4 therefore requires partial disulfide reduction/reoxidation and controlled linker-payload stoichiometry.<sup>71,73</sup> The resulting ADCs are inescapably heterogeneous,

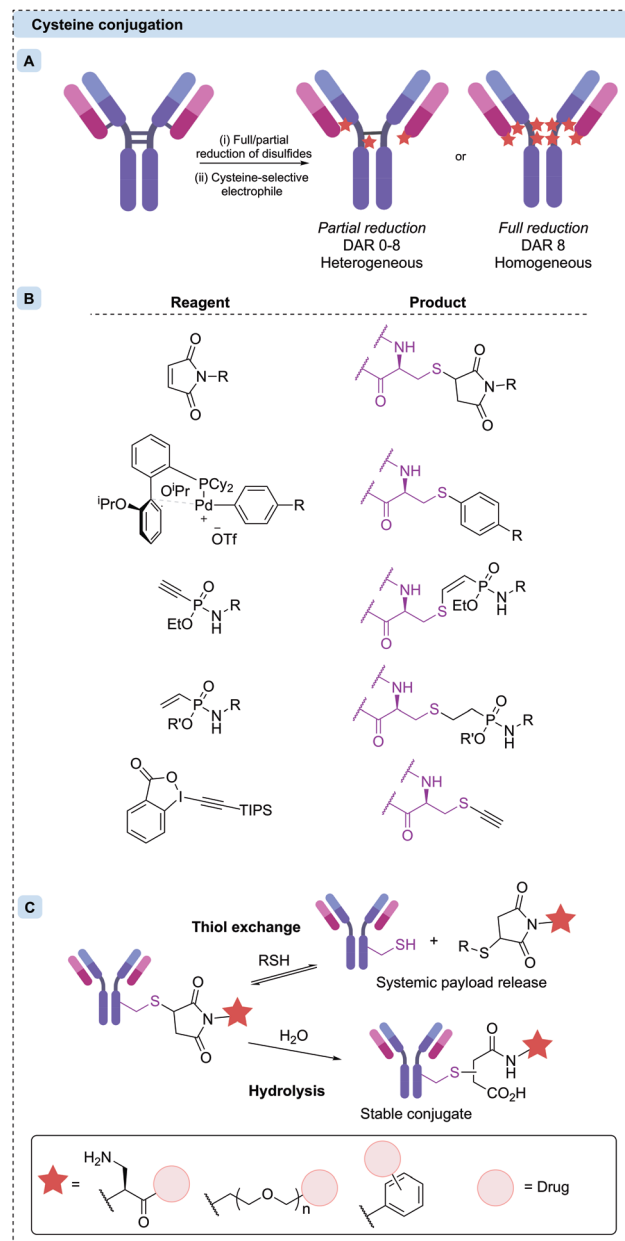


Fig. 5 (A) Reduction of interchain disulfides reveals thiol residues, reactive towards soft electrophilic reagents. Partial reduction results in heterogeneous product distributions, but full reduction and complete reaction of all eight reactive cysteines results in DAR 8 conjugates. (B) Structures of cysteine-selective reagents and their products upon conjugation. (C) The post-conjugation reactions of thiosuccinimide linkages (top). The retro-Michael addition and subsequent maleimide–thiol reaction, resulting in overall thiol-exchange (bottom). Hydrolysis of the succinimide moiety creates a stable chemical linkage. The structures of these self-hydrolysing maleimides are shown in the solid box.

although with less variability than is seen with stochastic lysine conjugation.

Cysteine modification occurs most commonly by 1,4-conjugate addition to *N*-substituted maleimides. Maleimides are particularly attractive reagents due to their synthetic accessibility and rapid reaction rates with cysteine under mild conditions.

Indeed, Adcetris®, Polivy®, Padcev®, Enhertu®, Trodelvy® and Blenrep® are all synthesised *via* maleimide modification of cysteines, as are the majority of ADCs currently in clinical trials. However, the resulting thiosuccinimide conjugates are inherently unstable, due to their propensity towards retro-Michael addition (Fig. 5C).<sup>74</sup> In circulation, the prematurely released maleimide-payload can then react with plasma thiols or diffuse into nearby cells, causing a reduction in efficacy and/or safety.<sup>38,75</sup> This instability can be mitigated by forcing post-conjugation hydrolysis of the thiosuccinimide, creating a stable chemical linkage. Accordingly, a number of “self-hydrolysing” maleimides have now been developed, with ring-opening catalysed by adjacent functional groups such as primary amine, polyethylene glycol (PEG) and *N*-aryl amongst the most promising.<sup>76–79</sup> Other reagents including  $\alpha$ -halocarbonyls,<sup>80</sup> palladium oxidative-addition complexes,<sup>81</sup> ethynylphosphonamidates,<sup>82,83</sup> vinylphosphonites<sup>84</sup> and ethynylbenziodoxolones<sup>85</sup> have also been used to synthesise ADCs with stable thioether bonds *via* modification of reduced interchain disulfides (Fig. 5B).

## 2.2 Engineered cysteines

Genetic modification of the number of accessible cysteine residues on an antibody surface has emerged as a popular method to achieve the desired site-selective and homogeneous modification. The earliest example using engineered antibodies decreased the number of interchain disulfides by replacing one of the cysteine residues with a different amino acid, resulting in fewer reactive cysteine residues. Mutants of the anti-CD30 IgG1 antibody cAC10, were generated by replacing select cysteine residues with serines.<sup>86</sup> Five mutants with different cysteine positions were modified with maleimidocaproyl-valine-citrulline-*para*-aminobenzoyl-monomethyl auristatin E (mc-Val-Cit-PABC-MMAE) to generate homogeneous ADCs with a DAR of either 2 or 4 (Fig. 6). Characterisation of these conjugates showed that mutagenesis did not impede antigen binding or *in vitro* cytotoxicity. However, *in vivo* mouse

xenograft models revealed these homogeneous ADCs had similar efficacy and therapeutic indices compared to analogous heterogeneous ADCs with similar average DARs. The authors concluded that the benefits from improved homogeneity may have been offset by the removal of interchain disulfide bonds.<sup>87</sup>

A significant advance was made by the development of antibodies with additional engineered cysteine residues. Introduction of non-native cysteine residues that are not involved in structural disulfide bonding can facilitate functionalisation with cytotoxic payloads. This approach offers a number of advantages: (1) modification of these unpaired cysteines with payloads will give homogeneous ADCs with a defined attachment site and drug stoichiometry; and (2) all native immunoglobulin disulfide bonds will be retained, potentially improving the stability and endogenous biology of the antibody. Identification of potential mutation sites is typically achieved using computational modelling, screening of model systems, or high-throughput scanning.<sup>88–90</sup> The mutated antibodies are then extensively characterised for stability, binding, aggregation, clearance and cytotoxicity.

Seminal work by Junutula *et al.* first introduced cysteine-engineered antibodies for biotherapeutic development, termed THIOMAB™.<sup>91</sup> In this study, the engineered cysteine was installed on an anti-MUC16 antibody by mutation of heavy chain alanine 114 (HC-A114). The authors found that expression of the mutated antibodies in Chinese hamster ovary (CHO) cells generated the THIOMAB with the engineered cysteine residues capped as disulfides with cysteine or glutathione. Therefore, a procedure of partial reduction (using tris(2carboxyethyl)phosphine [TCEP] or dithiothreitol [DTT]), purification, and re-oxidation of the interchain disulfide bonds (using CuSO<sub>4</sub> or dehydro-ascorbic acid) was required to reveal the reactive thiols. This partially reduced antibody was then treated with mc-Val-Cit-PABC-MMAE, producing a highly homogeneous ADC with an average DAR of 1.6 (Fig. 7A). This ADC was then compared with an analogous heterogeneous anti-MUC16 ADC (average DAR of 3.1) synthesised *via* modification

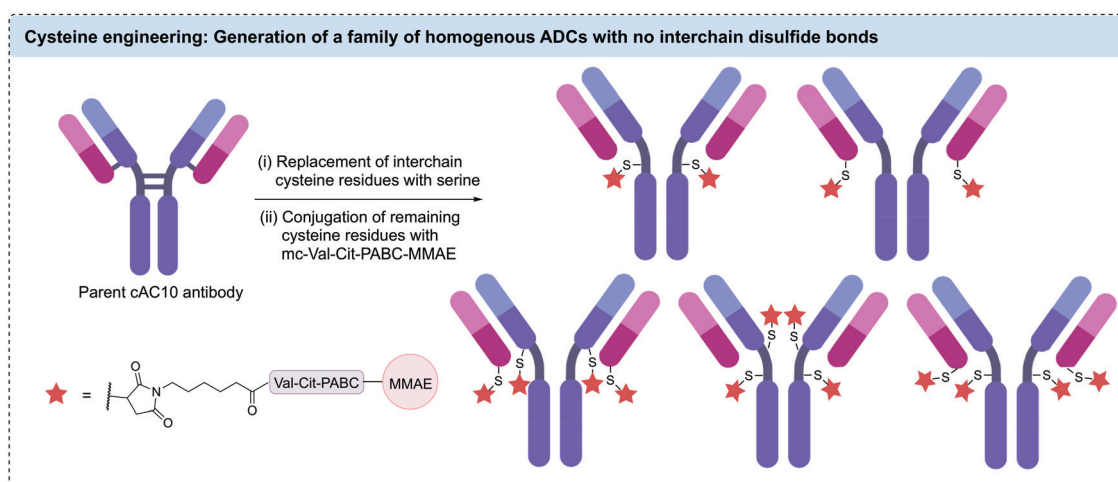
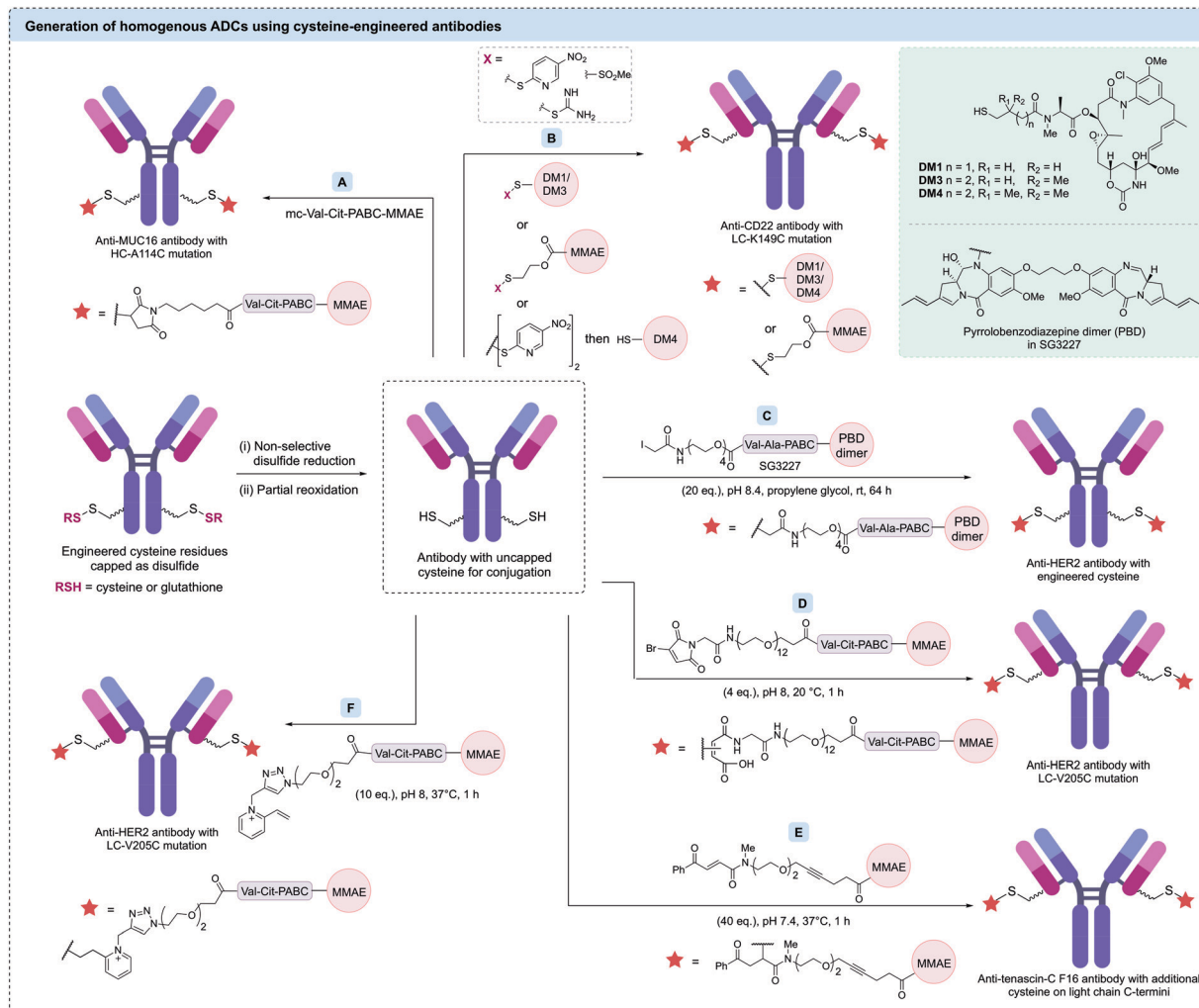


Fig. 6 Replacement of interchain cysteine residues with serine residues enables the generation of homogeneous ADCs with DARs of 2 or 4 *via* cysteine conjugation.





**Fig. 7** Strategies to functionalise cysteine-engineered antibodies to generate homogeneous ADCs. After revealing uncapped cysteine residues via reduction and re-oxidation steps, these cysteine-containing antibodies have been modified using (A) maleimides; (B) direct disulfide formation; (C) iodoacetamides; (D) bromomaleimides; (E) carbonyl acrylic reagents; (F) *N*-alkyl vinylpyridine salts.

of native interchain disulfides. An *in vivo* rat xenograft model revealed that the homogeneous ADC was at least as efficacious as the heterogeneous ADC despite its lower drug loading. Evaluation of the safety profile of both ADCs in rats and monkeys indicated that the heterogeneous ADC caused significant adverse effects. In contrast, the homogeneous ADC derived from the engineered antibody displayed no significant adverse effects, with all parameters essentially identical to vehicle-treated animals. Furthermore, the clearance rate for the homogeneous ADC was markedly slower than that of the heterogeneous ADC. Following these promising results, optimisation of the conjugation reaction yielded an ADC with a DAR of 2.

Many cysteine-engineered antibodies require the initial two-step reduction–reoxidation process reported by Junutula *et al.* to remove the capping disulfide prior to conjugation. However, one report by Shinmi *et al.* described the expression of a trastuzumab variant (LC-Q124C) that was isolated with no capping moiety, due to the sterically hindered location of the

cysteine.<sup>92</sup> Modification of this residue with mc-Val-Cit-PABC-MMAE produced a homogeneous ADC with a DAR of 2.

**2.2.1 Influence of cysteine microenvironment on pharmacological properties.** Several studies have reported the effect that the site of cysteine incorporation has on the stability of the conjugation linkage, thus potentially altering the pharmacological properties of the ADC. For example, to determine the effect of the cysteine microenvironment on the stability of the conjugate, Shen *et al.* compared three trastuzumab ADCs with engineered cysteines introduced at different positions.<sup>75</sup> Each engineered cysteine (LC-V205C, HC-A114C or HC-S396C) had varying levels of solvent accessibility and local charge. These cysteine residues were then modified with maleimide-MMAE linkers to generate the desired conjugates. All of the synthesised ADCs displayed similar DAR (1.7–1.9), *in vitro* target antigen binding, internalisation, and potency. Conjugates derived from cysteine residues with low solvent accessibility and positive local charge were more plasma stable, suggesting that steric hindrance prevents maleimide exchange with

plasma thiols and positively charged amino acid residues increase the rate of succinimide ring hydrolysis. These differences in stability resulted in significant increases in therapeutic efficacy, despite each of the ADCs displaying similar DAR (1.7–1.9), *in vitro* target antigen binding, internalisation, and potency.

In a related study by Sussman *et al.*, several anti-CD70 (h1F6) antibodies were engineered to contain cysteine mutations (heavy chain modifications of S239C, E269C, K326C or A327C), facilitating site-selective modification with a non-cleavable m-c-monomethyl auristatin F (MMAF) linker-payload.<sup>93</sup> These ADCs showed significantly different anti-tumour efficacies *in vivo*, despite similar *in vitro* potencies. To provide a rationale for this disparity, linker stability and thiosuccinimide ring opening were investigated. The authors found that ADCs with the slowest rate of thiosuccinimide ring opening also had the most stable linkage and *in vivo* potency. This trend is opposite to that reported by Shen *et al.*<sup>75</sup> and others,<sup>76</sup> who found that increased thiosuccinimide ring opening resulted in improved linkage stability and efficacy. Hydrophobic interaction chromatography (HIC) of the ADCs suggested that the conjugation site had a dramatic effect on the hydrophobicity of the conjugate. This in turn affected the stability of the thiosuccinimide linkage with the most hydrophobic ADCs demonstrating the slowest rate of hydrolysis and highest stability. The contrasting observations from these studies demonstrate the importance of optimising the site of cysteine engineering for each antibody to ensure sufficient stability.

In addition to traditional cysteine engineering methods *via* amino acid mutation, Dimasi *et al.* used cysteine insertion on an anti-EphA2 antibody.<sup>94</sup> Six cysteine-engineered antibodies comprising additional cysteines inserted before and after positions HC-S239, HC-A114, and LC-V205, were produced and evaluated for ADC development. Modification of the inserted cysteine with a maleimide-pyrrolobenzodiazepine (PBD) dimer linker-payload generated a series of homogeneous DAR 2 ADCs. It was found that the ADC synthesised from the antibody containing a cysteine insertion after HC-S239 displayed the most favourable characteristics, with high *in vivo* plasma stability and dose dependant *in vitro* cytotoxicity observed. Interestingly, although this ADC maintained binding with its target antigen and the neonatal Fc receptor (FcRn), it displayed significantly reduced binding with Fcγ receptors (FcγRs). Reduced binding with FcγRs may be beneficial, as emerging studies suggests that this binding mode can lead to non-specific uptake of ADCs.<sup>95</sup>

**2.2.2 Conjugation strategies for cysteine-engineered antibodies.** As mentioned in Section 2.2.1, the most common method of modifying a cysteine residue is to use an appropriate electrophilic moiety. Although maleimides are the most common cysteine-selective reagents, a variety of novel linkers have been used to functionalise engineered cysteines in this fashion. For example, iodoacetamides (Fig. 7C),<sup>96</sup> bromomaleimides (Fig. 7D),<sup>97</sup> carbonylacytic reagents (Fig. 7E),<sup>98,99</sup> and *N*-alkyl vinylpyridine salts (Fig. 7F)<sup>100</sup> and have been used to synthesise ADCs. Detailed reviews on cysteine-targeted protein modification are available elsewhere.<sup>51,101–103</sup>

Pillow *et al.* and Sadowsky *et al.* have also shown that drug attachment can be achieved through formation of a mixed disulfide.<sup>19,104</sup> Mixed disulfide bonds were formed by treating the antibody with an drug molecule bearing an activated thiol group, or alternatively by first activating the antibody's cysteine residues with 2,2'-dithiobis(5-nitropyridine), followed by reaction with a thiol-bearing drug molecule (Fig. 7B). Plasma stable constructs were generated using these methods on an anti-CD22 antibody with a cysteine mutation (LC-K149C). Drug release in disulfide-linked ADCs occurs by protein catabolism in the target cell to give a cysteine–drug conjugate, followed by disulfide reduction in the cytosol to release the free payload. The disulfide linkage approach could also be applied to amine-functionalised payloads (e.g. MMAE), using immolative 2-mercaptopethyl carboxy groups. In a related study, Vollmar *et al.* investigated the basis of the site-dependent stability of these disulfide bonds by comparing five trastuzumab mutants: HC-A118C, HC-A140C, LC-S121C, LC-K149C, and LC-V205C.<sup>105</sup> The authors found cysteine  $pK_a$  to have a greater influence on disulfide stability compared to steric effects – cysteine residues with the highest  $pK_a$  resulted in the most stable disulfide linkages.

Although the majority of cysteine engineered ADCs have a DAR of 2, a small number of reports have aimed to utilise engineered cysteines to generate higher DAR ADCs. For example, Pillow *et al.* generated a DAR 6 antibody-PROTAC by conjugating a chimeric BRD4 degrader (GNE-987) to engineered LC-K149C, HC-L174C, and HC-Y373C cysteine residues of an anti-CLL1 antibody *via* a methanethiosulfonyl (MTS) disulfide linkage.<sup>106</sup> In EOL-1 and HL-60 mouse xenografts, the anti-CLL1 ADC was shown to cause complete tumour regression after a single IV dose at either 5 or 10 mg kg<sup>-1</sup>. Separately, Neumann *et al.* generated DAR 10 ADCs *via* modification of the 8 interchain disulfide cysteines plus two additional engineered cysteines.<sup>107</sup> An anti-CD1232 antibody with two additional cysteine residues (HC-S239C) was conjugated to maleimide-modified nicotinamide phosphoribosyltransferase (NAMPT) inhibitors. In HNT-34 AML xenograft, the DAR 10 ADC induced rapid tumor regression after single administration of 10 mg kg<sup>-1</sup> and sustained the tumor regression after subsequent doses. Linker technologies have been developed to allow DAR 4 ADCs to be generated through modification of two cysteine residues. For example, Kumar *et al.* have combined a cysteine-engineered anti-HER2 antibody with a bis-functionalised maleimide reagent to generate DAR 4 ADCs with two different drug payloads (Fig. 8).<sup>108</sup> Cysteine modification with a maleimide reagent containing both ketone and alkyne reactive groups was followed by oxime ligation with an aminoxy-Val-Cit-PABC-MMAE payload and CuAAC with azido-Val-Ala-PABC-PBD to generate a homogeneous ADC with two MMAE and two PBD payloads. Although *in vitro* studies showed that the more potent PBD cytotoxin dominated the cytotoxic properties of the ADC, this study demonstrated that varied functional moieties can be installed on cysteine-engineered antibodies.

**2.2.3 Use of cysteine-engineered antibodies in clinical ADCs.** Since the introduction of cysteine-engineered antibodies,



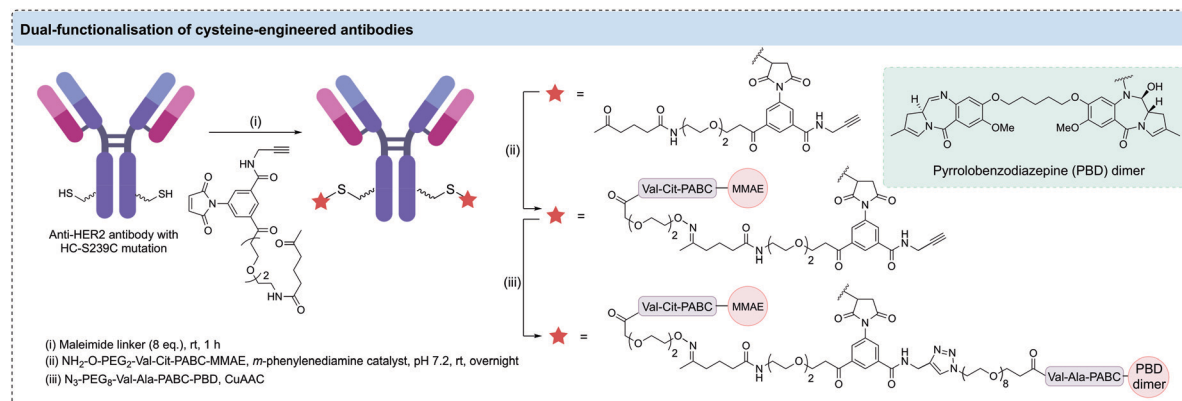


Fig. 8 Dual functionalisation of an anti-HER2 antibody containing two additional cysteine residues. A maleimide reagent containing orthogonal alkyne and ketone handles enabled conjugation of MMAE and PBD dimer payloads.

a number of cysteine-engineered ADCs have been developed against a range of cancer types.<sup>109–111</sup> Several of these ADCs have now advanced to clinical trials. For example, Immunogen's IMGN632 combines an anti-CD123 antibody with a novel, DNA-alkylating imine payload *via* a maleimide linkage.<sup>112</sup> Currently, Phase I/II clinical trials are underway for the treatment of acute myeloid leukemia (AML), blastic plasmacytoid dendritic cell neoplasm (BPDCN) and acute lymphoblastic leukemia (ALL) (ClinicalTrials.gov Identifiers: NCT03386513 and NCT04086264). Another example is ADC Therapeutics' ADCT-602, for the treatment of B-cell lymphoblastic leukaemia, in which an engineered variant of the humanised anti-CD22 antibody epratuzumab is functionalised with maleimide-Val-Ala-PABC-PBD (in Phase I/II; ClinicalTrials.gov Identifier: NCT03698552).<sup>113</sup> BAT8003 developed by Bio-Thera Solutions employs an antibody targeting Trop-2 to treat epithelial cancer.<sup>114</sup> This antibody has a HC-A114C mutation, which allowed the site-specific modification with a maytansine derivative (in Phase I; ClinicalTrials.gov Identifier: NCT03884517).

Although ADCs are usually developed for the treatment of cancer, cysteine-engineered ADCs have been developed as antibiotics. To target intracellular methicillin-resistant *S. aureus* bacteria, Lehar *et al.* designed antibody-antibiotic conjugates that are activated specifically inside mammalian cells.<sup>115</sup> A human IgG1 which targets wall teichoic acids of *S. aureus* was first engineered with a LC-V205C mutation and subsequently modified with a rifamycin derivative (an antibacterial that targets bacterial RNA polymerase) *via* a maleimide-Val-Cit cleavable linker. Compared to vancomycin treatment, these antibody-antibiotic conjugates were superior in treating MRSA *in vitro* and *in vivo*. A Phase I clinical trial demonstrated favourable safety and pharmacokinetic profile of the anti-*S. aureus* antibody-antibiotic conjugate in healthy volunteers (ClinicalTrials.gov Identifier: NCT02596399),<sup>116</sup> and further clinical trials are currently underway to treat patients with *S. aureus* infections (ClinicalTrials.gov Identifier: NCT03162250).

As demonstrated in this section, the use of cysteine-engineered antibodies provides reactive handles to reliably synthesise site-specifically modified, homogenous ADCs. Despite the requirement to optimise the most suitable position for cysteine

engineering, this method has been used to generate numerous ADCs comprising various antibody-linker-payload combinations against a range of malignancies. Further development of cysteine-engineered antibodies and their progression to clinical trials is expected.

### 2.3 Disulfide rebridging

Disulfide rebridging involves the reduction of the four inter-chain disulfide bonds in an IgG1 antibody followed by reaction with a cysteine-selective cross-linking reagent. The bis-reactive reagent enables the reconnection of the polypeptide chains while simultaneously installing drug molecules or bioorthogonal functionalities amenable to further modification. By covalently reconnecting the cysteine residues, the stabilising effect of the disulfide bonds is maintained and a controlled loading of one linker molecule per disulfide can be achieved. Depending on the number of drug molecules attached to each linker, a DAR of 4, 8 or 16 has been attained in this way.<sup>117</sup> Since the conjugation utilises native cysteine residues in the antibody hinge region, no alteration of the genetic code or the glycosylation pattern is required. The three most established disulfide rebridging technologies are bisulfone reagents, next-generation maleimides (NGMs) and pyridazinediones (PDs); however, in recent years numerous other methods have emerged, including the use of arylene dipropiolonitrile (ADPN), divinylpyrimidine (DVP), dibromomethyl heterocycles (C-Lock™), dichloroacetone or platinum(II) complexes. Here, we will give an overview of the applications and benefits of each strategy and discuss the overall utility of disulfide rebridging in ADC development.

**2.3.1 Bissulfones.** The development of bisulfones as disulfide rebridging agents and their application for the generation of antibody conjugates was first reported in 1990.<sup>118,119</sup> Mechanistically, the reaction occurs *via* *in situ* elimination of one of the sulfonyl groups which generates an  $\alpha,\beta$ -unsaturated carbonyl amenable to Michael addition of a cysteine residue to generate a thioether bond. Repetition of this elimination-addition process leads to the covalent rebridging of the two cysteine residues *via* a three-carbon bridge. This strategy was

first applied to the synthesis of ADCs in 2014 by Badescu *et al.* who reported the use of a bisulfone reagent attached to MMAE through a PEG<sub>24</sub> spacer and a cleavable Val-Cit-PABC motif to rebridge the disulfide bonds of trastuzumab (Fig. 9A).<sup>120</sup> HIC analysis of the resulting ADC suggested that the desired DAR 4 species was the major product of the reaction (78%). The remaining components were identified as the DAR 3 (10%) and DAR 5 (11%) species, resulting from under- or overreaction of the linker. The ADC displayed complete stability in the presence of human serum albumin (HSA) over a 5 day incubation period and was more efficacious than unconjugated trastuzumab in a mouse xenograft model after 5 doses at 20 mg kg<sup>-1</sup>. In a follow-up study by Bryant *et al.*, an analogous anti-HER2 trastuzumab ADC containing a shorter PEG<sub>6</sub> spacer was evaluated and compared to the approved HER2-targeting ADC T-DM1 (Kadcyla<sup>®</sup>).<sup>121</sup> In a JIMT-1 mouse xenograft model, both ADCs showed comparable activities at a dosage of 0.5 mg kg<sup>-1</sup> every 3 weeks.

5 mg kg<sup>-1</sup>; however the rebridged ADC was significantly more efficacious than T-DM1 at 10 mg kg<sup>-1</sup>.

It was hypothesised that premature degradation of the cleavable Val-Cit unit in circulation was lowering the efficacy of bisulfone-reacted ADCs. The mouse plasma stability of the Val-Cit motif is known to be affected by linker structure (including PEGylation pattern) and attachment point.<sup>39,122</sup> Therefore, Pabst *et al.* investigated the effects of PEGylation on the potency and stability of bisulfone-conjugated ADCs containing a Val-Cit-PABC cleavage mechanism and found that ADCs with branched or non-PEGylated linkers were significantly more stable *in vivo* in mice than bisulfone ADCs with linear PEGylated linkers.<sup>123</sup> Furthermore, the branched linker ADC demonstrated superior stability compared to the approved heterogeneous anti-CD30 ADC Adcetris® and showed excellent *in vivo* efficacy with complete tumour regression observed after treatment with a single dose at 1 mg kg<sup>-1</sup> in a CD30-positive

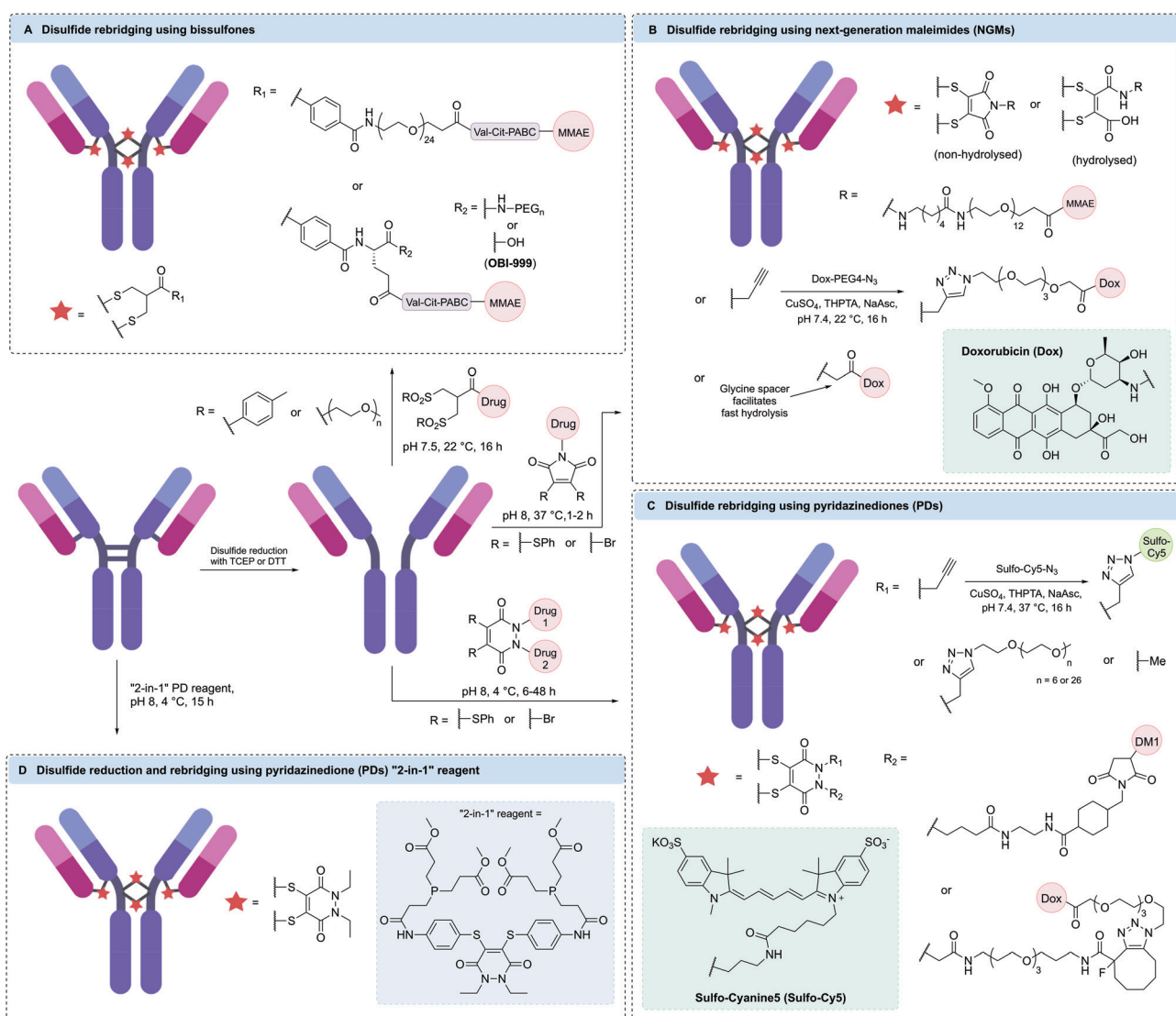


**Fig. 9** Selected examples of homogenous ADCs generated via disulfide rebridging using (A) bisulfones, (B) next-generation maleimides (NGMs), (C) pyridazinediones (PDs) or (D) “2-in-1” PD reagents.

mouse xenograft (Fig. 9A). In a different study, it was found that cyclisation of the branched PEG chains could improve the efficacy of bisulfone ADCs even further and allow for complete tumour regression in the same mouse model at a dosage of  $0.8 \text{ mg kg}^{-1}$ .<sup>124</sup>

Abzena is currently licensing bisulfone linker technology to various pharmaceutical companies under the tradename Thio-Bridge™. This arrangement has led to the development of multiple drugs in preclinical and clinical trials. For example, OBI-999 is an ADC developed by OBI Pharma composed of an MMAE payload attached to a humanised anti-Glob H antibody *via* a bisulfone linker (Fig. 9A).<sup>36,125</sup> The ADC has recently received FDA orphan drug designation for the treatment of pancreatic and gastric cancer based on promising preclinical data. OBI is currently recruiting patients with locally advanced or metastatic solid tumours, including gastric, pancreatic, oesophageal and colorectal cancers, for a Phase I/II study (ClinicalTrials.gov Identifier: NCT04084366). Another bisulfone-based ADC, HTI-1511, was developed by Halozyme and contains an MMAE payload conjugated to an EGFR-targeting antibody. This ADC has demonstrated promising tumour growth inhibition or regression in patient-derived xenograft models in mice, including models with KRAS/BRAF mutations typically associated with resistance to EGFR-targeted therapy and poor outcome.<sup>36,126</sup> Furthermore, HTI-1511 has been shown to be well tolerated in primate models.

A detailed procedure for the use of bisulfone reagents was recently published by Bird *et al.*, potentially aiding its more widespread use.<sup>127</sup> Typical reaction conditions are very mild and involve incubation of reduced antibody with 5–6 equivalents of bisulfone in pH 7.5 buffer at 22 °C for 16 hours. Conversion to the desired DAR 4 species is typically in the range of 75–85% and further purification by HIC is often performed to attain fully homogenous ADCs with a DAR 4 content of >95%.<sup>123</sup> Sodium dodecyl sulfate polyacrylamide gel electrophoresis (SDS-PAGE) data of OBI-999 suggests that the ADC exists as a mixture of two isomeric species; one being the natively rebridged species in which all polypeptide chains are rebridged in an interchain fashion and the other being a “half-antibody” species which has lost the covalent linkage between the antibody heavy chains due to the formation of non-native intrachain bridges between the cysteines in hinge region of the heavy chains. Whether this heterogeneity has any impact on ADC performance is unclear (*vide infra*).

**2.3.2 Next-generation maleimides (NGMs).** Next-generation maleimides (NGMs) are a class of maleimide reagents modified with two halide or thiophenol leaving groups. The use of such NGMs for disulfide rebridging was first introduced by Smith *et al.* in 2010 when it was found that these reagents could efficiently effect disulfide rebridging *via* consecutive addition-elimination reactions, inserting a two-carbon bridge between the two cysteine residues in the process.<sup>128</sup> In 2014, Schumacher *et al.* first demonstrated the use of this method for the generation of ADCs.<sup>129</sup> It was reported that complete rebridging of reduced trastuzumab could be achieved by reaction with 5 equivalents of dibromomaleimide or dithiophenomaleimide in less than one hour, showcasing that

the reaction proceeds with rapid kinetics, similar to those observed with traditional maleimide bioconjugation. The authors noted that the resulting conjugates were not homogenous, but rather existed as a mixture of natively rebridged “full antibody” and non-natively rebridged “half-antibody” species. By switching to an *in situ* protocol, in which reducing agent and linker are added simultaneously, half-antibody formation could be reduced drastically, indicating that lowering the residence time of the reduced cysteine residues decreases their potential for scrambling. This improved protocol was used to react trastuzumab with a dithiophenomaleimide reagent containing an alkyne handle which was subsequently functionalised with doxorubicin *via* click chemistry to yield a DAR 4 ADC with excellent homogeneity (Fig. 9B).

Like traditional maleimides, NGMs are unstable in the presence of free thiols unless hydrolysed to the maleamic acid form.<sup>103</sup> Nunes *et al.* showed that complete hydrolysis of an NGM-containing antibody-conjugate could be achieved by incubation in pH 8.4 buffer for 72 hours and the resulting hydrolysed conjugate was fully stable in human plasma for 7 days.<sup>130</sup> This hydrolysis protocol was used in the synthesis of a DAR 4 ADC *via* reaction of trastuzumab with a dithiophenomaleimide linker containing a non-cleavable PEG<sub>12</sub> spacer and an MMAE payload (Fig. 9B). The ADC was more efficacious than unmodified trastuzumab *in vivo*, with three doses at  $20 \text{ mg kg}^{-1}$  affording complete tumour regression in mouse models.<sup>131</sup>

Building on this work, the *in vivo* stability and efficacy of an NGM ADC was directly compared to a heterogeneous ADC with an average DAR of 4 synthesised *via* maleimide modification of interchain disulfides.<sup>132</sup> A non-cleavable dibromomaleimide linker was employed to connect MMAF to trastuzumab or the anti-CD98 antibody IGNX, generating homogenous DAR 4 ADCs. In both cases, the NGM ADCs had remarkably increased circulation half-life in mice (184 h vs. 130 h) and achieved improved tumour regression compared to their heterogeneous counterparts.

Despite these promising results, the requirement for 72 hour-hydrolysis to ensure stability was still considered a major drawback of NGMs. This process was accelerated by Moraes *et al.* by increasing electron deficiency and steric bulk around the maleimide motif.<sup>133</sup> More specifically, it was found that the incorporation of a glycine-derived motif adjacent to the maleimide ring reduced the hydrolysis time from 72 hours to just 1 hour (Fig. 9B).

Most reported NGM ADCs utilise non-cleavable linkers; however, their usage with cathepsin-cleavable linkers has also been reported. Bryden *et al.* showed that Val-Ala and Val-Cit dipeptides could be incorporated into NGM linkers.<sup>134</sup> In the first instance, the hydrophobic nature of the Val-Ala motif was reported to cause a significant reduction in reactivity and only the Val-Cit-NGM linker was able to yield >50% of the desired DAR 4 ADC. However, later incorporation of PEG chains off-set the hydrophobicity issue and allowed for the generation of viable ADCs with either dipeptide motif.

Recently, significant effort has been invested into exploring the effects of different substitution patterns on NGM stability and homogeneity. For example, Forte *et al.* have reported that



diiodomaleimides might be superior to dibromomaleimides in terms of reagent stability.<sup>135</sup> Furthermore, Feuillâtre *et al.* reported the use of hybrid thiobromomaleimides (TBMs) which were shown to produce homogenous ADCs with a marginally narrower DAR distribution compared to dibromomaleimide and dithiophenolmaleimide reagents.<sup>136</sup>

NGMs have repeatedly demonstrated the ability to generate ADCs with high levels of homogeneity. Optimisation of the ring hydrolysis has significantly improved the utility of this method and allowed for the synthesis of ADCs with excellent plasma stability. In addition to being compatible with a large range of traditional payloads such as MMAE and doxorubicin, NGM linkers have recently been shown to allow for the generation of ADCs with PROTAC payloads, showcasing their broad applicability.<sup>137</sup> The NGM linker platform is currently marketed by ThioLogics.

**2.3.3 Pyridazinediones (PDs).** Pyridazinediones (PDs) were first developed by Chudasama *et al.* as thiol-cleavable linkers for peptide stapling and prodrug development.<sup>138</sup> Similar to NGMs, PDs possess two leaving groups and react with cysteine residues *via* consecutive addition-elimination reactions, resulting in the insertion of a two-carbon bridge between the two residues. However, PDs distinguish themselves through their intrinsic stability. Although the linkage can be cleaved in the presence of other thiols, high concentrations of thiol are usually required, and numerous reports have documented the stability of PD-derived conjugates in human plasma. In 2017, Robinson *et al.* synthesised DAR 4 anti-HER2 ADCs with PD linkers containing either cathepsin-cleavable or non-cleavable MMAE payloads.<sup>131</sup> Mass spectrometry and HIC analysis showed excellent conversion to the DAR 4 species (90%) with only small amounts of DAR 3 (3%) and DAR 5 (7%) species present. Both ADCs were highly potent against antigen-positive cell lines with the cleavable ADC demonstrating 100-fold more potency than the non-cleavable variant. Both ADCs were efficacious and well tolerated in mice models.

PD reagents can be modified for the generation of dual-functional conjugates, as each of the two ring nitrogens are easily decorated with orthogonal click handles. In 2015, Maruani *et al.* utilised this capability by modifying trastuzumab with a dibromopyridazinedione linker containing both a terminal alkyne and a strained alkyne.<sup>139</sup> These handles were subsequently functionalised with a doxorubicin payload and a fluorophore *via* orthogonal CuAAC or SPAAC reactions to yield a DAR 4 ADC containing four cytotoxic payloads and four fluorophores (Fig. 9C). Despite the double modification, the ADC maintained high affinity for its target antigen and was completely selective for antigen-positive cell lines *in vitro*.

The ability to add a second functional moiety to an antibody using PD reagents has also been exploited to mask the hydrophobicity of the attached payload.<sup>140</sup> PD reagents functionalised with a DM1 payload and either a PEG<sub>6</sub> or PEG<sub>26</sub> chain were shown to react efficiently with reduced trastuzumab to generate DAR 4 ADCs of similar homogeneity (Fig. 9C). *In vivo*, both ADCs showed comparable activity to T-DM1 and lead to complete tumour regression after administration of 2 doses at 10 mg kg<sup>-1</sup> in a mouse xenograft model.

Whilst regular PD linkers react with one disulfide each to generate DAR 4 ADCs, Lee *et al.* exploited the second functionalisation vector of the PD scaffold to connect two reagents, thus creating a single linker that could react with four cysteine residues.<sup>141</sup> This modality was amenable to attachment of a single alkyne handle, which enabled the synthesis of antibody conjugates with a controlled loading of 2 payload molecules. The concept was validated by the generation of a homogenous DAR 2 doxorubicin ADC.

In another approach, incorporation of a dendritic spacer into a dibromopyridazinedione reagent enabled the synthesis of a homogenous trastuzumab ADC with a DAR of 16 *via* attachment of four porphyrin-based photosensitiser payloads to each PD-dendrimer.<sup>142</sup> This ADC showed excellent cytotoxicity in antigen-positive cell lines when exposed to light but exerted no effect in the dark, thus demonstrating the compatibility of PD linkers with photosensitiser payloads.

Post-conjugation functionalisation of PD linkers has mainly been achieved *via* CuAAC or SPAAC reactions; however, other types of click chemistry may also be used. For example, Marquard *et al.* recently reported the synthesis of a dibromopyridazinedione reagent with a *trans*-cyclooctene (TCO) functionalisation handle. This PD-TCO reagent was successfully conjugated to three therapeutically relevant IgG1 antibodies (trastuzumab, cetuximab and rituximab) and were further functionalised with tetrazine-containing fluorophores.<sup>143</sup> All three conjugates were highly homogenous and could be recovered in high yields. Notably even rituximab, which is known to exhibit >90% protein loss after TCO modification *via* traditional NHS-ester chemistry, could be recovered in 83% yield after PD-TCO modification. This showcased a clear advantage of disulfide rebridging chemistry over stochastic lysine modification in terms of protein recovery when dealing with aggregation-prone antibodies.

PD reagents are currently considered to be among the best disulfide rebridging agents in terms of ADC homogeneity and have resulted in >90% conversion to the desired DAR 4 conjugate in most of the studies discussed above. However, variable patterns of cysteine connectivity have been reported with half-antibody content ranging from 5% to 95% depending on reagent and reaction conditions.<sup>139,140</sup> Although the effect of variable cysteine connectivity on ADC performance remains unknown, methods for reducing half-antibody formation with PD linkers have been explored. For example, Lee *et al.* found that half-antibody formation could be lowered by the use of a “2-in-1” reagent. The reagent was designed to effect both disulfide reduction and rebridging, thus lowering the residence time of the reduced cysteine residues and their potential for scrambling.<sup>144</sup> The dithioaryl(TCEP)pyridazinedione reagent was used for the modification of trastuzumab and led to reduced half-antibody formation in comparison to a two-step reduction-rebridging protocol using TCEP and a regular dibromo- or dithiopyridazinedione linker (Fig. 9D). However, the reagent was not suitable for long-term storage due to poor stability. For this reason, Bahou *et al.* sought to optimise the PD bioconjugation protocol as an alternative way of maximising



full antibody formation without the need for bespoke “2-in-1” reagents.<sup>145</sup> It was thus found that the application of an *in situ* protocol, in which the addition of the PD linker precedes addition of the reducing agent, in combination with a decrease in reaction temperature from 37 °C to 4 °C, led to a significant reduction in half-antibody formation and an improvement in overall ADC homogeneity.

PDs, like NGMs, are among the best disulfide rebridging reagents in terms of reaction kinetics and product homogeneity. Furthermore, the “plug-and-play” aspect allows for facile functionalisation with multiple different payloads *via* orthogonal click handles is appealing for the synthesis of dual-functional ADCs. Like NGMs, PDs are currently marketed by ThioLogics.

**2.3.4 Other methods.** The extensive work conducted with bisulfones, NGMs and PDs has clearly demonstrated the practicality of using disulfide rebridging for the generation of homogenous ADCs. In recent years, this success has inspired the development of various new rebridging methods.

C-Lock™ is a proprietary technology developed by Concoris Biotherapeutics encompassing the use of dibromomethyl heterocycles such as dibromomethylquinoxaline as disulfide rebridging linkers (Fig. 10A). In 2013, Concoris was acquired by Sorrento Therapeutics which used C-Lock™ technology to develop STI-6129, an ADC comprising a duostatin payload and a CD38-targeting antibody, for the treatment of haematological malignancies. STI-6129 showed promising activity in preclinical studies and has recently entered Phase I clinical trials for the treatment of relapsed or refractory systemic AL amyloidosis (ClinicalTrials.gov Identifier: NCT04316442). C-Lock™ technology has also been applied by Zova Biotherapeutics who in 2019 published the development of ZV0508 – an ADC composed of a duostatin payload linked to an antibody targeting 5T4 oncofetal

glycoprotein *via* a dibromomethylquinoxaline linker.<sup>146</sup> HIC analysis of this ADC showed excellent conversion (>90%) to the DAR 4 ADC after incubation with just 5 molar equivalents of linker. However, as with other ADCs derived from disulfide rebridging, analysis by CE-SDS showed that Zova's C-Lock™ ADC was comprised of a mixture of full and half-antibody species. Nonetheless, ZV0508 displayed excellent tolerability and potency in preclinical *in vivo* investigations where it outperformed an analogous ADC generated using maleimide conjugation. Zova Biotherapeutics has since filed patent applications for several anti-HER2 and anti-5T4 ADCs containing C-Lock™ linkers.<sup>147,148</sup>

Concurrently, Novartis has reported the use of 1,3-dihaloacetone reagents such as 1,3-dichloroacetone or 1,3-dibromoacetone for the rebridging of antibody disulfides. In the resulting conjugates, each pair of cysteines is connected through a three-carbon tether containing a reactive ketone. This ketone can then be further reacted with a hydroxylamine-modified payload *via* oxime ligation (Fig. 10B). In one application, this approach was used for the construction of an anti-HER2 ADC with a DAR of 3.8.<sup>149</sup> In a different application, the introduced ketones were linked together by a linker-payload containing two hydroxylamine groups, thus enabling the generation of a MMAF-containing anti-HER2 ADC with a reported DAR of 1.8.<sup>150</sup> Both ADCs were shown to be highly homogenous by mass spectrometry and SDS-PAGE with approximately 90% conversion to the desired product and minimal half-antibody formation.

Invictus oncology has developed platinum(II) reagents for disulfide rebridging (Fig. 10C).<sup>151</sup> A Pt(II)-based linker-payload was generated by tethering the topoisomerase inhibitor camptothecin to a bivalent amine ligand which was subsequently complexed with Pt(II) chloride. This linker-payload reacted with

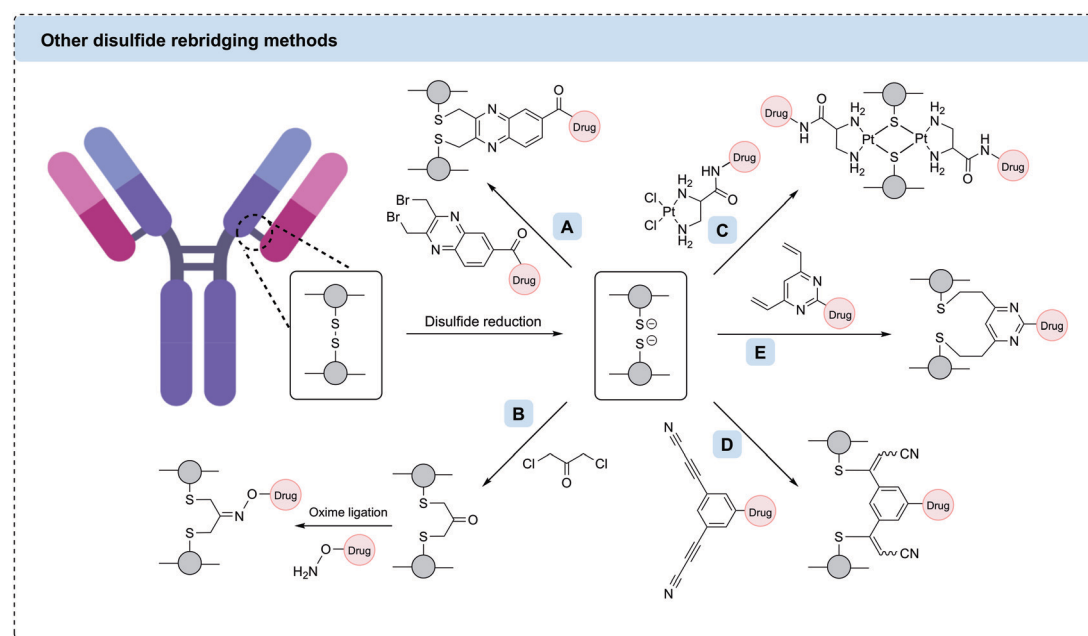


Fig. 10 Other disulfide rebridging methods for the generation of homogenous ADCs. (A) C-Lock™ reagents such as dibromomethylquinoxaline; (B) dichloroacetone conjugation followed by oxime ligation; (C) Pt(II)-based reagents; (D) arylene dipropiolonitrile (ADPN); (E) divinylpyrimidine (DVP).



reduced disulfides in trastuzumab, rituximab or cetuximab to generate ADCs with a DAR of 8. The ADCs showed increased stability and homogeneity *versus* analogous maleimide conjugates, although a significant amount of half-antibody formation was observed. The biological activity of the cetuximab ADC was validated *in vitro* and *in vivo*. The ADC was only marginally more active than unmodified cetuximab; however, this may be due to the choice of payload or release mechanism rather than the linker.

In addition to these industrially developed methods, multiple academic labs have partaken in the expansion of disulfide rebridging methods. For instance, Koniev *et al.* published a reduction-rebridging strategy for the generation of ADCs using arylene dipropiolonitrile (ADPN) linkers in 2018 (Fig. 10D).<sup>152</sup> This work was inspired by previous findings that arylene monopropiolonitrile linkers formed very stable linkages with cysteine residues.<sup>153</sup> To translate this into a rebridging strategy, three regioisomers of ADPN were compared. It was found that *meta*-ADPNs gave superior conversion over *ortho*- or *para*-ADPNs, albeit yielding a mixture of full and half-antibody species. The *meta*-ADPN linker was subsequently utilised to generate a trastuzumab ADC containing MMAE and a  $\beta$ -galactosidase-cleavable linker. Native mass spectrometry revealed  $\sim 50\%$  conversion to the desired DAR 4 species, with significant amounts of DAR 3 and DAR 5 species present. The ADC showed comparable cytotoxicity to T-DM1 when evaluated *in vitro*.

In 2019, Walsh *et al.* reported the use of divinylpyrimidine (DVP) reagents as disulfide bridging reagents for the generation of ADCs.<sup>154</sup> Like *meta*-ADPNs, DVPs enable rebridging *via* two consecutive Michael-addition reactions; however, rather than installing a five-carbon bridge, DVPs insert a flexible seven-carbon bridge between the two cysteine residues (Fig. 10E). This approach was used for the synthesis of several trastuzumab-based DAR 4 ADCs containing cathepsin-cleavable, sulfatase-cleavable, or non-cleavable spacers and an MMAE, hemiasterlin or doxorubicin payload.<sup>25,154,155</sup> In all cases  $>90\%$  conversion to the desired DAR 4 species was observed, which existed as mixtures of full and half-antibody formats. The conjugates displayed complete stability in human plasma over 14 days and were highly potent and selective *in vitro*. Recently, the scope of the methodology was further expanded by the development of a dual-functional DVP linker.<sup>156</sup> This linker enabled efficient dual functionalisation of trastuzumab with MMAE and a fluorophore without causing any negative effects on the activity of the antibody or either payload. Divinyltriazine reagents have also been shown to generate antibody conjugates with a payload loading of 4, with the rebridging proceeding efficiently using near-stoichiometric quantities of reagent.<sup>157</sup>

Many of the current rebridging methods suffer from the formation of half-antibody species which originate from non-native intrachain rebridging of the hinge region disulfides (*vide supra*). Such half-antibody species lack the native covalent link between the two heavy chains but remain held together by strong non-covalent interactions. The impact of these species on the physicochemical properties and binding of ADCs

depends on the particular system. In 2015, Lyon *et al.* compared the plasma clearance rate of unmodified disulfide-containing antibodies and maleimide-modified antibodies in which all interchain disulfides had been reduced. No significant difference was observed, indicating that interchain disulfide bonds are not essential to antibody stability and their absence does not negatively affect clearance.<sup>42</sup> However, a more recent investigation by Bahou *et al.* produced contrasting results.<sup>158</sup> Dibromo- and dichloropyridazinedione linkers were used to generate antibody-conjugates with varying homogeneity ranging from 10–50% half-antibody content. The thermal stability, aggregation potential and antigen-binding affinity of these conjugates were compared and the conjugate with the higher half-antibody content was shown to perform marginally worse than its more homogenous counterpart in many of the assays. No comparison between the performance of analogous half-antibody and full-antibody ADCs was undertaken. Therefore, it appears that more research into the nature and importance of half-antibody formation is warranted.

## 2.4 Non-canonical amino acids

**2.4.1 Genetic code expansion.** With the notable exceptions of the rare amino acids selenocysteine (Sec) and pyrrolysine (Pyl), all proteins are synthesised from a limited set of 20 natural amino acids. The canonical genetic code includes 64 codons encoding these 20 amino acids and three stop signals (UAG, amber; UAA, ochre; and UGA, opal). However, in recent years expansion of the genetic code has enabled the site-specific incorporation of non-canonical amino acids (ncAAs) into a range of proteins.<sup>159–161</sup> To achieve this, a tRNA/aminoacyl-tRNA synthetase (aaRS) pair that is orthogonal to the collection of tRNA/aaRS pairs found in the expression host is used to incorporate an ncAA into a protein in response to an unassigned codon, typically a stop codon, which has been introduced into the desired site of a gene.<sup>162</sup> The reassignment of a stop codon, known as stop codon suppression, competes with release factors (eRF1 in eukaryotes and RF1 in *E. coli*) that terminate protein synthesis in response to these codons. Nonetheless, a number of tRNAs have been found to effectively suppress stop codons, introducing alternative amino acids at these positions. For example, Pyl is genetically incorporated into methyltransferase enzymes in *Methanoscincina barkeri* in response to the amber stop codon.<sup>163</sup> The tRNA and tRNA synthetase required for this installation are not natively found in *E. coli* or mammalian cells. As such, introduction of this tRNA/aaRS pair into these cell types can be used to incorporate Pyl into proteins whose gene sequences contain an amber stop codon. Directed evolution of the tRNA/aaRS pair has enabled charging of the tRNA with a ncAA in place of Pyl, which can subsequently be installed in a growing peptide chain in response to the amber stop codon. The synthetase must also be engineered to specifically acylate a tRNA molecule with the ncAA, whilst avoid acylating the endogenous tRNAs.<sup>159,160</sup> In a similar way, several other engineered tRNA/aaRS pairs have been developed for genetic code expansion (GCE) applications, including the engineered *Methanocoldococcus jannaschii* tyrosyl-tRNA

synthetase (TyrRS) tRNA<sup>Tyr</sup> pair.<sup>164</sup> *De novo* generation of tRNA/aaRS pairs is also possible but generally proves far more challenging.<sup>165</sup>

**2.4.2 ncAA incorporation platforms.** In recent years, GCE techniques have enabled the incorporation of ncAAs into antibody sequences, resulting in an efficient approach to the site-specific modification of antibodies, and therefore homogeneous ADCs. This can be achieved *via* cell-based or cell-free systems. In cell-based systems the use of mammalian cell hosts is common due to their ability to ensure correct protein folding and post-translational modification. CHO cells in particular are routinely used for recombinant antibody production, including those engineered to contain ncAAs for ADC generation.<sup>166–168</sup> However, unlike bacterial expression systems mammalian cells require prolonged amber suppression, which can be damaging to cells.<sup>167</sup> Thus, as an alternative approach, cell-free protein synthesis (CFPS) systems have been developed. These systems lack the cell membrane, enabling unrestricted ncAA access to the engineered RS enzymes. Furthermore, the production of a stable cell-line to produce large quantities of recombinant antibodies is not required, although the resulting antibodies are aglycosylated due to lacking the necessary machinery for post-translational modifications. In recent years, numerous ADCs based on aglycosylated IgGs have entered clinical trials despite concerns over their stability, pharmacokinetics and immunogenicity.<sup>169–172</sup>

**2.4.3 ncAA position dependence.** In addition to the platform used for ncAA incorporation, the position at which the ncAA is introduced is another important consideration for ADC generation. For a given ADC, the yield of ncAA incorporation and subsequent modification efficiency of a specific positional variant depends on a number of factors, such as the ability to incorporate the ncAA into a specific position during translation, which has been shown to be dependent on the local sequence context of the nonsense codon.<sup>173</sup> Indeed, ncAA position is typically optimised for each ncAA, antibody, and payload to ensure the generation of ADCs capable of efficient antigen binding, without impacting functional domains that control pharmacokinetics and stability.<sup>167,174,175</sup> For example, VanBrunt *et al.* used a crystal structure of an IgG1 to select four conjugation sites that were distal to the antigen binding sites and avoided the hinge region, as well as residues known to be critical for Fc receptor binding.<sup>175</sup> In addition, the selected sites were predicted to be solvent exposed and outwardly oriented to enable efficient conjugation. Two IgG heavy chain positions (HC-274 and HC-359) and two light chain positions (LC-70 and LC-81) were found to satisfy these criteria. Incorporation of *N*<sup>6</sup>–((2 azidoethoxy)carbonyl)-L-lysine (AzK) at each site in turn allowed >95% conjugation efficiency with BCN-functionalised auristatin F (AF), thus generating four ADCs, each with a DAR ~ 2. Two further ADCs with a DAR ~ 4 were also produced by expressing antibodies with amber codons at both heavy and light chain locations (HC-274/LC-70 and HC-274/LC-81). *In vitro* cytotoxicity assays showed all six ADCs were potent and specific against HER2-expressing cells. However, one of the DAR 2 variants (HC-359) resulted in a more

hydrophobic ADC, prone to aggregation. Notably, the DAR 4 HC-274/LC-70 ADC was slightly more potent than the other five ADCs, whereas the other DAR 4 ADC HC-274/LC-81 was equipotent to the DAR 2 HC-274 conjugate. Thus, it was demonstrated that ADC activity is not only influenced by drug loading. Indeed, a decrease in potency was observed for the DAR 2 LC-81 variant compared to the DAR 2 HC-274 variant in the BT474 cell line, showing that the position of the AF toxin on the antibody also influenced ADC activity.

**2.4.4 Conjugation to ncAAs *via* oxime ligation.** A third important consideration for ADC generation *via* GCE is the choice of ncAA. As with all recombinant approaches to ADCs, incorporation of an ncAA results in a risk of possible immunogenicity. With this in mind, commonly used ncAAs are structural analogues of natural amino acids. In addition, the incorporated ncAAs must undergo efficient conjugation reactions. Following these criteria, ncAAs bearing unique functionalities, such as ketones, azides, cyclopropenes or diene functional groups, have been developed and incorporated into antibodies (Fig. 11).<sup>166,175–177</sup> In particular, the incorporation of ncAAs bearing ketones has been widely used to construct homogeneous ADCs with potent anti-tumour pharmacology. For example, Axup *et al.* have reported the development of a tyrosyl-derived tRNA/aaRS pair from *E. coli* capable of incorporating *p*-acetyl-phenylalanine (pAcF) into a peptide chain in response to the amber stop codon. This system was used to generate a variant of trastuzumab containing two pAcF residues through mutation of HC-A121 to pAcF.<sup>166</sup> Schultz and co-workers also used CHO cells to express pAcF-containing anti-CXCR4 antibodies with yields of expression in mammalian cells similar to those of wild-type proteins.<sup>178</sup> The mutant trastuzumab and anti-CXCR4 antibodies both underwent efficient and selective conjugation to auristatin payloads *via* oxime ligation to produce homogeneous ADCs with DARs ~ 2 (Fig. 11A). The resulting ADCs displayed both excellent pharmacokinetics and *in vitro* activity. *In vitro* assays showed the anti-CXCR4 ADC to be highly potent against CXCR4 expressing cancer cell lines with an EC<sub>50</sub> of 80–100 pM. Next, the *in vivo* efficacy of the ADC was evaluated in a mouse xenograft model, with the ADC displaying complete eradication of pulmonary tumour lesions with 3 doses of the ADC at 2.5 mg kg<sup>−1</sup>. Notably, further studies have also shown that ADCs generated through oxime-ligation at pAcF display improved circulatory half-life, efficacy and safety relative to analogous heterogeneous ADCs.<sup>168,179</sup>

Antibodies engineered to incorporate pAcF have also been used to selectively target immune cells through the CD11a antigen. Using an anti-CD11a antibody conjugated to a liver X receptor agonist, Lim *et al.* were able to target macrophages to reverse cholesterol transport and limit inflammation, whilst preventing undesirable lipogenic effects in hepatocytes.<sup>180</sup> To achieve this, pAcF was site-specifically incorporated into a single site on both heavy chains of an anti-CD11a antibody. Next, an aminoxy-functionalised Liver X receptor agonist was conjugated to the engineered antibody through an oxime linkage, affording the desired DAR 2 ADC. Yu *et al.* were also able to use an anti-CD11a antibody engineered to incorporate



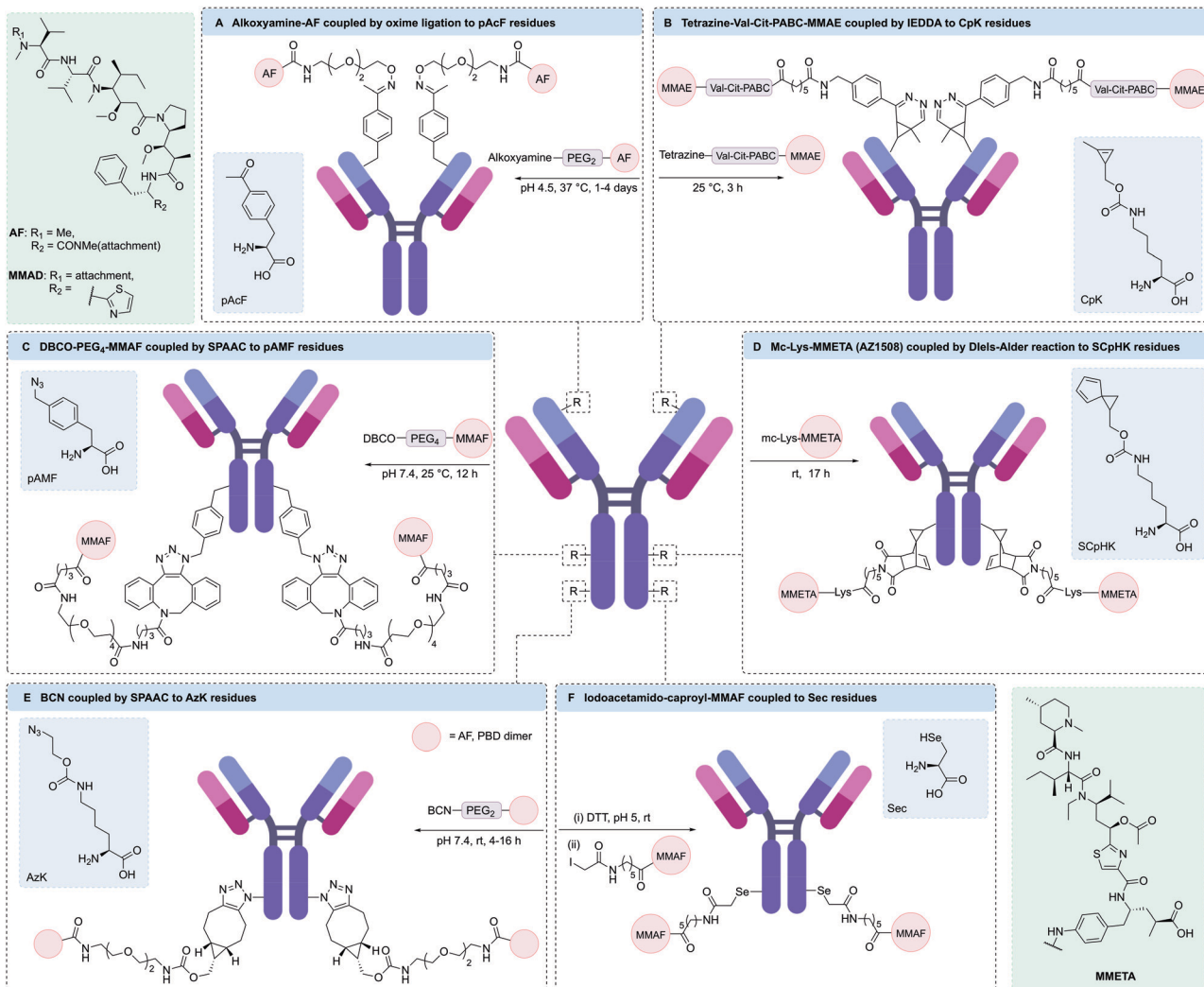


**Fig. 11** Unnatural amino acids and site-specific bioconjugation. (A) pAcF has a ketone side chain which can participate in oxime ligation reactions; (B) CpK has a cyclopropene side chain which can participate in IEDDA reactions; (C) pAMF has an azide side chain which can undergo click reactions; (D) SCpHK has a spiro[2.4]hepta-4,6-diene side chain which can participate in Diels–Alder reactions; (E) AzK has an azide side chain which can undergo click reactions; (F) Sec has a selenol side chain which can undergo reduction and subsequent nucleophilic substitution reactions.

pAcF in both heavy chains to selectively deliver a phosphodiesterase 4 inhibitor for the treatment of inflammatory conditions.<sup>181</sup> Modification of the engineered antibody with an analogue of GSK256066, a known phosphodiesterase 4 inhibitor, *via* an oxime linkage proceeded efficiently to give an ADC with a DAR of 2. The resulting ADC was shown to rapidly internalise into immune cells and suppress lipopolysaccharide-induced TNF $\alpha$  secretion in monocytes, as well as significantly reducing inflammatory cytokine production.

**2.4.5 Conjugation to ncAAs *via* azide-alkyne cyclo-additions.** Drawbacks to the use of pAcF for antibody modification include the acidic conditions required for oxime ligation ( $\text{pH} \sim 4.5$ ) and the slow reaction kinetics.<sup>166</sup> This has led to growing interest in azide-containing ncAAs, which can undergo rapid CuAAC or SPAAC reactions under physiological conditions.<sup>182,183</sup> One widely used azide-containing ncAA is *para*-azidophenylalanine (pAzF).<sup>21,22</sup> Indeed, Brandish *et al.*

engineered an amber codon to alter HC-A114 of an anti-CD74 human antibody to pAzF.<sup>184</sup> This enabled SPAAC modification with a glucocorticoid payload attached *via* a cyclooctyne-functionalised diphosphatase-cleavable linker, generating an ADC with a DAR  $\geq 1.7$ . An impermeable payload was chosen in order to increase the intracellular concentration, thus resulting in greater *in vitro* potency.

To aid the synthesis of more homogenous ADCs, Sato and co-workers have developed a novel platform for cell-free expression of ncAA-containing antibodies with faster reaction kinetics for conjugation *via* SPAAC.<sup>185</sup> This involved the engineering of an aaRS/RNA pair to enable incorporation of either pAzF or *para*-azidomethylphenylalanine (pAMF) into aglycosylated trastuzumab. It was hypothesised that pAMF would enable more rapid SPAAC conjugation compared to pAzF, due to the azido group being further from the electron withdrawing phenyl ring, hence generating ADCs with more precise drug-loading.



A number of pAMF containing antibodies have since been produced *via* this CFPS expression system, with the resulting engineered antibodies being successfully conjugated to dibenzyl-cyclooctyne (DBCO)-MMAF, DBCO-maytansinoid or DBCO-Val-Cit-hemiasterlin payloads to give highly potent ADCs (Fig. 11C).<sup>174,185–187</sup> Ahn *et al.* were also able to use this technology to introduce two DBCO-functionalised bifunctional chelators to trastuzumab, thus enabling the incorporation of radioisotopes for positron emission tomography.<sup>188</sup> A modified CFPS system enabled incorporation of 2, 4, 6, or 8 pAMF residues into an anti-HER2 antibody, which could then undergo conjugation to DBCO-maytansine to yield ADCs with DAR values of 1.77, 3.83, 5.82 and 7.43, respectively.<sup>174</sup> These ADCs were tested against several HER2-expressing cell-lines (SKBR3, BT474, MDA-MB-453, and JIMT1), showing a general trend of higher potency with increasing DAR.

In addition to alanine-based ncAAs, several lysine analogues, such as AzK, have also been site-specifically incorporated into antibodies. For example, Zhou and co-workers used AzK-containing rituximab to generate a dodecane tetraacetic acid-rituximab conjugate *via* SPAAC.<sup>189</sup> Subsequent radiolabelling of the chelate-modified antibodies with <sup>64</sup>Cu resulted in a homogeneous radioconjugate with two chelates per antibody. Marelli and co-workers were also able to express AzK in antibodies, enabling the subsequent generation of ADCs with AF, PBD dimer, or tubulysin payloads (Fig. 11E).<sup>167,175</sup> In one example, an anti-HER2 antibody expressing AzK on each heavy chain was conjugated to DBCO-tubulysin to give an ADC with a DAR  $\sim$  2. *In vitro* assays demonstrated the potent and selective cytotoxicity of the resulting ADC.<sup>167</sup>

#### 2.4.6 Conjugation to ncAAs *via* Diels–Alder cycloadditions.

As an alternative to ketone- and azide-containing ncAAs, Koehler *et al.* have reported the incorporation of several highly reactive ncAAs based on propargyl-lysine (PrK), *trans*-cyclooctene-lysine (TCOK), cyclooctyne-lysine (SCOK) and BCN-lysine (BCNK) into antibodies. These reactive handles were then used to site-selectively label antibodies with imaging agents or glycans. Unfortunately, this expression system resulted in relatively low yields (0.5 mg L<sup>-1</sup>) and the modified antibodies were highly prone to aggregation due to the use of larger and more hydrophobic amino acids.<sup>190</sup> To avoid these issues, Chin and co-workers have reported the incorporation of a cyclopropene derivative of lysine (CypK) into trastuzumab *via* GCE.<sup>176</sup> This engineered antibody could then undergo a rapid and efficient inverse-electron demand Diels–Alder (IEDDA) reaction with tetrazine-Val-Cit-PABC-MMAE to give ADCs with a defined DAR of 2 (Fig. 11B). Similarly, Christie and co-workers developed cyclopentadiene-containing ncAAs, spiro[2.4]hepta-4,6-diene-lysine (SCpHK) and cyclopentadiene-lysine (CpHK), that underwent irreversible Diels–Alder cycloadditions with maleimide-modified drugs.<sup>177</sup> Conjugation of SCpHK-antibodies with several maleimide payloads including Val-Cit-PABC-MMAE, AZ1508 (a tubulysin), or SG3249 (a PBD dimer) produced ADCs with DARs of 2 that were shown to be potent both *in vitro* and *in vivo* (Fig. 11D). However, the successful generation of ADCs incorporating CpHK proved more challenging; introducing CpHK

at HC-K274 resulted in successful reaction with maleimide-functionalised AZ1508, whereas introduction of CpHK at HC-S239 resulted in dimerization of the heavy chains.<sup>191</sup> Following on from this work, Marelli and co-workers successfully used both SCpHK and CpHK antibodies to generate ADCs through conjugation to maleimide-bearing tubulysin payloads.<sup>167</sup>

**2.4.7 Selenomabs.** Over the past two decades GCE strategies have also been applied for the incorporation of the naturally occurring atypical amino acid selenocysteine (Sec) into monoclonal antibodies, resulting in engineered antibodies known as selenomabs. Since the selenol group ( $pK_a \sim 5$ ) is more acidic than the thiol group of cysteine ( $pK_a \sim 8$ ), Sec is deprotonated at lower pH, thus exhibiting more rapid, efficient and site-selective reactions under near physiological conditions.<sup>192,193</sup> These reactions can occur in the presence of other reactive amino acids without the need for catalysis, or the reoxidation of the disulfide bridges required for engineered cysteine conjugation.

In eukaryotes, Sec is incorporated into polypeptides in response to the UGA stop codon when a Sec incorporation sequence (SECIS) is present in the 3' untranslated region of the mRNA.<sup>193,194</sup> First-generation selenomabs were engineered to incorporate one or two C-terminal Sec residues by inserting the UGA codon and SECIS at the 3' end of its encoding gene.<sup>193,195</sup> The resulting recombinant antibodies were shown to fully retain their antigen binding capabilities. However, competition between Sec incorporation and termination at the UGA codon, led to low Sec incorporation efficiency.<sup>195</sup> Indeed, inefficient Sec incorporation *via* the UGA stop codon and SECIS element remains a challenge that requires further optimisation.

Rader and co-workers have exploited the high reactivity of Sec under mildly acidic conditions for selective modification of a trastuzumab-based selenomab *via* reaction with iodoacetamide-modified MMAF.<sup>196</sup> Initial studies positioned the Sec residue at the C-terminus of the antibody. However, competition between Sec insertion and termination at the UGA codon resulted in a mixture of IgG-stop and IgG-Sec-MMAF proteins, thus yielding a selenomab-drug conjugate with an average DAR of 0.6. Alternatively, by positioning Sec residues in the CH3 domains of trastuzumab at HC-396 the incorporation of two Sec residues was achieved. In addition, higher conjugation efficiency of the resulting selenomab with iodoacetamide-modified MMAF was observed due to the higher solvent accessibility of the Sec residues (Fig. 11F). Indeed, a DAR 2 iodoacetamide-based selenomab-drug conjugate was produced, which showed excellent stability, selectivity, and potency in both *in vitro* and *in vivo* mouse models.

**2.4.8 Dual functionality.** The incorporation of ncAAs for ADC generation has largely been limited to insertion of a single type of ncAA in a full-length antibody. However, the ability to efficiently incorporate two or more different ncAAs into an antibody would allow for the synthesis of more complex conjugates. To achieve this dual functionalisation, distinct aaRS/tRNA pairs are required, which each suppress a different nonsense codon and do not cross-react with each other or host



aaRS/tRNA pairs.<sup>197</sup> To date, up to three different ncAAs have been incorporated into a single polypeptide chain using multiple orthogonal aaRS/tRNA pairs.<sup>198</sup> However, there is only one example of multiple ncAAs being used for the synthesis of a dual-functional ADC (Fig. 12A). Schultz and co-workers used the UAA-suppressing PylRS/MmttRNA<sub>UUA</sub><sup>Pyl</sup> pair alongside the UAG-suppressing TyrRS/tRNA<sub>CUA</sub><sup>Tyr</sup> pair to simultaneously and site-specifically incorporate two orthogonally reactive ncAAs (pAcF and AzK) into a single antibody.<sup>199</sup> The resulting antibody, anti-HER2-IgG-pAcF/AzK, contained a pAcF residue on each heavy chain and a AzK residue on each light chain. Selective modification of the pAcF residues was then achieved through reaction with an alkoxy-amine-derivatized AF drug-linker to form an oxime linkage, which was followed by modification of the AzK residues *via* a SPAAC reaction with AlexaFluor 488-dibenzocyclooctyne (DIBO). This gave the desired dual labelled antibody, HER2-IgG-AF/AF488, in greater than 90% conjugation yield. The ADC demonstrated utility as both a therapeutic and imaging/diagnostic agent.

More recently, thio-selenomabs have also facilitated the generation of dual functional antibodies through genetic incorporation of an ncAA.<sup>200,201</sup> These antibodies contain both engineered Sec and cysteine residues, enabling bioorthogonal conjugation of two distinct payloads. Indeed, this dual conjugation method was used by Nilchan *et al.* to generate an anti-HER2 ADC that combined both the tubulin-targeting payload MMAF and the DNA-damaging payload PNU-159682 (Fig. 12B).<sup>200</sup> This required engineering of trastuzumab to contain Sec (HC-S396) and additional cysteine residues (HC-A114C) in both heavy chains. Subsequent site-selective dual modification was achieved *via* reaction of Sec with iodoacetamide-functionalised PNU-159682, followed by reaction of cysteine residues with methylsulfone phenyloxadiazole-MMAF to produce a serum stable bioconjugate. Treatment of human breast cancer cells with the resulting ADC suggested distinct mechanisms of action for each payload upon analysis of cell cycle arrest. However, the ADC combining PNU-159682 and MMAF did not demonstrate improved potency compared to an ADC functionalised with PNU-159682 alone.

**2.4.9 ncAA-containing ADCs in clinical trials.** The success of GCE as an approach to the generation of ADCs is evident, as several ADCs generated in this way have entered clinical trials. For instance, AmbrX have developed the mammalian expression system EuCODE to allow manufacturing of ncAA containing antibodies in CHO cells with titers over  $1\text{ g L}^{-1}$ . Using this strategy, two ADCs, ARX788 and AGS62P1, which are composed of auristatin payloads conjugated to pAF-containing antibodies *via* oxime ligation, have been developed and are now in Phase I clinical trials (ClinicalTrials.gov Identifiers: NCT03255070 and NCT02864290, respectively).<sup>202,203</sup> ARX788 is a DAR 1.9 ADC comprising an anti-HER2 monoclonal antibody site-specifically conjugated to the potent microtubule inhibitor MMAF *via* a non-cleavable PEG linker.<sup>202</sup> In preclinical models, ARX788 displayed improved efficacy and safety profiles compared to current marketed HER2-targeting ADC Kadcyla®, which has led to ARX788 being evaluated in Phase I trials for the treatment HER2-positive breast or gastric cancer. AGS62P1 is an ADC composed of an anti-FLT3 antibody conjugated to an auristatin-based payload, AGD-0182, which is an analogue of dolastatin 10.<sup>203</sup> Preclinical studies have shown AGS62P1 is well-tolerated and displays potent *in vitro* cytotoxic activity ( $\text{IC}_{50} = 0.2\text{--}12\text{ nM}$ ) in AML cell lines, which prompted progression to on-going Phase I trials for AML.<sup>204</sup>

Two further ADCs currently in Phase I clinical trials, STRO-001 and STRO-002, have been developed by Sutro.<sup>186,187</sup> These ADCs were generated using a cell-free platform, XpressCF+™, which has an engineered RF1 mutant to facilitate efficient incorporation of pAMF at positions designated by a UGA codon.<sup>174</sup> In STRO-001, pAMF was incorporated into each heavy chain of an anti-CD74 antibody by replacing the codon corresponding to HC-F404 with an amber codon.<sup>187</sup> Subsequent SPAAC between each pAMF and a DBCO-functionalised maytansinoid payload conjugated *via* a non-cleavable linker gave STRO-001; an ADC with a DAR of 2. Preliminary trial data has shown that STRO-001 is generally well tolerated and has encouraging anti-tumour activity in a group of patients with pre-treated diffuse large B-cell lymphoma (ClinicalTrials.gov Identifier: NCT03424603).<sup>169</sup> In contrast, STRO-002 is a DAR 4

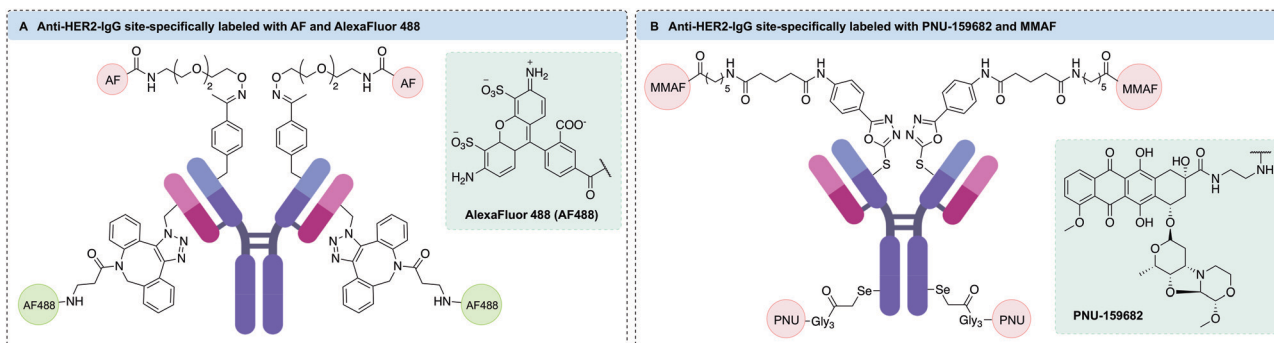


Fig. 12 Dual functional ADCs generated *via* GCE. (A) Microtubulin inhibitor AF and fluorescent dye AlexaFluor 488 were conjugated to a HER2-targeting antibody *via* site-specific conjugation at the engineered pAcF and AzK residues, respectively; (B) DNA crosslinking agent PNU-159682 and tubulin polymerisation inhibitor MMAF were conjugated to a HER2-targeting thio-selenomab *via* site-specific conjugation at the engineered Sec and Cys residues, respectively.



ADC composed of an anti-folate receptor alpha human IgG1 antibody conjugated to a cleavable drug-linker (SC239) containing the tubulin-targeting 3-aminophenyl hemiasterlin payload SC209.<sup>186</sup> To generate this ADC, four pAMF residues were incorporated into the antibody at two defined sites on each heavy chain. These sites were then conjugated to SC239 *via* a cleavable Val-Cit-PABC linker functionalised with DBCO. Studies in patients with solid tumours have shown that this ADC is also well-tolerated, with mostly mild adverse effects, and the clinical benefits are promising (ClinicalTrials.gov Identifier: NCT03748186).<sup>170</sup> Indeed, based on a trial of 20 ovarian cancer patients STRO-002 dose levels of 2.9 mg kg<sup>-1</sup> or higher led to one partial response and 14 patients with stable disease in initial post-baseline scans. Furthermore, 13 patients had a  $\geq 50\%$  reduction or normalisation of cancer biomarkers.

In addition to these aforementioned ADCs in clinical trials, several more ADCs containing ncAAs are also progressing towards Phase I trials. Whilst production challenges still exist, recent efforts have successfully increased both protein expression and reaction kinetics. Thus, the applicability of this approach for the generation of clinically useful ADCs is rapidly increasing.

## 2.5 C/N-terminal modifications

Modification of either the N- or C-terminus of an antibody has proven to be a viable strategy for generating homogeneous ADCs. Antibody modification at these positions enables simple and site-specific introduction of bioorthogonal motifs or affinity tags that facilitate further functionalisation. Importantly, the C-terminal positions are generally distal from critical antigen binding regions, which typically leads to complete retention of antibody binding specificity upon modification. Accordingly, C-terminal modifications have broad applicability across antibodies and the wider protein modification field. N-Terminal modifications have also been prolifically used for site-specific protein conjugation.<sup>205</sup> However, this approach is more challenging to apply to antibodies due to the close proximity to the vital receptor binding region. Hence, modifications at the N-terminus must be carefully monitored to ensure that conjugation does not hinder antigen binding affinity. The terminal  $\alpha$ -amine group has a  $pK_a$  of 6–8, making it more nucleophilic than lysine residues under milder conditions.<sup>205</sup> Hence, this terminal position can be selectively targeted in the presence of other aliphatic amines at low or neutral pH. Furthermore, the microenvironment at the terminal positions often differs to that of other regions within the protein structure, a factor that has been harnessed to enhance selectivity for conjugation.

Bioorthogonal functionalities suitable for site-selective conjugation can be introduced to the terminal positions of an antibody using synthetic strategies. For example, several chemical methods detail the introduction of reactive aldehyde handles onto the antibody termini, which can be further modified to enable the generation of homogeneous ADCs.

N-Terminal transamination is one strategy used to synthesise ADCs in a site-selective manner *via* conversion of the amino

N-terminus to an aldehyde functional group. N-Methyl-pyridinium-4-carboxaldehyde benzenesulfonate salt (Rapoport's salt) was found to transaminate glutamate-terminal proteins,<sup>206</sup> installing an aldehyde or ketone functional handle suitable for conjugation through oxime or hydrazone linkages (Fig. 13A). Trastuzumab was used to examine the efficiency of this conjugation approach in an antibody context. Initially, unaltered trastuzumab containing an EVQ motif at the heavy chain N-terminus was treated with Rapoport's salt, yielding 67% of the conjugation product. No modification of the light chain terminal, which contained a DIQ sequence, was observed. Next, modified antibody constructs were prepared whereby the N-termini of both the heavy and light chains were modified to append an EES peptide motif, which was discovered to have enhanced and more selective reactivity with Rapoport's salt. Conjugation of this modified antibody *via* oxime ligation gave 56% and 68% yield on the light and heavy chains, respectively. Using this technique, AlexaFluor 488 antibody conjugates were prepared and analysis demonstrated that N-terminal modification did not hinder antigen binding, validating this approach for ADC preparation.

The aldehyde moiety has also been exploited for the modification of cysteine residues appended to antibody N-termini (Fig. 13A).<sup>207</sup> This technique generated a homogeneous thiazolidine linked ADC through reaction of the 1,2-aminothiol functionality found on the anti-fibronectin F8 antibody N-terminus cysteine residues with an aldehyde-containing drug. The drug used in this proof-of-concept study was cemadotin, an analogue of dolastatin-15. The aldehyde-containing derivative was found to have comparable cytotoxicity to the parent compound, validating its use in ADC development. The resultant ADC enabled slow *in vitro* release of the toxic payload through hydrolytic cleavage of the thiazolidine linkage. The antibody specifically targets cancer cells and upon internalisation, releases the free aldehyde-containing drug in a traceless fashion. An interesting application of this technology is in the masking of aldehyde functional groups present in drugs. Aldehyde functionalities generally suffer from oxidation, potential for epimerisation or reactivity with various biomolecules; therefore, antibody conjugation is a useful strategy to mitigate their off-target effects.

Another important strategy for homogeneous ADC generation involves the selective oxidation of a serine residue genetically appended to the antibody N-terminus (Fig. 13A). Such a serine-containing antibody can then undergo sodium periodate-mediated oxidation, generating an aldehyde handle. The aldehyde can subsequently react with alkoxyamine functionalised payloads under mild conditions to form oxime linked conjugates. This technology was reported by both ImmunoGen and MedImmune in 2015. ImmunoGen designated this serine modification strategy as SeriMabs and following the serine oxidation, condensed the resulting aldehyde with a dithiopyridine-containing heterobifunctional linker, generating a stable oxime bond.<sup>208</sup> The dithiopyridine groups could then be reacted with thiol-containing payloads, forming a disulfide linked DAR 2 ADC in  $>90\%$  yield. As such, the SeriMab technology was utilised to conjugate a mono-imine



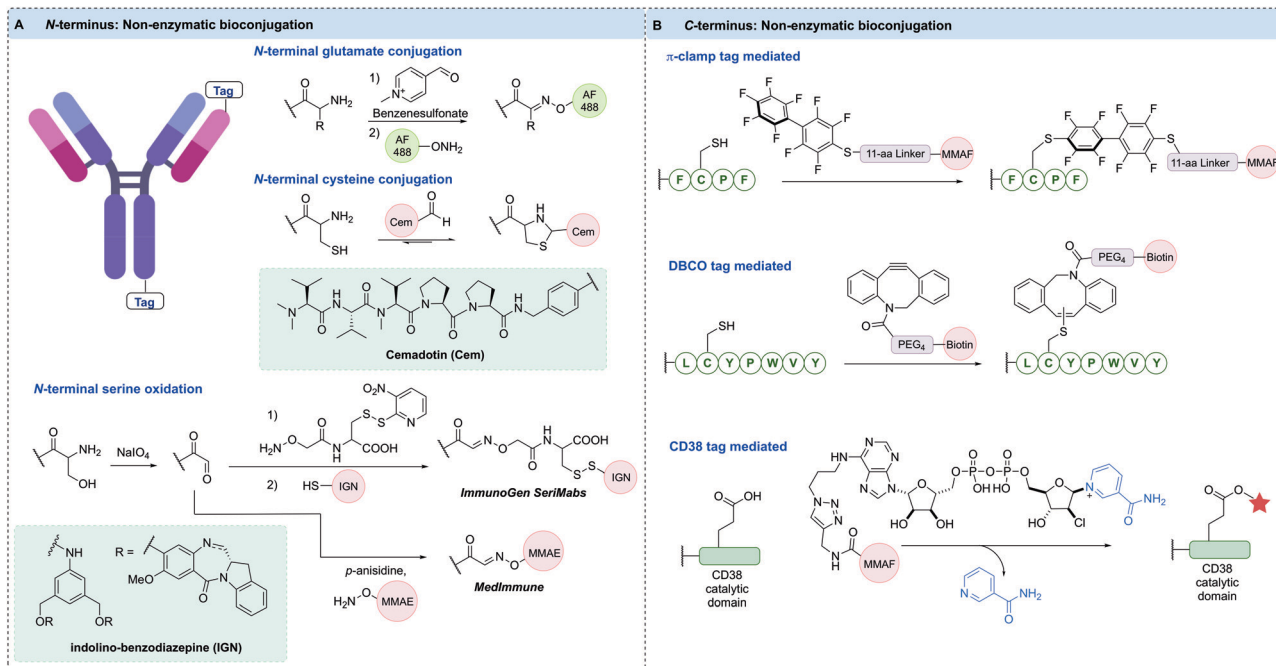


**Fig. 13** Non-enzymatic bioconjugation methods used to construct homogeneous ADCs at the: (A) N-terminal position, where terminal glutamate and cysteine residues can be selectively modified with aldehyde functionalised payloads, and Ser residues introduced can be oxidised to aldehydes, which can be trapped using alkoxyamine functionalised payloads to form oxime linked conjugates; (B)  $\pi$ -clamp peptide sequence selectively reacts with perfluoroaromatic probe, DBCO tagged antibody selectively reacts with DBCO reagents via the thiol–yne reaction, CD38 tag reacts with covalent inhibitor-tagged payload, forming a stable arabinosyl ester.

containing indolino-benzodiazepine (IGN) DNA-alkylating payload connected to the N-terminal aldehyde *via* oxime ligation.<sup>209</sup> The generated ADC exhibited comparable antigen binding affinity to the unconjugated antibody, and was highly potent *in vitro* and *in vivo*. Importantly, the oxime linkage was determined to be stable *in vivo* for 3 days, with an approximate payload release  $t_{1/2}$  of  $>10$  days. An MMAE-conjugated ADC with a DAR of 2 was also prepared by MedImmune using the same serine oxidation strategy applied to an anti-EphA2 antibody.<sup>210</sup> This ADC exhibited good hydrolytic and serum stability and had high potency *in vitro* against PC-3 cell lines whilst also displaying good *in vivo* efficacy. Additionally, a DAR 4 ADC was generated by modifying terminal serine residues on both the light and heavy chains.

Site-specific bioconjugation can also be achieved by modifying the microenvironment of an amino acid, which can activate a specific amino acid residue in the presence of other reactive species (Fig. 13B). One recent example of this approach installed a so-called  $\pi$ -clamp peptide sequence (FCPF) to direct site-selective modification of the peptide cysteine with perfluoroaromatic reagents in the presence of competing cysteine residues.<sup>211</sup> The  $\pi$ -clamp sequence was initially appended to the C-termini of trastuzumab heavy chains. Selective cysteine conjugation was achieved by introducing an MMAF-conjugated perfluoroaromatic probe, which rapidly reacted with the  $\pi$ -clamp cysteine residue *via* a  $S_NAr$  reaction under mild, reducing conditions. Notably, none of the native interchain cysteines displayed any reactivity with this reagent under reducing conditions. The resultant ADC retained HER2 affinity and exhibited high *in vitro*

potency and selectivity. The conjugation technology was also applied to the selective modification of a C225 antibody appended with the  $\pi$ -clamp, indicating the generality of this strategy.

A further example of microenvironment modification harnessed the thiol–yne reaction to achieve rapid and site-selective conjugation of DBCO reagents to a seven-residue peptide tag (LCYPWVY) introduced at the protein C-terminus (Fig. 13B).<sup>212</sup> The cysteine-containing peptide sequence (DBCO-tag) acts as an affinity tag to enable highly regioselective cysteine modification. A DBCO-tagged antibody was generated by genetically fusing the DBCO-tag to the heavy chain C-terminus of trastuzumab. The modified antibody was then treated with biotin-conjugated DBCO under reducing conditions, generating 90% mono-labelled antibody, and importantly, leaving the eight native cysteines intact. The antigen binding affinity of the resultant antibody was unaffected, and the thiol enol ether linkage was highly stable to glutathione under physiological conditions for over four days. This method is highly versatile due to the multitude of commercially available DBCO reagents, which may enable rapid and efficient synthesis of ADCs.

CD38 is an adenosine diphosphate (ADP)-ribosyl cyclase that catalyses the production of ADP-ribose and cyclic ADP-ribose from nicotinamide adenine dinucleotide ( $NAD^+$ ). Covalent inhibitors of CD38 have been developed that react with catalytic E226 to form a stable arabinosyl ester. Dai *et al.* exploited these developments *via* fusion of the catalytic domain of CD38 to the heavy chain C-terminus or light chain N-terminus of trastuzumab.<sup>213</sup> Subsequent reaction of the fusion antibody



with an MMAF-modified covalent inhibitor of CD38 generated a pair of DAR 2 ADCs, as evidenced by MS (Fig. 13B). The ADCs retained antigen affinity and selectivity, demonstrated high stability in mouse plasma, and were highly potent *in vitro* and *in vivo*.

Several different chemical methods for termini modification have been utilised for antibody modification. Importantly, modification at either the N- or C-termini of both heavy and light chains appears possible without detriment to antibody binding of target receptors or Fc receptors.

## 2.6 Other chemical methods

**2.6.1 Regioselective lysine modification.** While stochastic lysine modification has proved successful in producing many of the early generation of approved ADCs, the heterogeneity of the products has invariably led to sub-optimal pharmacological activity of many other investigated ADCs (*vide supra*). Recently, significant effort has been dedicated to developing methods that facilitate regioselective modification of antibody lysines. For example, Matos *et al.* have reported the exploitation of lysine microenvironment to controllably modify the most nucleophilic (lowest  $pK_a$ ) lysine residue in a protein with sulfonyl acrylate reagents (Fig. 14A).<sup>214</sup> This approach was used to modify trastuzumab with the kinase inhibitor crizotinib, generating a homogeneous DAR 2 ADC *via* selective modification of a single lysine residue on each light chain (LC-K207). Modification with the sulfonyl acrylate was highly efficient (>95% conversion) with near stoichiometric quantities of reagent required. In another example, Chilamari *et al.* also modified a single lysine residue in trastuzumab light chains *via* a phospha-Mannich reaction whereby the lysine amine first underwent imine formation with an aldehyde reagent, followed by attack of the imine with a triethylphosphite reagent (Fig. 14A). Using this approach, a doxorubicin ADC with a DAR of 0.92 was generated. The conjugation site was found to be located in the light chain and although the precise amino acid was not identified, studies on isolated trastuzumab Fab fragment indicated that K183 was the sole modification site.<sup>215</sup>

A unique approach to selective antibody modification has involved the introduction of the variable domain from the aldolase antibody 38C2 (or h38C2 for the human variant) into the antibody scaffold to generate a dual variable domain (DVD) antibody. The variable domain of 38C2 contains a catalytic lysine with low  $pK_a$  (~6) in its enzyme active site. In one use of this DVD format, Rader and co-workers generated a DVD based on trastuzumab and the variable domain of h38C2, which was site-selectively modified *via* reaction with 1,3-diketone reagents or a  $\beta$ -lactam derivative of MMAF in >95% conversion (Fig. 14A).<sup>216–218</sup> This anti-HER2 DAR 2 ADC demonstrated exquisite *in vitro* and *in vivo* activity and selectivity. Based on these results, anti-CD138 and anti-CD79b ADCs were also generated from DVD antibodies. Although these antibodies are ~50 kDa larger than typical IgGs, the authors noted that they retain similar pharmacokinetic properties. The reactive lysine in the catalytic pocket was also amenable to selective modification with methylsulfone phenyloxadiazole (MS-PODA) modified payloads (Fig. 14A).<sup>219,220</sup>

Mortensen *et al.* exploited the metal-binding ability of proteins to site-selectively modify lysine residues in a range of therapeutic antibodies.<sup>221,222</sup> Treatment of the antibody with a metal ( $\text{CuSO}_4$ ) and a small molecule metal coordination ligand, which was further functionalised with an aldehyde enabled modification of specific lysines in the vicinity of the metal binding site *via* reductive amination of the aldehyde (Fig. 14A). Incorporation of an azide in the metal chelator enabled further modification *via* SPAAC with a DBCO-Cy5 payload. Removal of the  $\text{Cu}^{2+}$  was also achieved by treatment with EDTA. This strategy was used to modify trastuzumab, rituximab and cetuximab with modification of trastuzumab shown to occur primarily at LC-K190 and HC-K136.

**2.6.2 Site-selective histidine modification.** Selective histidine modification poses a challenge due to competition from other more nucleophilic residues such as lysine or cysteine. In 2018, Adusumalli *et al.* reported the development of a “chemical linchpin” to enable selective histidine modification. This linchpin was a bifunctional reagent containing both aldehyde and epoxide reactive groups. First, all available lysine residues were transiently protected *via* reaction with the aldehyde moiety. Next, proximal histidine residues reacted with the pendant epoxide to afford irreversible modification. Finally, reformation of the aldehyde enabled modification of this installed bioorthogonal handle *via* oxime formation. Using this method, trastuzumab was selectively modified with doxorubicin or DM1 payloads to generate DAR 4 ADCs which demonstrated *in vitro* cytotoxicity (Fig. 14E).<sup>223</sup> A similar linchpin strategy has recently been described by Adusumalli *et al.* for site-specific lysine modification of trastuzumab (Fig. 14A).<sup>224</sup>

**2.6.3 Selective arginine modification.** The lower abundance of arginine residues in native antibodies compared to lysine residues makes arginine-selective modification attractive for the preparation of homogeneous conjugates. With this in mind, Dovgan *et al.* reported the modification of trastuzumab arginine residues *via* condensation of its guanidine side chain with a 4-azidophenyl glyoxal (APG) reagent (Fig. 14C).<sup>225</sup> This reaction enabled direct introduction of a bioorthogonal azido group onto trastuzumab, which was subsequently modified *via* SPAAC reaction to conjugate various payloads. The produced antibody conjugates maintained antigen selectivity and demonstrated high stability in human plasma. Modification of genetically inserted arginine residues in a DVD of h38C2 has also been achieved *via* reaction with a phenylglyoxal derivatised payload.<sup>226</sup> This method also enabled dual lysine and arginine modification by introducing one h38C2 variable domain containing a reaction lysine and one h38C2 variable domain containing a reactive arginine into an antibody. Selective modification was then achieved *via* treatment with  $\beta$ -lactam-modified MMAF and a phenylglyoxal-modified rhodamine dye (TAMRA) (Fig. 14B).

**2.6.4 Simultaneous conjugation of neighbouring lysine and aspartic acid/glutamic acid.** Sornay *et al.* have recently reported the simultaneous conjugation of neighbouring amino acids, lysine and aspartic acid/glutamic acid *via* a four-component Ugi reaction (Fig. 14D).<sup>227</sup> The Ugi reaction was



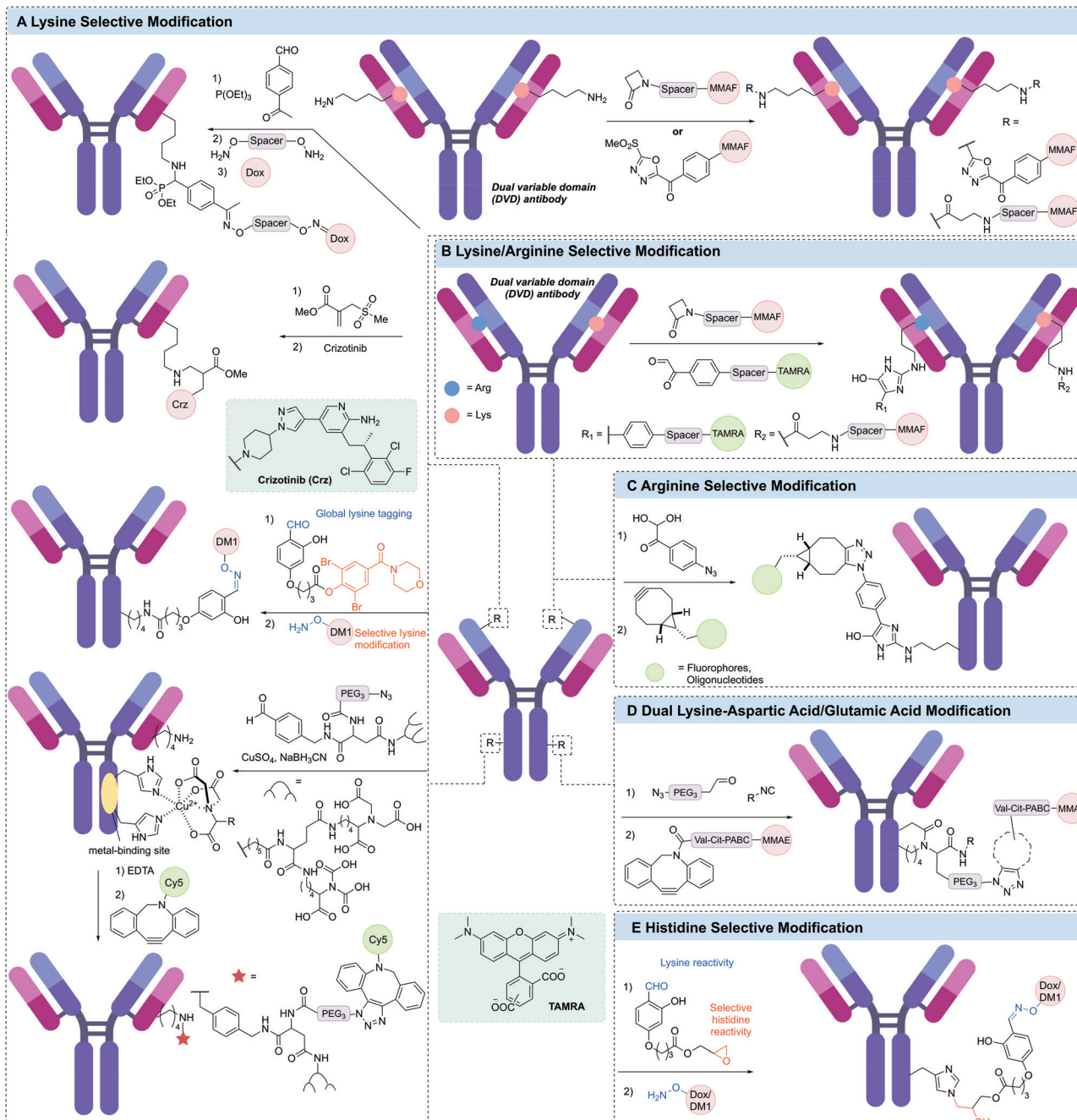


**Fig. 14** Other residue-selective modification for generating ADCs. (A) Lysine selective modification via a phospha-Mannich reaction (left top), using sulfonyl acrylate reagents (left second), using linchpin directed modification reagent (left third), of catalytic lysine in variable domain using  $\beta$ -lactam derivative and methylsulfone phenyloxadiazole (MS-PODA) derivative (right top), and using metal-binding site-directed modification (bottom left); (B) lysine/arginine selective modification using  $\beta$ -lactam and phenylglyoxal derivatives; (C) arginine selective modification using 4-azidophenyl glyoxal (APG) reagent; (D) dual lysine-aspartic acid/glutamic acid modification using aldehyde and isocyanide-modified compounds; (E) histidine selective modification using linchpin directed modification.

used to conjugate the side-chain amine and carboxylate groups of two neighbouring lysine and aspartic acid/glutamic acid residues *via* reaction with an aldehyde and isocyanide-modified payload. It was reasoned that the requirement for two amino acids to be sufficiently spatially close to undergo reaction would increase the site-selectivity of the reaction. Indeed, it was found that the simultaneous modification

occurred primarily between LC-K126 and LC-D122/E123. However, single site Passerini reaction also competed with this process at several glutamic acid/aspartic acid residues. Nonetheless, a DAR 1.4 MMAE ADC demonstrated better *in vitro* potency than the approved T-DM1.

**2.6.5 Affinity peptide labelling.** Protein A or G are widely used in the purification or enrichment of antibodies from



complex media. A promising strategy for site-specific native antibody conjugation has emerged, involving the use of small protein domains or peptides that non-covalently bind to a conserved sequence in the antibody Fc domain with high affinity. These small proteins or peptides are often truncated versions of the IgG-binding domain of protein A/G or are developed from high throughput phage display libraries. Incorporation of a reactive moiety on the peptide can then facilitate covalent modification of the antibody in this region. Several examples of this approach have been reported, with the key advantages being that genetic engineering or glycan remodelling are not required, and that the same affinity peptide can be used to form bioconjugates with virtually all immunoglobulin of the same isotype.

Among the numerous Fc-binding domains (FcBDs), the ZZ-domain, a modified dimer of the IgG binding site of protein A from *Staphylococcus aureus*,<sup>228</sup> is widely used. Mazor *et al.* generated an IgG-binding peptide-toxin fusion, ZZ-PE38 by genetically fusing the ZZ-domain to a truncated *Pseudomonas* exotoxin A (PE38).<sup>229</sup> This strategy was used to generate non-covalent antibody-toxin conjugates targeting HER2, CD24 and

EGFR, with each demonstrating efficient tumour regression *in vivo*.<sup>230–232</sup>

Instead of the FcBD protein, Park *et al.* have reported a peptide-directed photo-crosslinking (PEDIP) approach to covalently modify the Fc region of an antibody.<sup>233</sup> A 13 residue peptide (called Fc-III) was identified as binding the Fc region of IgG antibodies. Incorporation of *para*-benzoyl-phenylalanine (BPA) into the Fc-III peptide enabled covalent modification of HC-M252 in trastuzumab upon irradiation with ultraviolet light (Fig. 15A). Further modification of Fc-III with another truncated analogue of *Pseudomonas* exotoxin A (PE24) enabled generation of a trastuzumab-PE24 conjugate with 1 toxin per antibody. Similarly, Vance *et al.* utilised the same BPA-containing Fc-III peptide to install a protected thiol site-selectively on trastuzumab. Subsequent thiol deprotection enabled further modification with maleimide-Val-Cit-PABC-MMAE to generate a DAR 1.9 ADC. The authors also demonstrated the high stability of the conjugate in human plasma and potent *in vitro* cytotoxicity.<sup>234</sup>

Kishimoto *et al.* have reported the use of an Fc-directed peptide (17 residues, similar to Fc-III) with an appended NHS

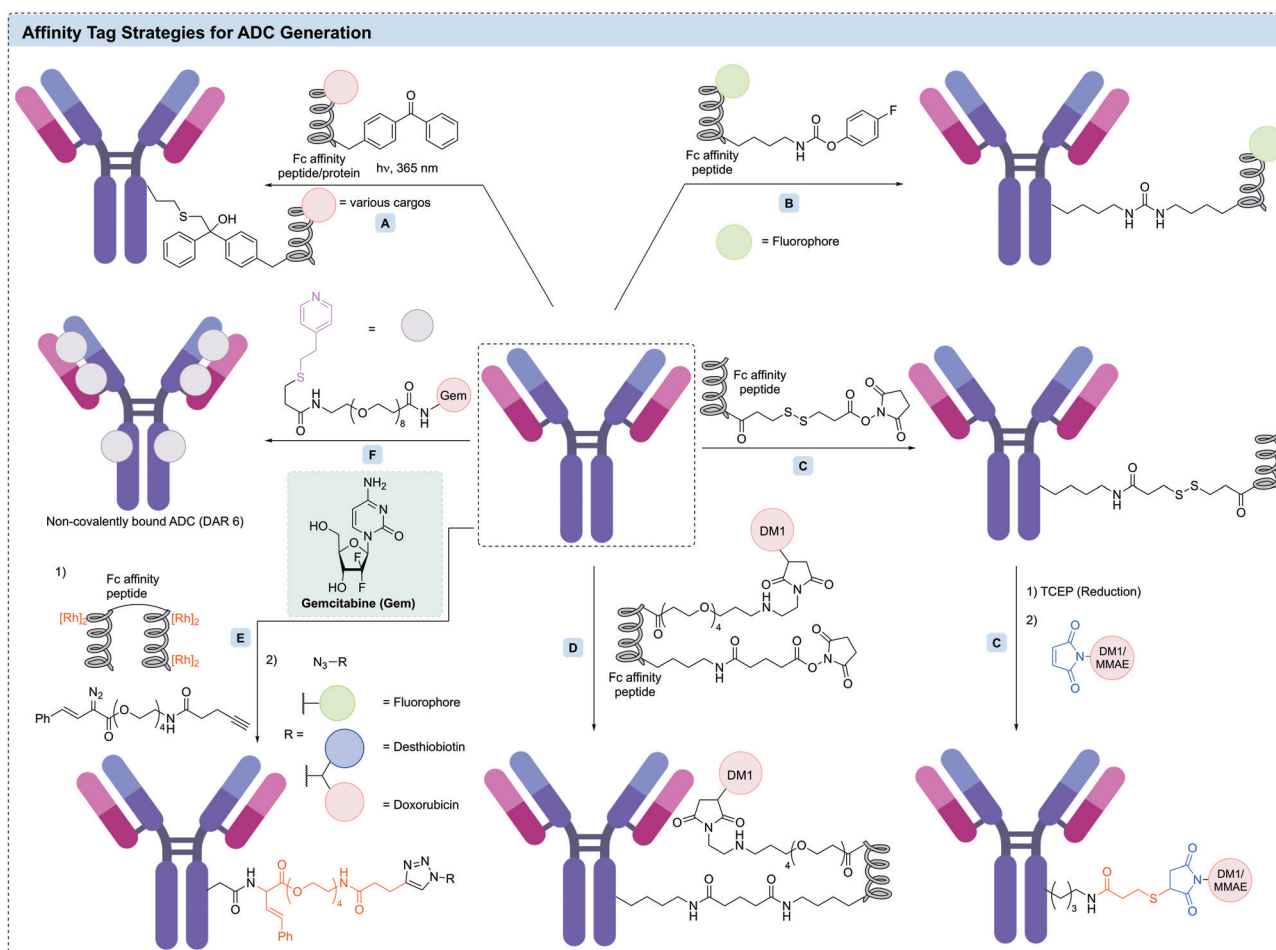


**Fig. 15** Affinity tag strategy for ADC generation. (A) Photoaffinity labeling strategy using Fc affinity peptide/protein; (B) affinity peptide in combination with the activated ester method to modify lysine residues; (C) traceless affinity peptide labeling using the cleavable linker in combination with activated ester method (AJCP); (D) the use of an Fc-affinity peptide with an appended *N*-hydroxysuccinimide ester (NHS); (E) traceless affinity peptide labeling using the metallopeptide method; (F) self-assembling strategy via interaction of the antibody with a mercaptoethylpyridine (MEP) derivative.

ester to enable selective modification of Fc lysines (Fig. 15D).<sup>235</sup> This conjugation reaction completed within 15 minutes under mild conditions and produced the desired conjugate in high yield. This method enabled site-specific modification of HC-K248 in the Fc region of trastuzumab. In one example, further functionalisation of the affinity peptide with DM1 yielded ADCs with a DAR of 1 or 2. The DAR 1 trastuzumab-peptide conjugate maintained its affinity for Fc receptors (FcRn, Fc $\gamma$ RI, and Fc $\gamma$ RIIIa); however, this affinity was completely lost in the DAR 2 ADC. It was hypothesised that this loss of FcRn binding was caused by overlap between the binding site of the Fc-III-derived peptide and FcRn.

Yu *et al.* have described the use of the B domain of protein A to direct site-selective modification of an Fc lysine in trastuzumab.<sup>236</sup> A library of modified B domains containing ncAAs with lysine-reactive side chains (*e.g.* acrylamide, isothiocyanate or carbamate) were reacted with trastuzumab. The carbamate-containing peptide was shown to cross-link efficiently with the antibody heavy chain K337, forming a stable urea linkage (Fig. 15B). This approach was used to obtain a fluorescein-labelled antibody with a fluorophore loading of 2.

**2.6.6 Traceless affinity peptide labelling.** Although peptide labelling has proven successful for modifying antibodies site-selectively, concerns include the immunogenic potential of the non-native peptide or its large size which may impede Fc biology. Traceless labelling methods with affinity tags offer a unique opportunity to obtain the same selective modification without the potential pitfalls of peptide attachment. Ohata and Ball reported a novel tool for traceless peptide labelling for ADC preparation based on the Fc region affinity strategy.<sup>237</sup> A hexarhodium metallopeptide catalyst was prepared using a truncated Z domain peptide, which enabled efficient site-specific antibody functionalisation of the Fc binding domain *via* reaction with a diazo payload (Fig. 15E). Cooperative interplay between multiple metal centres enabled the introduction of a bioorthogonal alkyne moiety into an asparagine residue in the CH2 domain of either mono- or polyclonal antibodies. Elaboration of this simple reactive group allowed the preparation of conjugates with appended fluorophores, affinity tags, or drugs. The modified residue in the conjugation reactions was identified as an asparagine residue in the CH2 domain by trypsin digestion and tandem MS, consistent with previous investigations which identified asparagine as the modified residue in rhodium-catalysed modification protein.<sup>238</sup> Attachment of doxorubicin generated an anti-HER2 ADC with a DAR of 1. An alternative strategy by Yamada *et al.* also used an Fc-III peptide derivative containing an NHS ester as an affinity tag to modify multiple lysine residues in the Fc region (Fig. 15C).<sup>239</sup> This method was named affinity peptide mediated regiodivergent functionalisation (AJICAP<sup>TM</sup>) and achieved selective modification of HC-K246 and HC-K248 in trastuzumab. Key to the design of this reagent was the incorporation of a cleavable disulfide between the NHS ester and the affinity peptide. Upon covalent lysine modification, reduction of the disulfide followed by treatment with maleimide-modified DM1 generated a DAR 1.9 anti-HER2 ADC that achieved complete tumour

eradication after 4 doses at 5 mg kg<sup>-1</sup> in an NCI-N87 mouse xenograft. The utility of this approach as well as optimisation of the preparation and analysis of AJICAP<sup>TM</sup> ADCs have subsequently been described.<sup>240–244</sup>

Gupta *et al.* reported the novel type of non-covalent ADCs that self-assemble *via* interaction of the antibody with a small molecule affinity ligand (Fig. 15F).<sup>245</sup> 4-Mercaptoethylpyridine (MEP), which is used in antibody purification because of its ability to selectively bind distinct regions within both the Fab and Fc fragments was used to facilitate this non-covalent conjugation.<sup>246,247</sup> This method yielded homogeneous DAR 6 ADCs *via* reaction of trastuzumab or cetuximab with MEP-modified gemcitabine. The modification reaction proceeded rapidly (<8 min) by binding at two conserved binding sites on each Fab and two in the Fc region. Furthermore, the structure, binding specificity, and affinity of the antibody were retained after modification. Remarkably, the conjugates were highly stable in plasma and showed excellent anti-tumour efficacy in mice with non-small cell lung cancer xenografts.

#### 2.6.7 Conjugation on isolated LCs followed by mAb assembly.

Farràs *et al.* have recently reported a novel strategy to elicit homogeneous ADC synthesis. Independent expression of the light and heavy chains of trastuzumab in HEK293 cells was followed by modification of the sole reduced cysteine in the light chain *via* reaction with mc-Val-Cit-PABC-MMAE. Finally, combination of the modified light chain with the heavy chain was achieved to obtain the complete IgG with a DAR of 2 (Fig. 16).<sup>248</sup> Analysis *via* HIC revealed good recombination efficiency to reform the full antibody, while enzyme linked immunosorbent assay (ELISA) demonstrated retained binding affinity for the HER2 receptor, suggesting that this strategy could be possible for the modification of other therapeutic antibodies. Similar to traditional interchain cysteine modification, covalent linkage of the light and heavy chains is lost using this method.

### 3 Amino acid modification – enzymatic methods

Enzymes have been frequently used to achieve site-selective antibody modification due to their high specificity and mild reaction conditions. Enzymes can either directly attach a payload to a specific amino acid sequence or introduce a reactive functionality on the antibody that can be further functionalised with the desired payload. Both approaches have been successfully utilised to generate homogenous ADCs.

#### 3.1 Transglutaminase

Amongst the enzymatic methods available for attachment of a payload to an antibody, microbial transglutaminases (mTG) have proven themselves particularly useful.<sup>249</sup> Protein-glutamine  $\gamma$ -glutamyltransferases (transglutaminases) are a class of enzyme that catalyse the acyl transfer reaction between the  $\gamma$ -carboxyamide group of glutamine residues and 6-amino-groups of lysine residues, to form intra- and intermolecular N<sup>6</sup>-(5-glutamyl)-lysine isopeptide crosslinks with subsequent



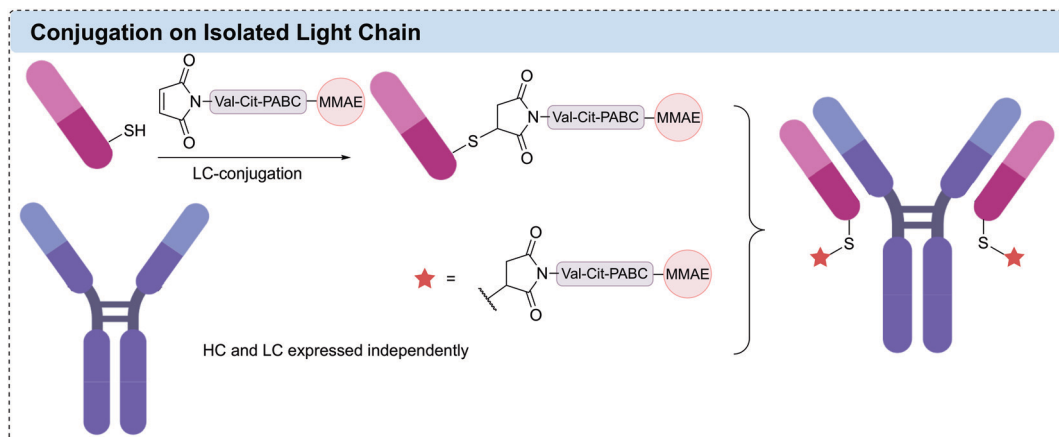


**Fig. 16** Strategy to obtain DAR 2 homogeneous ADCs via assembly from independently produced heavy chain and MMAE-conjugated light chain. Each chain was independently produced and purified, and the LC modified via reaction with mc-Val-Cit-PABC-MMAE

release of ammonia.<sup>250</sup> The unique reactivity of transglutaminases has been exploited as a diverse tool for the post-translational modification of proteins. The transglutaminase from actinobacterium *Streptomyces mobaraensis* was first isolated by Ando *et al.* in 1989,<sup>251,252</sup>

In the context of IgG modification, a number of distinct approaches to effecting specific modification have emerged (Fig. 17). Native or engineered residues can be targeted; however, large proteins such as human IgG contain a high number of surface-exposed Gln and Lys residues, presenting a potential challenge to control the site-selectivity and loading of a proposed transamidation.<sup>253</sup> In many successful approaches, the antibody adopts the role as the acyl-donor substrate, given that amino acids neighbouring Gln are known to exert a greater influence on mTG specificity.<sup>251</sup>

### 3.1.1 Early examples and the importance of glycosylation.

The first example of an mTG-mediated modification of an IgG was reported in 2000 by Josten *et al.*,<sup>254</sup> expanding upon their methodology for mTG-mediated synthesis of hapten–protein conjugates.<sup>255</sup> The authors used mTG to successfully biotinylate a monoclonal IgG against the herbicide 2,4-dichlorophenoxyacetic acid (2,4-D). Conjugation was performed at room

temperature overnight, either in PBS, or Tris-HCl (pH 7.5). Conjugation was explored with two different biotin derivatives, and their conjugation ratios with respect to IgG determined *via* MALDI-MS to range between 1 and 2, depending upon the biotin derivative and the buffer. From this, the authors concluded that approximately two glutamine residues of the anti-2,4-D IgG were accessible to mTG, consistent with the 'mirror image character' of the antibody. Importantly, competitive ELISA suggested antigen binding was unaffected by the conjugation.

The first systematic investigation of TG-mediated conjugation to native antibodies was reported in 2008 by Schibli and co-workers.<sup>256</sup> mTG (from *S. mobaraensis*), and recombinant His-tagged human transglutaminase 2 (TG2) were comparatively investigated for their ability to catalyse attachment of a Cy3 fluorescent probe to three types of IgG. A wide screen of conditions was undertaken, encompassing pH, enzyme/substrate concentrations, and the side chain used for attachment (lysine or glutamine). In-gel fluorescence following SDS-PAGE revealed an almost exclusive labelling of the heavy chain. Reflecting the increased number of exposed lysine residues and the known specificity of TGs towards glutamine-containing

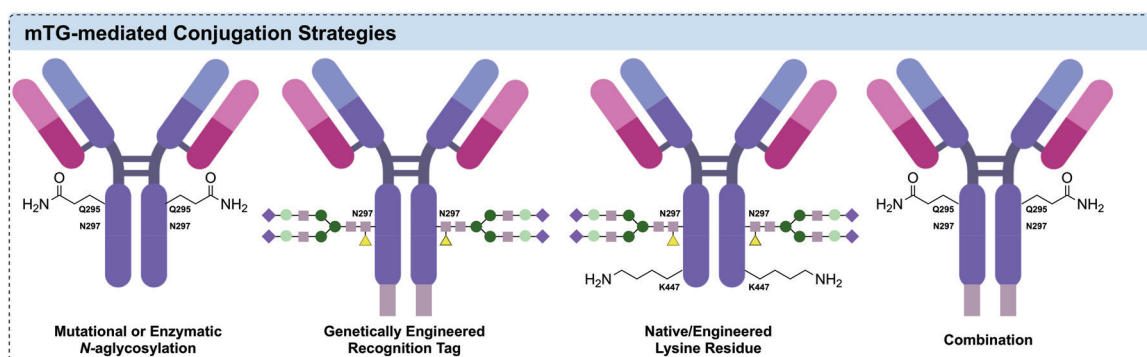


**Fig. 17** Approaches to mTG-mediated site-specific conjugation to IgG<sub>1</sub> for the generation of ADCs (L to R): exposure of native Q295 via enzymatic or mutational removal of *N*-linked heavy chain glycans; genetic incorporation and expression of mTG specific recognition motif; conjugation via native/engineered lysine residue; combination of multiple approaches allowing for dual functionalisation.

sequences, conjugation with glutamine-modified substrates was found to give a 6-fold increase in labelling compared to that of lysine-modified payloads. Modification of native lysine residues could be achieved however, with antibody-to-fluorophore ratios (FAR) ranging between 0.3 and 0.5. Crucially, the authors observed that conjugation with lysine-substrates was far superior when attempted on an aglycosylated antibody, producing a FAR of 1.0. It was suggested that the single-site mutation (N297Q), which either provides an additional glutamine coupling site or induces structural changes in the IgG to increase accessibility of other glutamine residues. More light was shed on the surprising influence of aglycosylation towards lysine-substrate conjugation in a follow-up study, in which it was demonstrated that mTG-mediated functionalisation yielded immunoconjugates with defined stoichiometry of loading at site-specific positions in the Fc region (Fig. 18B).<sup>257</sup> With the aglycosylated anti-L1-CAM antibody chCE7 (bearing the N297Q mutation), controlled attachment of four labels per antibody was achieved. Tryptic digestion followed by MALDI-TOF MS analysis unambiguously assigned Q295 and N297Q as

the sites of conjugation. Prior work had suggested that removal of the Fc glycans results in greater mobility of the C/E (Q295-T299) loop near the proposed site of modification,<sup>258–260</sup> and so *N*-glycosidase F (PNGase F) was applied to enzymatically deglycosylate native chCE7 and rituximab (Fig. 18A). Specific attachment to the now-accessible Q295 residue was achieved *via* mTG-mediated conjugation following the deglycosylation, was again confirmed by MS. This approach was similarly adopted to functionalise aglycosylated chCE7 with a DOTA metal chelator.<sup>261</sup>

The deglycosylation approach was augmented by Dennler *et al.* in 2014, with their development of a two-step chemoenzymatic protocol for the controlled assembly of ADCs comprising MMAE and MMAF payloads (Fig. 18C).<sup>262,263</sup> The anti-HER2 antibody trastuzumab was first deglycosylated with PNGase F, followed by mTG-mediated enzymatic ligation of a small molecular weight amine substrate (40-fold molar equivalents per conjugation site) overnight in PBS at 37 °C. This substrate contained a reactive vector to facilitate post-conjugation payload functionalisation, either a sulphydryl group for subsequent

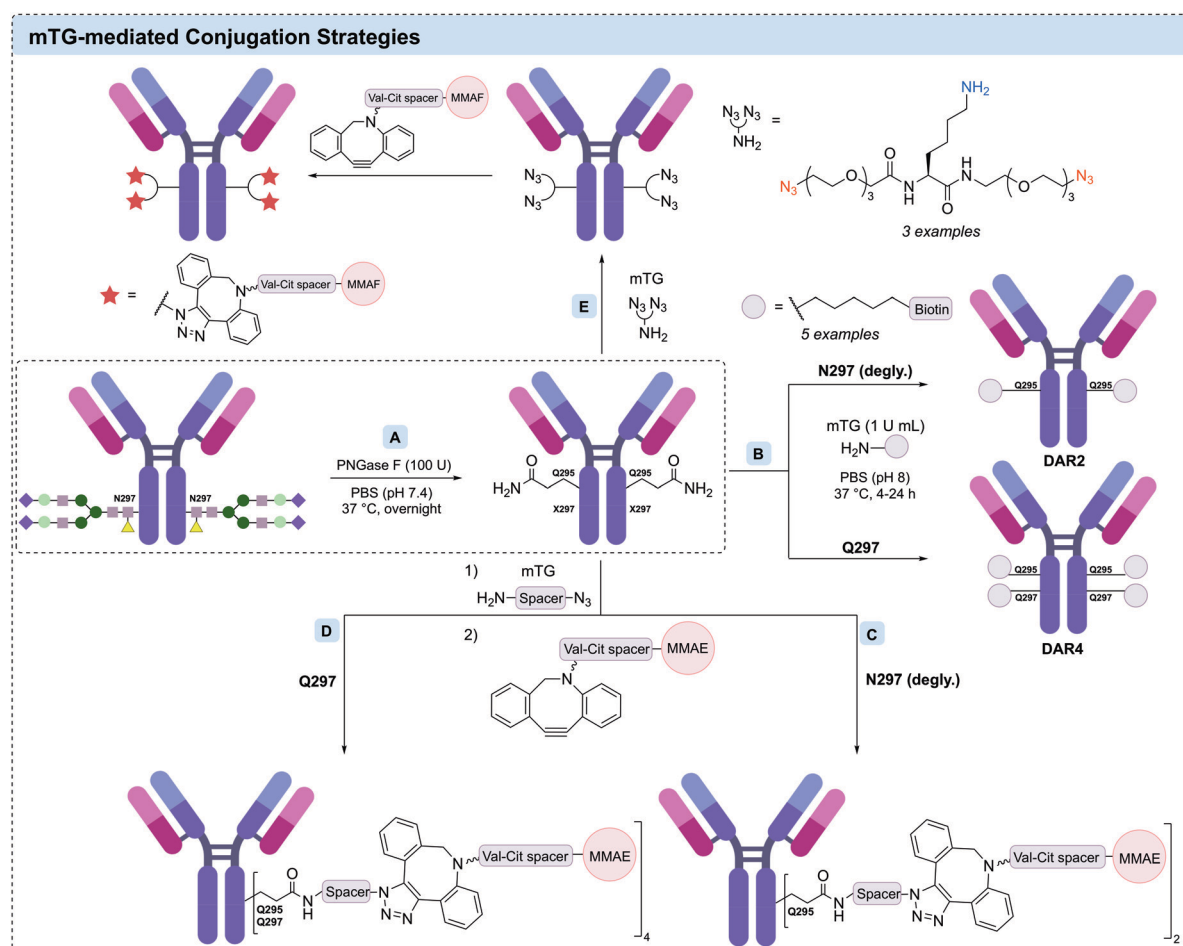


Fig. 18 mTG-mediated conjugation strategies via heavy chain Q295: (A) deglycosylation of N297 with PNGase F, enabling accessibility of Q295; (B) conjugation of amine payloads yields final products with controlled substrate: antibody ratio of either 2 (N297) or 4 (where N297Q mutation provides additional accessible glutamines); (C and D) two-step chemo-enzymatic method for site-specific functionalisation enables assembly of DAR2 or DAR4 ADCs depending upon residue 297; and (E) branched azide-linkers (example shown) facilitate installation of two payloads per antibody attachment site via chemo-enzymatic protocol.



conjugation with a maleimide, or an azide allowing for SPAAC. A DAR of 2.0 was achieved *via* the SPAAC route, and 1.8 for the thiol-maleimide. In comparison, direct enzymatic ligation of the spacer-auristatin derivatives proved inferior for a multitude of reasons. Apart from eliciting DARs between 1.0 and 1.6, extensive optimisation of each substrate was deemed necessary, and the hydrophobicity of the payloads likely to necessitate addition of organic co-solvent, which lowers mTG activity. Furthermore, the increased reactivity and selectivity of the initially attached small substrate allowed the authors to use near-stoichiometric quantities of the toxins (2.5 equivalents), exemplifying the potential cost benefit to this approach.

Lhospice *et al.* utilised this chemoenzymatic approach to produce novel ADCs from an aglycosylated variant of anti-CD30 antibody cAC10, containing the N297Q mutation (Fig. 18D).<sup>47</sup> The antibodies were assembled either through direct conjugation of the amine-Val-Cit-MMAE, or an amino-azide reagent followed by SPAAC to attach the payload. The latter, two-step approach required only 10 molar equivalents of the azide reagent, and 5 molar equivalents of the MMAE-payload—compared to the 80 molar equivalents required for direct enzymatic conjugation of the amine-Val-Cit-MMAE payload. LC-MS analyses confirmed the two-step chemoenzymatic approach to elicit products with higher homogeneity (DAR 4.0) than that of the direct ligation (DAR 3.6). The conjugates were found to exhibit *in vitro* EC<sub>50</sub> levels comparable to that of Adcetris<sup>®</sup>. All four ADCs were stable in cynomolgus monkey, human, and rat plasma for at least 1 week. *In vivo* pharmacokinetic studies in rat were consistent with this result, with no change in DAR observed after 2 weeks. Furthermore, <sup>125</sup>I radiolabelling revealed superior tumour uptake, and slower blood clearance, in mice compared to those of Adcetris<sup>®</sup>. Crucially, *in vivo* studies estimated the maximum tolerated dose of the homogeneous ADCs in Wistar rats to be greater than 3 times that of Adcetris<sup>®</sup>.

In the wake of failures in efficacy studies of ADCs comprising payloads of extremely high potency (*e.g.* auristatins, maytansines), there has been renewed consideration for the use of less potent cytotoxins.<sup>264</sup> Newer linker formats that facilitate higher drug loadings of moderately active chemotherapeutic agents have therefore been developed, to maintain efficacy without the associated toxicity. In 2017, Anami *et al.* reported a series of branched azide linkers that were suitable as acyl-acceptor substrates for mTG-mediated conjugation.<sup>265</sup> Each linker contained two azide groups (Fig. 18E), which was attached *via* mTG-mediated conjugation to an N297A mutant anti-HER2 antibody. This facilitated attachment of a Val-Cit-MMAF unit *via* SPAAC, yielding an average DAR of 3.9. The same protocol was undertaken with an N297Q mutant anti-HER2 antibody, producing an average DAR of 7.4. The ADCs exhibited poor stability in mouse plasma, due to the known susceptibility of the Val-Cit motif to extracellular carboxylesterase.<sup>122</sup> The authors sought to remedy this in further investigations, where they developed variants of the Val-Cit motif, which were incorporated through their branched azide linker.<sup>266</sup> In this study, mTG-synthesised ADCs containing Glu-Val-Cit or Asp-Val-Cit demonstrated superior

stability, retained cathepsin activity and efficacy in a series of *in vivo* investigations.

mTG-conjugation to mutationally or enzymatically aglycosylated antibodies has been utilised in several broader investigations and applications, including dual modification.<sup>267</sup> A one pot dual functionalisation, pairing mTG-mediated conjugation with lipoate-acid ligase A-mediated ligation with genetic incorporation of a peptide tag into either the heavy or light chain of trastuzumab has been reported.<sup>268,269</sup> These two conjugation methods were used to install linkers containing orthogonal functional vectors (azide, and strained alkene), allowing for ‘click’-installation of FRET-paired fluorophores. A variety of constructs were assembled, with or without orthogonal cleavable spacers, allowing for removal of the payload from a desired position with either MMP2 or cathepsin B. Additionally, Puthenveetil *et al.* developed a methodology for solid-phase, site-specific dual conjugation of linker-payloads to antibodies.<sup>270</sup> The procedure comprised binding of deglycosylated mutant trastuzumab containing engineered cysteine residues to protein A agarose beads, allowing for solid-phase mTG-mediated conjugation of an amino-BCN linker. The capped mutant cysteines were then exposed under reducing conditions, allowing for maleimide conjugation. Finally, an azide-bearing payload underwent a SPAAC with the BCN motif to generate the dual functional ADCs. Non-glycosylated approaches to antibody modification are not limited to toxin attachment. Other reports have detailed the attachment of azide polymers,<sup>271</sup> photosensitiser motifs<sup>272</sup> or virus nanoparticles.<sup>273</sup>

Recent research offers some reservations concerning the selectivity of mTG for the conserved PWEEQYNST sequence (containing Q295) in the Fc region.<sup>274</sup> Trastuzumab was deglycosylated with PNGase F, and then a small azidoamine was attached with mTG. LC-MS and SDS-PAGE analysis suggested complete conversion with no evidence of light-chain modification. Tryptic digestion followed by tandem MS of the conjugate confirmed modification at the expected position. However, under more forcing conditions, triply modified species were also detected. The third site was unambiguously identified as Q3<sub>H</sub> (trastuzumab labelling), close to the N-terminal CDR1 epitope-binding region. The revelation is potentially problematic, highlighting the need for continued development of analytical methods for assessing homogeneity, and the possible scope for enhancing specificity through advances in areas such as engineered transglutaminases.

All of the methods described above require the absence of the Fc N-glycans in order to facilitate access to the conserved Q295 site. IgG glycosylation influences the stability and conformation of the Fc region and is critical for antibody recognition by Fc receptors.<sup>275</sup> The consequence of glycosylation upon antibody pharmacokinetics in humans is unclear, with investigations on aglycosylated antibodies revealing variable stability, aggregation propensity, and half-life.<sup>276,277</sup> Advances in engineered mTGs may preclude this dilemma, a recent example of which was reported by Dickgiesser *et al.*<sup>278</sup> Utilising a semi-rational combinatorial approach based upon sequence alignments with related TGs, the authors generated a library of mTG



mutants was generated, which facilitated efficient and site-specific conjugation to native glycosylated antibodies at Q295. Remarkably, ADCs with DAR ranging between 1.9 and 2.1 were achieved with several of the mutant mTGs despite the presence of the *N*-glycans. Tandem MS confirmed Q295 as the conjugation site, with only a minor by-product of DAR 3 (the attachment site of which was not identified). This emerging approach promises to simply expand the Q295 strategy, without detriment to the pharmacokinetic properties of the produced conjugates.

**3.1.2 mTG recognition motifs.** A common strategy to direct the site of mTG-mediated transglutaminase is *via* the insertion of a glutamine-containing recognition sequence ('Q-tag'). The position of insertion is not limited to the termini, thus a range of positions and any consequent effects on conjugation efficiency, binding affinity, pharmacokinetics, *etc.* can be optimised. However, the identification of mutational sites is non-trivial. Whether conjugation is possible, and to what extent, is likely to be influenced by the tertiary structure of the antibody, and the local amino acid sequence. Moreover, the effect of conjugation upon physiochemical properties of the ADC will differ between sites, and the selected drug. In a pioneering study on the influence of the site of conjugation upon stability and pharmacokinetics, Strop *et al.* developed a glutamine tag (LLQG) that was engineered into a wide variety of surface accessible regions of an anti-EGFR (epidermal growth factor receptor) IgG1 antibody.<sup>38</sup> mTG-mediated site-specific ligation at the inserted glutamine residue was undertaken with amine-functionalised monomethyl auristatin D (MMAD) or cadaverine-AlexaFluor payloads. Twelve sites were found to result in good biophysical properties and a high degree of conjugation. The utility of the method was further exemplified with the successful modification of mutant anti-M1S1 C16 and anti-HER2 antibodies. Conjugation was conducted at pH 8 with

5–10-fold molar equivalents of AcLys-Val-Cit-MMAD linker-payload at either 22 or 37 °C for 16 hours. The DAR of the produced conjugates ranged between 1.2 and 2.0, depending upon the antibody, payload, and site of glutamine tag incorporation. To probe the relationship between the site of conjugation and the properties of the ADC, two C16 ADCs were synthesised with conjugation respectively performed at the modified heavy (LLQGA; DAR 1.9) and light chain C-termini (GGLLQGA; DAR 1.8). Both C16 ADCs exhibited impressive *in vitro* cytotoxicity against M1S1-positive cells, with IC<sub>50</sub> values (~50 pM) comparable to a DAR 3.6 C16 Val-Cit-MMAD ADC assembled by conventional cysteine conjugation (~40 pM) despite the lower drug loading. Antitumour efficacy was also observed *in vivo*, with sustained tumour regression observed over 10 weeks in mice implanted with BxPC3 cells. Slightly accelerated clearance of the C16 ADC conjugated through the heavy chain was observed over that conjugated through the light chain, which may be due to the ADCs' differential tissue distribution. Analysis of FcRn binding revealed no significant difference between the C16 ADCs.

Farias and co-workers developed a methodology for the characterisation of mTG-mediated amino-PEG<sub>6</sub> propionyl MMAD (AmPEG<sub>6</sub>-MMAD) payload attachment.<sup>279</sup> The authors attached the AmPEG<sub>6</sub>-MMAD payload to engineered glutamine tags (LLQGA) installed at various positions of an anti-M1S1 antibody C16 (Fig. 19A). The conjugates were investigated with a combination of native MS, peptide mapping and in-source fragmentation analysis. A small amount of off-target conjugation was observed at Q295, which was attributed to the small amount of aglycosylated antibody typically produced when expressed in CHO or HEK293 systems. This off-target conjugation was mitigated by utilising a Q295N mutant antibody, resulting in approximately 99.8% site-specificity at the installed tag.

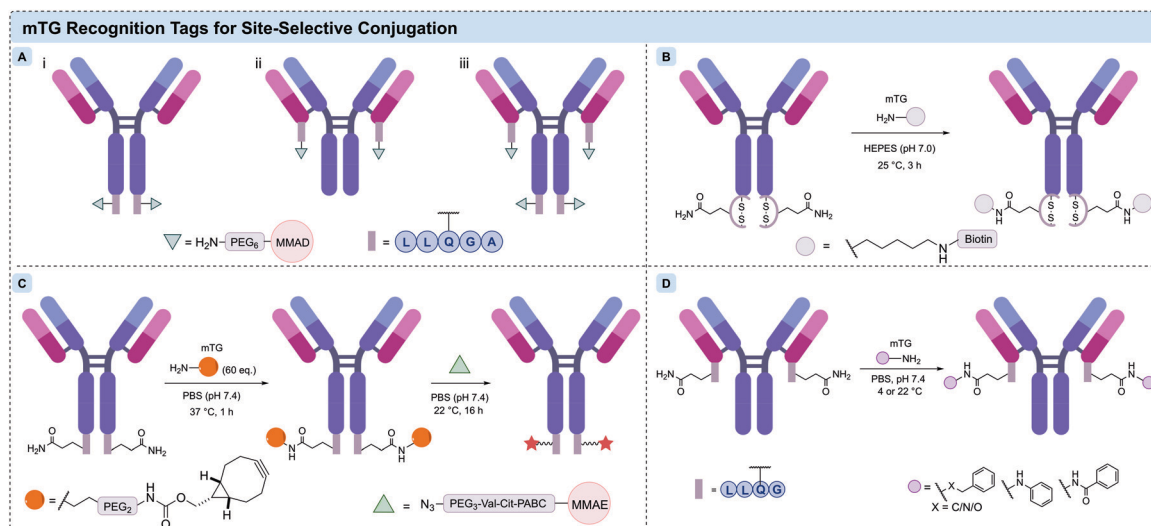


Fig. 19 Approaches to mTG-mediated conjugation via recognition tags: (A) incorporation of AmPEG<sub>6</sub>-MMAD linker-payloads with LLQGA tag at antibody heavy chain C-termini (i), light chain C-termini (ii), and light and heavy chain C-termini (iii); (B) conformationally strained DAIP-derived sequence facilitates efficient mTG-conjugation; (C) two-step chemo-enzymatic attachment via SPI<sub>p</sub> derived recognition motif; (D) recent expansion in scope of substrates amenable to mTG-mediated conjugation.



The C-termini LLQGA approach is a commonly adopted mTG-ligation strategy and has seen use in the assembly of related biologics, such as antibody–oligonucleotide conjugates.<sup>280</sup>

Strop *et al.* utilised the engineered recognition motif strategy, in combination with N297Q glycosylation, to investigate whether the pharmacokinetic limitations of high DAR ADCs could be overcome through control over the site of conjugation.<sup>281</sup> ADCs comprising the anti-M1S1 antibody C16 and a non-cleavable MMAD payload, were assembled with DARs of 2, 4, 6 and 8. *In vitro* toxicity assays against BxPC3 (high M1S1 expression) and Colo205 (moderate M1S1 expression) cell lines were conducted, comparing the response to that of similarly loaded ADCs assembled *via* conventional maleimide–cysteine conjugation. Expectedly, the higher DAR ADCs were the most potent. All ADCs exhibited pM toxicity against BxPC3, however those of DAR 6 and 8 maintained this level of potency against Colo205. *In vivo* studies revealed that the mTG-assembled DAR 8 conjugate outperformed its conventionally assembled counterpart, inducing long-term tumour growth inhibition. Schneider *et al.* recently reported the development of ‘dextramabs’, a novel linker platform for ADCs comprising a hydrophilic polysaccharide scaffold of desired length, allowing for the assembly of high DAR ADCs.<sup>282</sup> The polysaccharide scaffold contains repeating azide-bearing glucose units, allowing for SPAAC functionalisation following mTG-mediated conjugation to the antibody. Functionalisation with DBCO-PEG<sub>3</sub>-Val-Cit-PABC-MMAE payloads generated ADCs of 2, 4, 8 and 11. Sub-nanomolar inhibitory activity was observed for DAR 8 and 11 ADCs ( $IC_{50} = 0.1$  nM). No significant change in binding was observed, and thermal shift assays suggested no loss in stability compared to trastuzumab.

A focused study on the influence of conjugation site on the stability of Val-Cit-PABC linkers was undertaken by Dorywalska *et al.* in 2015.<sup>39</sup> A range of anti-M1S1 C16 conjugates bearing aminocaproyl-Val-Cit-PABC-Aur0101 (an auristatin payload) linker-payloads at a variety of engineered Q-tags were synthesised and incubated in mouse, rat, cynomolgus monkey, and human plasmas, followed by purification and analysis *via* HIC and MS. The ADCs remained stable independent of conjugation site, and blood type—with the exception of mouse blood, in which stability varied widely depending upon the site of attachment. Cathepsin B activity for the Val-Cit cleavage was also found to depend upon the site of conjugation. A positive correlation between linker stability (in mouse plasma) and anti-BxPC3  $IC_{50}$  values was observed in *in vitro* cytotoxicity studies. Further systematic characterisation was later reported.<sup>283</sup>

Wong *et al.* have also reported the development of epidermal growth factor receptor (EGFR) targeting ADCs.<sup>284</sup> A low-affinity anti-EGFR ADC (RN765C) was produced by insertion of a glutamine tag (GQLLQGPP) at the C-terminus of the light-chain of the antibody, followed by mTG-mediated conjugation with the linker-payload AcLys-Val-Cit-PABC-PF-06380101. Conjugation to the antibody was undertaken with 10-fold molar excess of the linker-payload at 37 °C for 24 hours, resulting in a DAR of 1.93–2.0 following purification. This ADC exhibited subnanomolar *in vitro*  $EC_{50}$  across a range of cell lines—yet was

less potent towards normal human keratinocytes, which also express EGFR albeit at lower levels. RN765C was highly efficacious *in vivo*, with sustained solid tumour regression achieved with a single dose of 1.5 mg kg<sup>-1</sup>. The same linker-payload was used by Strop *et al.* in designing a novel Trop-2-targeting ADC, RN927C.<sup>285</sup> Accordingly, under similar conditions to RN765C, the AcLys-Val-Cit-PABC-PF-06380101 linker-payload was attached *via* mTG-mediated conjugation to an mTG-tag (LLQGA) fused to the heavy chain C-terminus. A single HIC purification step resulted in a homogeneous conjugate with a measured DAR of 2.0. Cell line and patient-derived xenograft *in vivo* mouse models exhibited sustained regression with a single dose of RN927C at 0.75–3 mg kg<sup>-1</sup>. A Phase I dose-escalation study was undertaken with RN927C on thirty-one patients with advanced or metastatic solid tumours (ClinicalTrials.gov Identifier: NCT02122146). Disappointingly, no partial or complete responses were observed, and the study was terminated early due to excess toxicity.<sup>286</sup>

Researchers from Pfizer utilised mTG-mediated conjugation to construct ADCs to investigate the dependency between intracellular trafficking and non-cleavable ADC-mediated cell killing.<sup>15</sup> The investigated conjugates comprised anti-Trop-2 or anti-APLP2 (known to travel directly to lysosomes following endocytosis) IgGs. DAR 2 ADCs were constructed *via* mTG-mediated attachment to GQLLQGPP glutamine tags fused to the light chain C-termini, and DAR 4 ADCs *via* Q295/Q297 on N297Q mutant IgGs. Am-PEG<sub>6</sub>-MMAD was used as the linker-payload, conjugated under standard conditions. In growth inhibition studies against SKOV3 cells, APLP2-ADC (0.11 nM) exhibited a significantly lower  $EC_{50}$  compared to Trop-2-ADC (5.95 nM), despite SKOV3 Trop-2 expression being approximately double that of APLP2. The superior efficacy of APLP2-ADC over Trop-2-ADC was maintained in *in vivo* xenograft models.

The demonstrated stability and homogeneity of mTG-mediated conjugation techniques have prompted their application in ADC designs where safety is especially critical. In 2019, Ratnayake *et al.* (Pfizer) developed a series of HER2-targeting ADCs bearing depsipeptides, an extremely potent class of cytotoxins, at different attachment sites.<sup>287</sup> The lead conjugate PF-06888667, comprising the depsipeptide SW-163D conjugated *via* a cleavable AcLys-Val-Cit-PABC-DMAE (dimethylethlenediamine) linker, exhibited subnanomolar *in vitro* cytotoxicity against N87 and MDA-MB-361-DYT2 cell lines. Complete tumour regression was observed in an N87 xenograft mouse model at a dosage ten-fold lower than that of the approved T-DM1. The study highlights the importance of rational design in payload site and attachment method.

There is a growing body of work on the optimisation of the sequence and location of recognition tags to improve conjugation efficiency and specificity. In 2015 Siegmund *et al.* reported the development of a rationally designed glutamine tag (GEC-TYFQAYGCTE), informed from a sequence analysis and crystal structure of dispase autolysis inducing protein (DAIP), a natural substrate for bacterial transglutaminase.<sup>288</sup> Flanking cysteine residues were included to mimic the loop in DAIP by rigidifying the  $\beta$ -turn following disulfide formation (Fig. 19B). Kinetic studies of the mTG-mediated biotinylation of this oligopeptide



resulted in significantly faster conjugation in comparison to an analogous sequence containing two asparagine residues instead of the two cysteine residues. Both tags were incorporated to the C-termini of the heavy chains of anti-EGFR antibody cetuximab. Both sequences were found by Western blot and MALDI TOF-MS analysis to mediate site-specific conjugation. Microscopy and flow cytometry demonstrated that the conjugation did not impair EGFR binding.

A novel recognition motif derived from a native substrate from the host of the *S. mobaraensis* bacterial transglutaminase, *Streptomyces* papain inhibitor (SPI<sub>P</sub>), was recently reported (Fig. 19C).<sup>289</sup> An analysis of the substrate preference of mTG within a series of synthetic peptides derived from sequences within the papain inhibitor, as well as DAIP, was conducted. Anti-HER2 ADCs were assembled *via* recognition tags fused to the heavy chain C-termini, attachment with amino-PEG<sub>2</sub>-BCN linkers, followed by SPAAC with the azido-PEG<sub>3</sub>-Val-Cit-PABC-MMAE payload. For the ADC assembled from the lead sequence, a DAR of 1.81 was determined by HIC, and an IC<sub>50</sub> of 151 pM against HER2+ SK-BR-3 cells. In contrast, a comparable ADC assembled *via* a simpler LLQG tag yielded a DAR of 0.48 and exhibited an IC<sub>50</sub> of 1.9 nM. Yamazoe *et al.* have recently reported a high-throughput protocol for assisting the determination of optimal locations for drug conjugation.<sup>290</sup> mTG-conjugation was utilised to generate a library of ADCs from a pool of mutated antibodies, which were analysed and validated *via* MS. The screening allowed for several new tags and sites to be identified and may prove to be an important tool for future development and optimisation of homogeneous ADCs.

**3.1.3 Other advances.** Given the greater influence that neighbouring sequences exert upon mTG selectivity for glutamine over lysine, research has focused primarily upon glutamine residues. Limited success however has been reported for lysine-targeted mTG modification.<sup>251,291–294</sup> As can be appreciated, most acyl acceptors have tended to be primary amines for simplicity. A recent publication has reported an expansion of the substrate repertoire to include hydrazines, hydrazides and alkoxyamines—which produces isopeptides of varied susceptibility (Fig. 19D).<sup>295</sup> Modification of genetically installed glutamine residues in the light or heavy chain was demonstrated with these nucleophiles with minimal modification of native glutamines observed. Furthermore, conjugation with unsubstituted hydrazine and dihydrazines facilitated introduction of bioorthogonally reactive aldehydes or ketones to produce further functionalised bioconjugates. Another example introduced a thiol *via* mTG catalysis, followed by modification with an mc-Val-Cit-PABC-MMAE payload.<sup>296</sup> Widespread use of mTG has driven efforts to improve its activity, specificity and stability with several reports describing advances in each of these.<sup>297–303</sup> The unique specificity and high activity constitute the novel mTG as a useful complementary tool for site-specific enzymatic conjugation. Although many of these studies are not specifically focused on the optimisation of mTG-mediated antibody-modification, they highlight a potential direction from which further advances might be pursued.

### 3.2 Enzymatic C/N-terminal modification

Several enzymatic protocols have been developed over the past decade to facilitate selective modification of the N- or C-termini of the antibody chains, often by genetic fusion of an enzyme-specific recognition tag. One such protocol involves the use of formylglycine-generating enzyme (FGE), which oxidises cysteine residues to a formylglycine unit in a CXPXR consensus sequence (X = any amino acid except proline).<sup>304</sup> Aldehyde modified antibodies generated using this SMARTag® technology have been conjugated with hydrazine- or hydroxylamine-functionalised payloads (Fig. 20A). The hydrazine-iso-Pictet-Spengler (HIPS) ligation achieves rapid bioconjugation under mild conditions, forming hydrolytically stable protein conjugates.<sup>305</sup> An in-depth study on the HIPS ligation revealed that C-terminus tagging resulted in improved pharmacokinetics and *in vivo* efficacy compared to alternative conjugation positions.<sup>306</sup> A CD22-targeting ADC, TRPH-222 (CAT-02-106), generated using the SMARTag® HIPS bioconjugation technology, has recently entered Phase I clinical trials for the treatment of lymphoma with an expected completion date of 2022 (NCT03682796). TRPH-222 comprises a CD22-targeting antibody, which contains a formylglycine residue on each heavy chain, conjugated to a maytansinoid payload *via* a non-cleavable linker. TRPH-222 has a DAR of 2, and exhibited promising efficacy and safety properties during pre-clinical evaluation.<sup>307,308</sup> Interim results from the Phase I clinical trial have recently indicated that TRPH-222 was well-tolerated in 19 non-Hodgkin's lymphoma patients with manageable side effects.<sup>309</sup> Additionally, this ADC has shown early signs of efficacy at doses of 0.6 to 5.6 mg kg<sup>-1</sup> administered every three weeks, including five complete responses. Additionally, an anti-HER2 DAR 2 ADC generated *via* FGE-mediated aldehyde insertion at the C-terminus fusion CXPXR tag followed by HIPS conjugation of a DM1 payload, has shown promising preclinical activity and tolerability compared to the approved T-DM1.<sup>310</sup>

A recently reported alternative strategy for formylglycine conjugation developed novel *N*-pyrrolyl alanine Pictet-Spengler reagents that exchanged the indole heterocycle for a pyrrole ring.<sup>311</sup> This approach enabled rapid antibody bioconjugation with an easily synthesised reagent. Additionally, formylglycine-tagged antibodies generated by FGE have also been exploited using pyrazolone reagents, whereby ligation occurs *via* tandem Knoevenagel condensation-trapping reactions (Fig. 20A).<sup>312,313</sup>

Further enzymatic conjugation technologies include protein prenyltransferases, a family of enzymes that can append isoprenoid groups to a cysteine residue within a CaaX recognition tag (where a is an aliphatic amino acid, and X is an amino acid that determines specificity for a particular isoprenoid transferase). These enzymes are typically responsible for post-translational modifications and have been successfully applied to the single and dual modification of proteins, achieving high conversions and selectivity.<sup>314–316</sup> Additionally, the technology has been used for the generation of homogeneous ADCs (Fig. 20B). Initial work involved the modification of an antibody C-terminus CaaX tag with an isoprenyl derivative containing a reactive group (e.g. ketone, azide) that was subsequently modified using bioorthogonal chemistry, including oxime



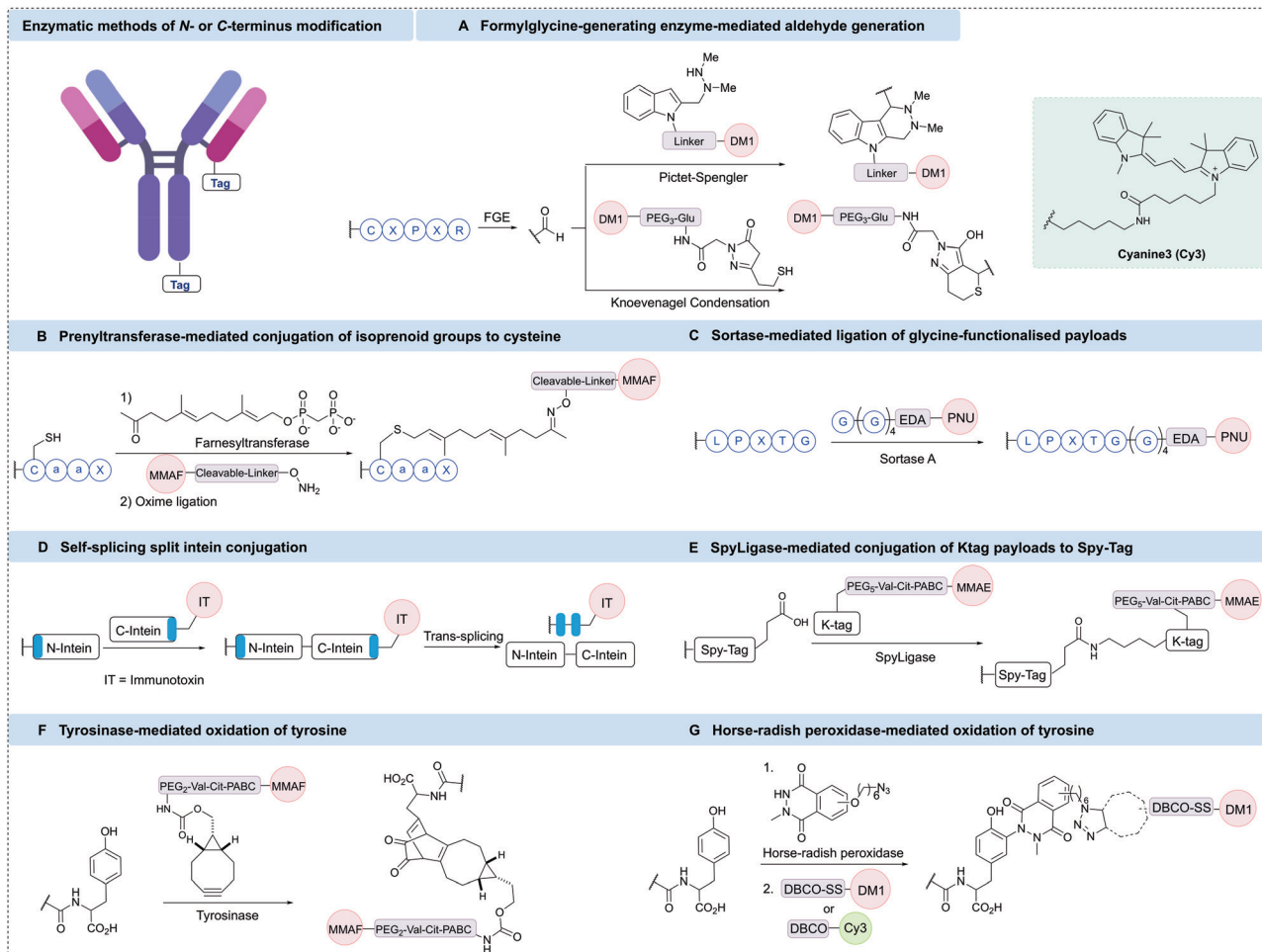


**Fig. 20** Enzymatic bioconjugation methods for C-terminal modification; (A) formylglycine-generating enzyme (FGE) oxidises a specific Cys residue to an aldehyde suitable for Pictet-Spengler or Knoevenagel conjugation; (B) prenyltransferase-mediated conjugation of functionalised isoprenoid groups to cysteine in CaaX and subsequent oxime ligation reaction; (C) sortase-mediated antibody conjugation (SMAC) technology; (D) self-splicing split inteins form a new amide bond between extein units (blue) whilst excising to form intein protein; (E) SpyLigase-mediated conjugation of a SpyTag and KTag sequence; (F) tyrosinase-mediated strategy for the oxidation of tyrosine and subsequent strain-promoted cycloaddition; (G) Horse-radish peroxidase tyrosine oxidation strategy.

formation or azide–alkyne cycloadditions.<sup>317</sup> This technology is known as ConjuALL™ and was developed by LegoChem Biosciences. Recently, the prenylation conjugation platform has been utilised to generate a HER2 targeting ADC, LCB14-0110. This ADC was synthesised through prenyltransferase-mediated conjugation of a ketone-functionalised isoprenoid to trastuzumab with a C-terminus appended CaaX motif, which was then subjected to an oxime ligation with a  $\beta$ -glucuronidase-cleavable MMAF payload.<sup>318</sup> The ADC exhibited high stability during pre-clinical evaluation with a promising PK profile, and is currently in Phase I clinical trials in China.

Sortase-mediated antibody conjugation (SMAC) technology™ is an additional enzymatic ligation approach developed by NBE-therapeutics. SMAC-technology™ uses *S. aureus* sortase A, which is a transpeptidase that cleaves the amide bond between threonine and glycine residues in the LPXTG (X = any amino acid) pentapeptide motif, and subsequently catalyses the attachment of glycine-functionalised payloads to the newly

generated C-terminus (Fig. 20C). The sortase recognition motif and a Strep II tag, which was used to aid removal of unreacted antibody, were fused to the light and heavy chain C-terminus of different antibodies, including brentuximab and trastuzumab. Sortase-mediated conjugation was then used to attach a series of penta-glycine tagged payloads containing maytansine or MMAE to generate homogeneous ADCs analogous to Kadcyta® and Adcetris®.<sup>319</sup> The sortase conjugated analogues were found to exhibit similar *in vitro* potency to the clinically approved ADCs in cell viability assays. Additionally, conjugation of the payload to the antibody was shown to have no adverse effect on the antigen binding. Reaction efficiencies exceeding 80% were typically achieved with various payloads and antibodies, indicating the generality of this approach. Next, the *in vivo* potency of the trastuzumab derived ADC was studied in a HER2-positive SKOV3 cell line xenograft mouse model. Once more, the sortase conjugated ADC exhibited comparable potency to Kadcyta®. In another example, sortase-mediated

conjugation was used to generate an anthracycline based ADC targeting HER2. This ADC demonstrated high serum stability and efficacy in a HER2-positive *in vivo* model.<sup>320</sup> Typically, the conjugation efficiency was *ca.* 85%, corresponding to a DAR of  $\sim 3.4$ , which could be increased to 4.0 after StrepTactin affinity chromatography purification. However, the conjugation efficiency was highly dependent on the linker-payload composition. When the extremely toxic nemorubicin metabolite PNU-159682 was used as the payload, over 95% conjugation efficiency to the anti-HER2 antibody was achieved without enrichment (DAR *ca.* 4.0). The non-cleavable ADCs generated were shown to be highly potent, effective on cells that expressed only moderate target antigen levels and had high *in vitro* and *in vivo* serum stability. Interestingly, incorporation of a cleavable linker component had little effect on the cytotoxicity of these ADCs, implying that the mechanism of action of the payload was unaffected by the linker in the non-cleavable variants. Additional mechanistic *in vivo* studies on the PNU-based ADC found that some breast cancer resistance mechanisms could be overcome using these novel ADCs.<sup>321</sup> With promising preclinical data, NBE-therapeutics expects the first SMAC-derived ADC, NBE-002, to reach Phase I clinical trials in mid to late 2020.

Sortase-mediated conjugation has also been applied to dual-labelling strategies in combination with butelase 1, an enzyme that ligates a specific NHV amino acid motif to nucleophilic payloads. These two enzymes have recently been harnessed in an orthogonal fashion for the one-pot site selective generation of dual-labelled ADCs.<sup>322</sup> Additional methods that combine sortase A with the  $\pi$ -clamp conjugation technology have also been developed to achieve an efficient antibody dual labelling technology.<sup>323</sup>

Self-splicing split inteins can be used for the generation of homogeneous antibody immunotoxin conjugates (Fig. 20D). Inteins are proteins flanked by exteins that self-excite to assemble proteins after mixing the N- and C-terminal intein components. A new amide bond is generated between the extein units, which can be used for conjugation of a payload to an antibody. Pirzer *et al.* applied the split inteins strategy to antibody modification by appending a Gly-Ser linker connected to the 11 amino acid intein sequence to the heavy chain C-termini of trastuzumab and an EGFR-targeting antibody.<sup>324</sup> The immunotoxins used in this study were a truncated variant of *Pseudomonas* Exotoxin A, and gelonin. These immunotoxins were appended with a 143 amino acid C-terminal intein sequence connected to a maltose binding protein, which was designed to improve solubility and expression reproducibility. The tagged antibody and toxin were then combined under reducing conditions and protein trans-splicing occurred with an overall coupling efficiency of 50–70%. Unconjugated antibody was removed through immobilised metal affinity chromatography, yielding highly toxic final constructs with a toxin-antibody ratio of *ca.* 1.3. Importantly, immunotoxin conjugation to the antibody did not hinder antigen binding for either antibody. Next, *in vitro* cell viability assays demonstrated high levels of both selectivity and cytotoxicity for the ADCs. For the Exotoxin A derived ADCs,  $IC_{50}$  values ranged between

0.8–3.9 pM, approximately 10-fold more potent compared to the gelonin ADCs ( $IC_{50}$  values of 12–68 pM). The difference in activity was proposed to be a result of more efficient transport of the Exotoxin A payload from endosomes to the cytosol, observed by confocal microscopy. This split intein technology is a valuable addition to the conjugation toolbox, and future optimisation of linker lengths and composition has been proposed to improve the conjugation efficiencies.

SpyLigase has also been used to generate homogeneous ADCs (Fig. 20E).<sup>325</sup> This enzyme catalyses formation of an isopeptide bond between SpyTag and KTag recognition peptides. In a recent report, an MMAE payload was connected to the KTag 10 amino acid sequence, and the SpyTag 13 amino acid sequence was fused to the C-terminus of the anti-EGFR antibody cetuximab. In the presence of SpyLigase, combination of the antibody and the KTag payload generated homogeneous ADCs under mild conditions with *ca.* 80% conjugation efficiency and a DAR of *ca.* 1.7. Following purification by protein A chromatography, the *in vitro* cytotoxicity of the resulting ADC was analysed. High potency was observed against EGFR-positive breast cancer cell lines for both non-cleavable and cleavable ADCs, with  $IC_{50}$  values of 0.2 and 0.1 nM respectively.

Tyrosine-specific bioconjugation has recently shown great promise for controlled protein conjugation.<sup>326</sup> Factors including its relatively low abundance, hydrophobicity, and  $\pi$ - $\pi$  stacking generally limits the surface exposure of tyrosine residues, which leads to low accessibility for protein conjugation. Tyrosinase is an enzyme that efficiently oxidises exposed tyrosine residues to 1,2-quinones, which can react with various functionalities to conjugate payloads (Fig. 20F). One example utilised a BCN-tagged MMAF linker-drug for strain promoted, oxidation-controlled quinone-alkyne cycloadditions (SPOCQ).<sup>326</sup> A tyrosine residue connected to a tetra-glycine linker (G<sub>4</sub>Y) was genetically fused to the light chain C-terminus of trastuzumab and an anti-influenza AT1002 antibody. The antibodies were then oxidised with tyrosinase and treated with the BCN-tagged cleavable MMAF payload to rapidly form ADCs with reasonable conjugation efficiency under mild conditions. Overall, this approach was somewhat limited by the non-specific reaction of nucleophilic amino acid residues proximal to the 1,2-quinone, reducing the conjugation efficiency.

### 3.3 Other enzymatic methods

In another approach to tyrosine modification, Sato *et al.* have reported selective modification of surface-exposed trastuzumab tyrosines (Fig. 20G).<sup>327</sup> In this protocol, horseradish peroxidase (HRP) catalysed single electron transfer modification of tyrosine phenol with *N*-methylated luminol derivatives containing a pendant azide. Modification was found to occur on tyrosines in the complementarity determining region (HC-Y53). The installed azide was then treated with DBCO-functionalised payloads, including Cy3 or Cy5 fluorophores or toxin DM1, which generated a DAR 2 ADC. The resulting conjugates were used for *in vivo* imaging or therapeutic evaluation.

Similar to histidine, serine modification often proves difficult due to competition from other more nucleophilic residues.



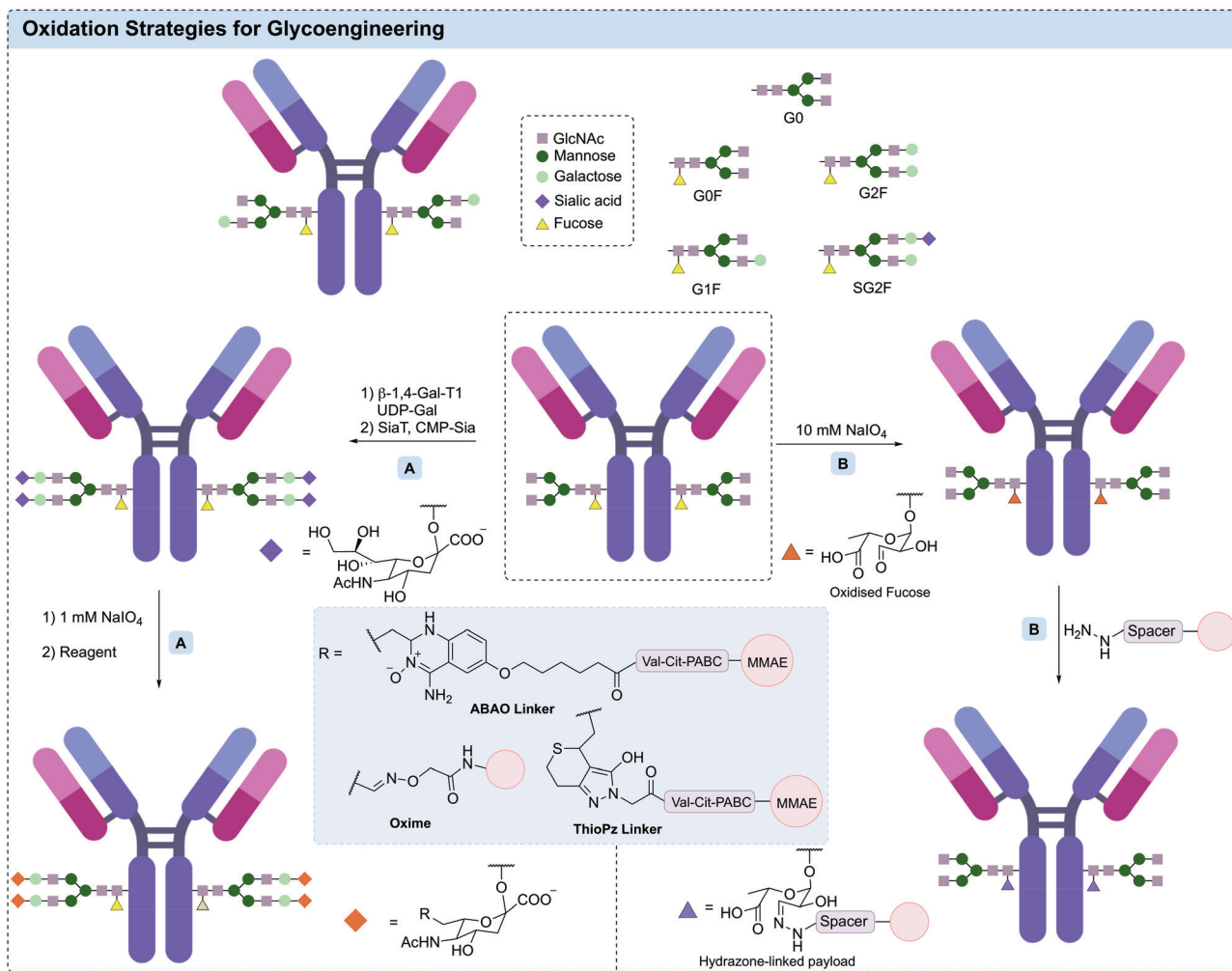


**Fig. 21** Glycosylation pattern of IgG1 antibodies (top) and oxidation strategies for antibody glycan modification (bottom). (A) Oxidation of sialic acid residues followed by reaction with aminoxy, ThioPz or ABAO payloads. (B) Oxidation of fucose residues followed by hydrazone formation.

However, Grünwald *et al.* have reported an efficient enzymatic strategy using phosphopantetheinyl transferases (PPTases), which recognise serine residues in specific amino acid sequences and can transfer payloads from coenzyme A (CoA)-modified substrates.<sup>328</sup> PPTase recognition sequences (*ca.* 11 amino acids) were inserted into the CH3 domain of trastuzumab. Treatment of the serine-tagged antibody with an MMAF-coenzyme A reagent generated a homogeneous DAR 2 ADC, which exhibited cytotoxicity *in vitro* against HER2-positive cell lines and significant tumour regression *in vivo* in a HER2-positive xenograft model. Further developments by Grünwald *et al.* applied a two-step strategy, in which CoA analogues containing bioorthogonal functional groups were first introduced using a shorter 6 amino acid PPTase recognition sequence, prior to chemical payload conjugation.<sup>329</sup>

## 4 Glycan modification

Within the CH2 domain of all IgG antibodies, there is a conserved site for glycosylation at HC-N297. The complex

biantennary *N*-glycan exists as a mixture of glycoforms, for example, serum IgG purified from a healthy individual may contain up to 33 different major and minor glycoforms.<sup>330,331</sup> Each glycoform contains a core heptasaccharide alongside additional monosaccharides. The majority of therapeutic mAbs produced in CHO or HEK293 cell lines contain a mixture of G0F, G1F and G2F glycoforms where G = galactose, F = fucose, and numbers (0–2) indicate the number of terminal galactose moieties (Fig. 21).<sup>332</sup> Conjugation of ADC payloads to the *N*-glycan is attractive as: (1) it is spatially distant from the complementarity determining regions (CDRs) through which antibody-antigen recognition occurs; (2) the glycosylation pattern is well conserved across antibody types, which simplifies widespread modification of antibodies; and 3) the carbohydrate is chemically distinct from the polypeptide backbone of the antibody, enabling site-specific conjugation.

#### 4.1 Antibody glycoengineering *via* oxidation

Since the 1960s, glycans of glycoproteins have been utilised as a site for conjugation for a variety of labelling applications.

Early methods relied on the oxidation of vicinal *cis* diols present at the glycan terminus.<sup>333</sup> In 1984, O'Shannessy *et al.* described a new method for antibody biotinylation *via* sodium periodate ( $\text{NaIO}_4$ )-mediated oxidation of terminal monosaccharide *cis* diols to aldehydes.<sup>334</sup> Reaction with biotin-hydrazide then produced a biotin labelled antibody containing a hydrazone linkage. In a similar approach, Chua *et al.* reported the use of both periodate and galactose oxidase to produce reactive aldehydes on terminal galactose residues, which similarly utilised hydrazide-functionalised payloads to afford antibody modification.<sup>335</sup>

This strategy was first applied to ADC production in 1989 by Laguzza *et al.* who modified a series of antibodies *via* reaction of hydrazide-modified vinca alkaloid cytotoxins with periodate-generated aldehydes on the antibody glycan. Using this method, ADCs were obtained in high yield with DARs ranging from 4–6.<sup>336</sup> Similarly, in 1993, Hinman *et al.* prepared hydrazide-functionalised calicheamicin derivatives, which were conjugated to the oxidised glycans of an anti-MUC1 antibody. The produced ADCs retained target antigen binding and were selectively cytotoxic to antigen positive cells *in vitro* and efficacious in an *in vivo* mouse model.<sup>337</sup> Finally, in 1999, Stan *et al.* produced ADCs by a procedure involving antibody desialylation (using neuraminidase) followed by galactose oxidation (using galactose oxidase).<sup>338</sup> Conjugation of doxorubicin was subsequently achieved *via* reaction of its daunosamine motif with the oxidised galactose units to produce ADCs with a DAR of 3.7. This ADC was almost four times more efficacious than an analogous lysine-conjugated ADC with an average DAR of 7.8 in an *in vivo* xenograft mouse model. It was hypothesised that the superior homogeneity of the site-specific galactose conjugated ADC generated an enhanced pharmacokinetic profile, thus explaining these observations.

These approaches effectively demonstrated that the *N*-glycan offers an alternative modification site to amino acids. However, early methods did not account for the innate heterogeneity of antibody glycans, which exist as a mixture of glycoforms. Therefore, the direct oxidation of antibodies with varying levels of oxidisable glycan fucose, galactose and sialic acid residues still resulted in a heterogeneous mixture of conjugates. To overcome this, Neri and co-workers developed a cell line that enabled the production of an anti-fibronectin F8 antibody consisting solely of the G0F glycoform.<sup>339</sup> Periodate oxidation of the antibody fucose residues produced in this cell line then provided excellent conversion to the desired product (>95% conversion) with a single aldehyde on each heavy chain (Fig. 21B). Treatment of the aldehyde-containing antibody with a hydrazine-modified auristatin cytotoxin, produced a homogeneous ADC with a DAR of 2.

A drawback of this fucose oxidation method is the high concentrations of  $\text{NaIO}_4$  (10 mM) required. Such high concentrations are known to cause unwanted oxidation of other amino acid side chains of the antibody. Particularly, oxidation of the methionine residues (HC-M252 and HC-M428) in the neonatal Fc receptor (FcRN) binding site can decrease FcRN binding and thus reduces the serum half-life of the antibody and the overall efficacy of the therapeutic.<sup>340,341</sup> To avoid such high oxidant

concentrations, Zhou *et al.* have developed a method to introduce periodate-sensitive sialic acid residues into the antibody *N*-glycan.<sup>342</sup> The *N*-glycan was first enzymatically remodelled *in vitro* using  $\beta$ -1,4-galactosyltransferase ( $\beta$ -1,4-Gal-T1) and  $\alpha$ -2,6-sialyltransferase (Sia T) to transfer galactose and sialic residues onto the native glycans (Fig. 21A). This produced near homogeneous monosialylated glycans. The two installed terminal sialic acids could then be oxidised with just 1 mM  $\text{NaIO}_4$  and conjugated to aminoxy functionalised drugs to produce homogeneous ADCs with oxime linkages. This strategy was shown to be effective on three antibodies; in one such example, an anti-HER2 antibody was modified with two different cytotoxic payloads, producing ADCs with DARs of 1.6 and 3.9. These ADCs demonstrated good *in vitro* activity and specificity toward HER2 positive cells. Despite the significant decrease in  $\text{NaIO}_4$  required, ~30% of HC-M252 and ~10% of HC-M428 residues were oxidised during this reaction, resulting in a 10% reduction in FcRN binding compared to the trastuzumab control. However, this small reduction of FcRN binding only had a marginal effect on serum half-life *in vivo*. In addition to the use of 10-fold lower periodate concentrations, this method also produces stable oxime linkages, superior to hydrazone linkages that have displayed liability in circulation and associated off-target payload release.<sup>336</sup>

A drawback of the oxidative sialate method is the low drug loading capability compared to other amino acid conjugation methods: only one sialic acid is introduced per heavy chain, despite the presence of two galactose acceptors, and the oxime ligation reaction at these sites has garnered capricious conjugation efficiencies, with variable DAR ADCs produced. To fully exploit the utility of this method, optimisation of the conjugation reaction to improve the homogeneity of the synthesised ADCs is desirable. To this end, Huang *et al.* have recently reported the development of 2-aminobenzamidoxime (ABAO) and mercaptoethylpyrazolone (ThioPz) reagents to expand the structural diversity of linkers used in glycosite-specific ADCs (Fig. 21).<sup>343</sup> Both reagents were shown to react efficiently, rapidly and selectively with *N*-glycan aldehydes produced by chemoenzymatic glycan remodelling, as previously described.<sup>342</sup> The resulting ADCs displayed high levels of homogeneity and selective *in vitro* cytotoxicity. Importantly, the ADCs were also highly stable under physiological conditions, in contrast to hydrazone linked ADCs often generated by glycan conjugation. Furthermore, a ThioPz-derived antibody conjugate displayed a plasma half-life that was superior to that of an analogous oxime conjugate. Therefore, these reagents may enable further optimisation of the overall pharmacological properties of glycosite-specific ADCs and enable the wider application of glycan conjugation in the future.

#### 4.2 Endoglycosidase for glycan remodelling

Endoglycosidases are enzymes that catalyse the hydrolytic cleavage of polysaccharide chains between non-terminal sugar residues.<sup>344</sup> Their complementary glycosynthases, typically generated from site-specific mutations at the active sites, can catalyse transglycosylation, whereby upon hydrolysis, a sugar



moiety is attached to the new terminal residue. Several endoglycosidases have been discovered that exhibit specific activity to trim and functionalise the core structure of the glycan chains on antibodies. For example, both Endo-A from *Arthrobacter protophormiae* and Endo-H from *Streptomyces plicatus* are specific for high-mannose type *N*-glycans and Endo-D from *Streptococcus pneumoniae* targets the chitobiose core of *N*-glycans.<sup>345–348</sup> However, the use of wild-type endoglycosidase for the modification of antibody glycans is limited as only native *N*-glycan donors are tolerated and both the products and substrates can be hydrolysed *via* a substrate-assisted mechanism resulting in low transglycosylation yields (5–20%) (Fig. 22).<sup>332,348</sup> To overcome these limitations, several studies have explored the use of sugar oxazolines, (intermediate mimicking substrates), as the activated donor substrates for the modification of glycoproteins.<sup>348</sup> This strategy generally involves two steps; first, *N*-glycan chains are trimmed by a native endoglycosidase, which is subsequently followed by transglycosylation with an engineered endoglycosidase to attach a new, non-native sugar moiety.<sup>332</sup>

In 2012, Goodfellow *et al.* reported that Endo-S, a bacterial endoglycosidase from *Streptococcus pyogenes*, performs efficient remodelling of complex biantennary antibody *N*-glycan chains.<sup>349</sup> Later that year, Wang and co-workers identified D233 in Endo-S as a key residue in promoting the formation of oxazolinium ion intermediate, which thus contributes to the undesired hydrolysis of polysaccharide substrates.<sup>350</sup> The mutation of D233 to alanine or glutamine prevents the catalytic hydrolysis of polysaccharides while maintaining the glycosylation efficiency with sugar oxazoline donors. Thus, two resulting glycosynthase mutants, Endo-S-D233A and Endo-S-D233Q, were generated. Indeed, both enzymes showed remarkable efficiency in transglycosylating the core-GlcNAcs of intact antibodies from glycan oxazolines with high yield (Fig. 22). To demonstrate the utility of this strategy, rituximab was deglycosylated with wild-type Endo-S and transglycosylated by reaction with azide-oxazoline  $\text{N}_3\text{-Man}_3\text{-GlcNAc}$  under Endo-S-D233Q catalysis to generate a homogeneous antibody with four bioorthogonally reactive azide handles.

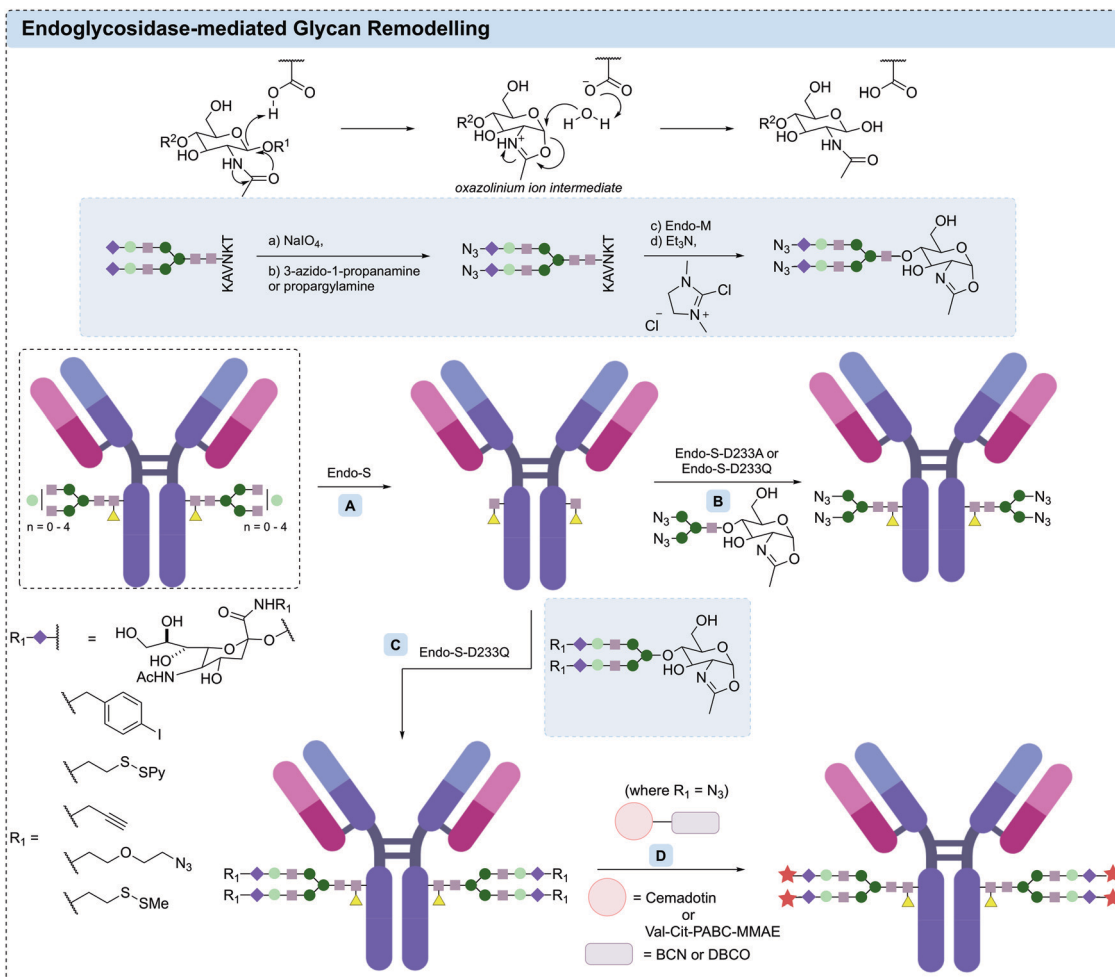


Fig. 22 Wild-type endoglycosidase can catalyse the hydrolysis of antibody glycans *via* a substrate-assisted mechanism. Endoglycosidases and their glycosynthases-mediated glycan remodelling strategy: (A) deglycosylating antibody with Endo-S to unveil the innermost GlcNAc; (B) transglycosylation of core-GlcNAc of intact antibody with  $\text{N}_3\text{-Man}_3\text{-GlcNAc}$  under the catalysis of either Endo-S-D233A or Endo-S-D233Q; (C) Endo-S-D233Q-catalysed transglycosylation of core-GlcNAc of intact antibody with biantennary sugar oxazolines bearing reactive handles; (D) subsequent SPAAC reaction with cytotoxic payloads to generate ADCs with controlled DAR ratio.



The homogeneous glycoforms generated from evolved Endo-S catalysed glycan-trimming or transglycosylation has been widely used to study the effect of glycan modification on the binding affinity of antibody towards Fc $\gamma$  receptors, probing other biological activity, and for the generation of ADCs.<sup>351–354</sup> For example, Davis and co-workers chemically functionalised the terminal sialic acid residues of biantennary sugar oxazolines with various reactive handles, including alkyne, azide, disulfide and phenyliodide moieties, and incorporated these oxazoline derivatives onto trastuzumab using the Endo-S-D233Q mutant (Fig. 22).<sup>353</sup> The remodelled trastuzumab bearing azide handles were

conjugated with cemadotin *via* a SPAAC reaction to generate heterogeneous ADCs with DARs of 2, 3 and 4 (Fig. 22). Compared to unfunctionalised trastuzumab, the DAR 3 ADC displayed enhanced *in vitro* cytotoxicity against HER2-positive SK-BR-3 cells with an EC<sub>50</sub> of ~800 pM.

Several studies have used directed evolution to optimise endoglycosidase transglycosylation of antibodies.<sup>355–361</sup> Huang and co-workers have recently described the use of two of these enzymes (Endo-M and Endo-S-D233Q) to facilitate the efficient attachment of azide-containing sialic acid residues (Fig. 23).<sup>362</sup> Subsequent CuAAC was used to attach cleavable

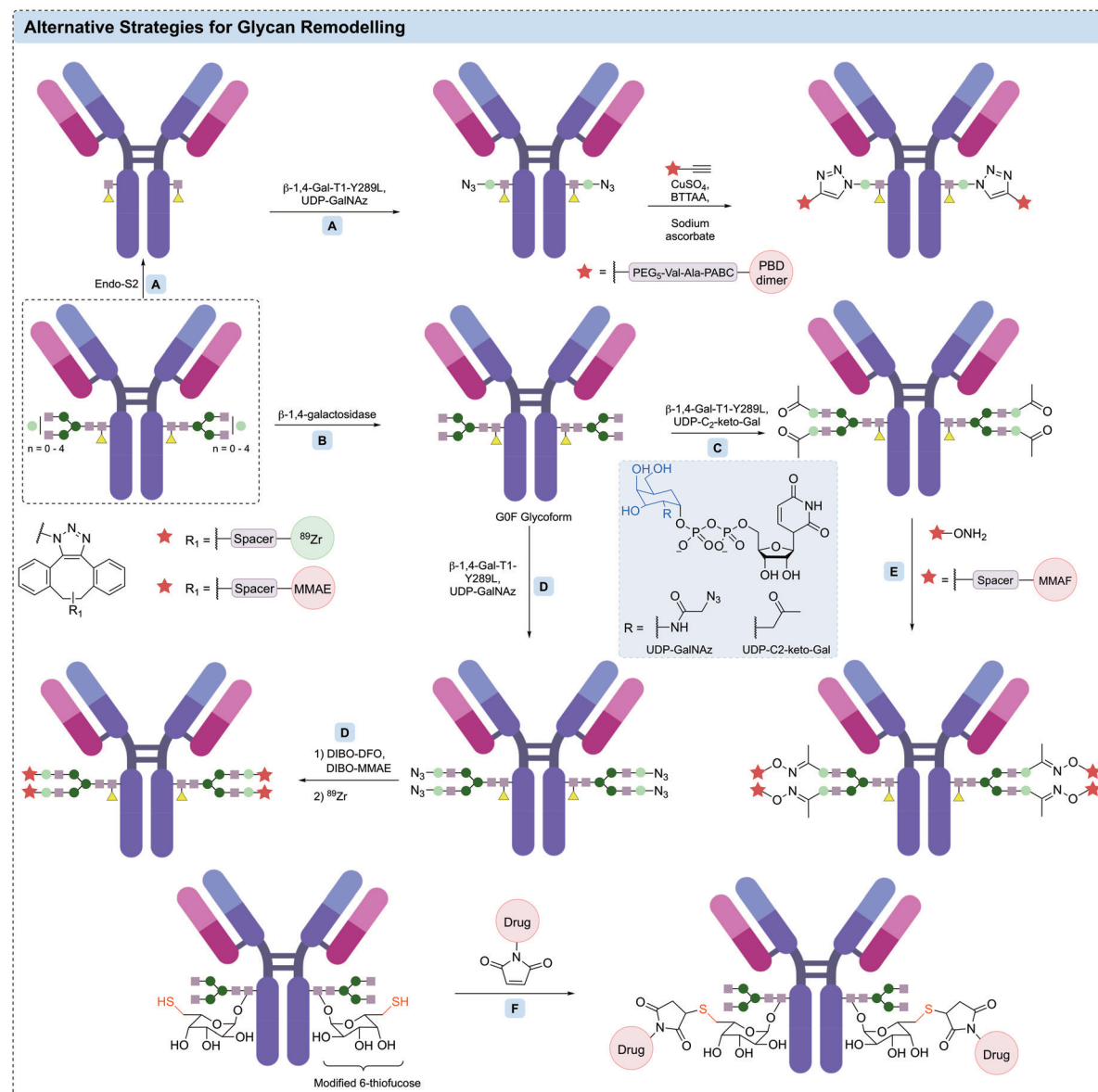


Fig. 23  $\beta$ -1,4-Galactosyltransferases and fucosyltransferase for glycan remodelling: (A)  $\beta$ -1,4-Gal-T1-Y289L-catalysed transglycosylation of core-GlcNAc of intact antibody followed by CuAAC reaction to PBD dimer led to the generation of a prostate-cancer-cell-targeting ADC; (B)  $\beta$ -1,4-galactosidase-catalysed trimming of heterogeneous antibody to give GOF glycoform; (C) incorporation of C2-keto-Gal on GOF glycoform under the catalysis of  $\beta$ -1,4-Gal-T1-Y289L; (D) incorporation of GalNAz on GOF glycoform under the catalysis of  $\beta$ -1,4-Gal-T1-Y289L followed by CuAAC reaction to generate a <sup>89</sup>Zr-MMAE dual labelled ADC; (E) oxime ligation with MMAF payload to generate an ADC with a DAR of 4; (F) Michael addition of maleimide-drug molecule to modified 6-thiogalactose residues of antibody glycans to generate an ADC with improved homogeneity.



and non-cleavable MMAE payloads, generating homogeneous ADCs with a DAR of 3.8. *In vitro* evaluation of these ADCs revealed that the ADC bearing a cleavable Val-Cit motif more efficiently inhibited the growth of HER2-positive SK-BR-3 cells with an EC<sub>50</sub> of 0.09 µg mL<sup>-1</sup>, compared to the commercial trastuzumab (EC<sub>50</sub> of 0.4 µg mL<sup>-1</sup>).

Overall, the development of glycan trimming techniques using endoglycosidases and their corresponding glycosynthases has proved to be an efficient method for providing access to homogeneous antibody glycoforms, which can then be functionalised using other glycan modification techniques (*i.e.* oxidation to terminal aldehydes) to allow bioconjugation of payloads and ultimately facilitate synthesis of homogeneous ADCs.

#### 4.3 β-1,4-Galactosyltransferases

Another key glycan remodelling method that has emerged in the past two decades is the use of evolved β-1,4-galactosyltransferase (β-1,4-Gal-T1) mutants, which have the ability to incorporate modified *N*-acetylgalactosamine (GalNAc) moieties to terminal *N*-acetylglucosamine (GlcNAc) residues on the antibody glycan. β-1,4-Gal-T1 is a type of glycosyltransferase that transfers galactose (Gal) from its uridine diphosphate (UDP)-precursor to GlcNAc residues at the non-reducing end of glycoprotein carbohydrates.<sup>363,364</sup> A single point mutation (β-1,4-Gal-T1-Y289L) was shown to significantly increase the efficiency of GalNAc transfer whilst retaining high GlcNAc transfer activity (Fig. 23).<sup>363</sup>

In 2009, Qasba and co-workers described the first site-specific antibody conjugation *via* β-1,4-Gal-T1-Y289L catalysis using C2-keto-Gal and *N*-azidoacetylgalactosamine (GalNAz) as donor substrates.<sup>365</sup> First, four therapeutic antibodies were trimmed by β-1,4-galactosidase to remove any terminal galactose residues. The resulting homogeneous G0 glycoforms were then galactosylated with either C2-keto-Gal and GalNAz in excellent efficiency *via* β-1,4-Gal-T1-Y289L catalysis, followed by functionalisation of the azide or ketone handles. For example, a fluorophore-antibody conjugate was generated by oxime ligation of C2-keto galactosylated trastuzumab with AlexaFluor 488 C<sub>5</sub>-aminoxyacetamide. Pleasingly, both ELISA and fluorescence activated cell sorting (FACS) analysis indicated that the antigen-binding function of the antibodies remained unaltered after glycan remodelling and functionalisation.

The first ADC generated using the β-1,4-Gal-T1-Y289L remodelling strategy was reported by Zhu *et al.* in 2014.<sup>366</sup> The G2F glycoform of the HER2 targeting antibody, m860 was modified using β-1,4-Gal-T1-Y289L to incorporate terminal C2-keto-Gal residues. Conjugation of an aminoxy MMAF derivative *via* oxime ligation generated an anti-HER2 ADC with a DAR of 4. This ADC maintained comparable binding affinity towards Fc<sub>γ</sub>RIIIa and Fc<sub>γ</sub>RI receptors to that of the native antibody, and exhibited potent *in vitro* cell-killing activity towards HER2-positive JIMT-1 breast cancer cells, which are trastuzumab-resistant.

A similar strategy has also been applied to the modification of an anti-EphA2 antibody.<sup>367</sup> First, the glycan of the anti-EphA2 antibody was almost completely removed using the

Endo-S2 glycosidase, which cut after the first GlcNAc on the antibody. GalNAz residues were then installed *via* β-1,4-Gal-T1-Y289L catalysis, followed by CuAAC reaction to conjugate the PBD dimer payload, SG3364. This generated a DAR 2 ADC, which displayed enhanced *in vitro* cell-killing activity against prostate cancer cells and successfully suppressed tumour growth over 42 days in an *in vivo* mouse xenograft model.

This three-step strategy (use of Endo-S glycan trimming, GalNAz addition *via* β-1,4-Gal-T1-Y289L followed by CuAAC-mediated payload attachment), termed GlycoConnect<sup>TM</sup>, has also been applied to the generation of superior anti-HER2 ADCs with enhanced activity compared to T-DM1.<sup>368</sup> In this study, doxorubicin, MMAF, maytansine and duocarmycin SA were all conjugated *via* click-reactions with the azido-modified trastuzumab variants, to generate a library of ADCs with a defined DAR of 2. ADCs bearing either cleavable or non-cleavable linkers all displayed remarkable cell-killing activity against a HER2-positive cell line (SK-BR-3), while having little effect against a HER2-negative cell line (MDA-MB-231). In a subsequent mouse PDX model, both cleavable and non-cleavable trastuzumab-MMAF conjugates resulted in complete tumour regression after a single administration at 9 mg kg<sup>-1</sup>. In contrast, at the same concentration, the approved anti-HER2 ADC Kadlecyl<sup>®</sup> was significantly less efficacious.

The deglycosylation-remodelling strategy has also been widely applied to generate radioimmunoconjugates. For example, in 2013, Zeglis *et al.* applied the chemoenzymatic strategy for site-selective radiolabeling of antibody glycans through a modular four-step approach.<sup>369</sup> After deglycosylating the prostate-specific membrane antigen (PSMA)-targeting antibody J591 with β-1,4-galactosidase, a GalNAz residue was incorporated on the glycan chains of J591 by β-1,4-Gal-T1-Y289L catalysis. A chelator-modified DIBO was then introduced to the glycan *via* a SPAAC reaction at room temperature, followed by radiolabeling with <sup>89</sup>Zr. This formed a radioimmunoconjugate with an average chelator-to-antibody ratio of 2.8. In their following work, the deglycosylation-remodelling strategy was optimised into a one-pot reaction in which GalNAz was incorporated into the Fc-glycan of a colorectal cancer-targeting antibody huA33, followed by modification with AlexaFluor 680 and radiolabelling with <sup>89</sup>Zr to generate a dual functionalised radioimmunoconjugate with 3.4 <sup>89</sup>Zr/mAb and 1.6 AlexaFluor 680/mAb.<sup>370</sup>

Recently, Zeglis and co-workers have applied this one-pot deglycosylation-remodelling strategy to generate a HER2-targeting ADC for use in PET imaging (Fig. 23). First, a GalNAz moiety was installed on native trastuzumab *via* β-1,4-galactosidase deglycosylation and subsequent β-1,4-Gal-T1-Y289L glycosidation.<sup>371</sup> Subsequent SPAAC reaction with a 1:1 mixture of MMAE-DIBO and chelator-DIBO, followed by <sup>89</sup>Zr radiolabeling lead to the formation of an ADC with an average DAR of 1.7 and 2.1 <sup>89</sup>Zr/mAb. This dual functionalised ADC was then evaluated in an *in vivo* study in athymic nude mice bearing subcutaneous HER2-expressing BT474 xenografts. Treatment at 10 mg kg<sup>-1</sup> resulted in a 90% reduction of tumour volume over 20 days, while the administration of 10 mg kg<sup>-1</sup> native trastuzumab did not result in significant tumour reduction (<30%).



#### 4.4 Other glycan remodelling techniques

Finally, site-specific glycan modification has also been achieved by hijacking the pathway that attaches fucose residues to antibody carbohydrates.<sup>372</sup> By introducing modified fucose-substrates into CHO cell lines, these unnatural fucoses can be incorporated in antibody glycans in place of fucose by fucosyltransferases. For example, 6-thiogalactose peracetate, which contains a reactive thiol handle for site-specific glycan conjugation has been incorporated into a range of antibodies with 60–70% efficiency. A reduction and re-oxidation strategy allowed specific attachment of drug payloads to the glycan 6-thiogalactose, producing ADCs with improved homogeneity compared to those produced by conjugation through hinge region disulfides (Fig. 23). Additionally, the conjugates had improved resistance toward retro-Michael addition reactions, resulting in improved stability compared to cysteine thiol-maleimide ADCs. Although further investigation of these ADCs *in vivo* is warranted, this method also avoids unwanted methionine oxidation encountered by glycan oxidation strategies, and the ADCs produced demonstrated superior cytotoxicity compared to their heterogeneous counterparts.

Glycan engineering encompasses a broad range of techniques to provide access to homogeneous ADCs, with specific conjugation at a site that does not negatively impact antibody–antigen binding. Additionally, glycoengineering approaches avoid the need to engineer the amino acid sequence. However, they do require specific reagents, enzymes and enzyme mutants and are limited in drug loading capabilities. Furthermore, evaluation of the effects of glycan modification on Fc–Fc receptor interactions on the overall pharmacology of these ADCs will be important in further development.

## 5 Conclusions and outlook

From first generation ADCs that were primarily synthesised *via* stochastic lysine or cysteine modification, it is clear that significant advances have been made in site-selective antibody modification enabling the widespread synthesis of homogeneous ADCs. Each of these new methodologies has their own advantages and disadvantages (Table 1). Indeed, there are several instances of contrasting biological results obtained for the same (or highly similar) synthetic strategies with differing antibodies or payloads.

In addition to the conjugation methodologies, it is paramount that suitable analytical techniques are available to study the reactions and the resulting ADC product. These techniques will also be required to study the *in vivo* metabolism or biotransformation of these ADCs. Combining techniques such as native mass spectrometry and chromatographic analysis (e.g. HIC or HPLC) will be useful in this regard.<sup>373</sup> It is clear that the technological capability is already in place to achieve this. However, widespread dissemination of the precise methods and set-up parameters is required to further expand their utility.

As we move into an era where a larger number of ADCs synthesised using site-selective modification methods are undergoing clinical evaluation, a significant increase in data regarding the clinical effects of site-selectivity will be obtained. Utilisation of artificial intelligence and machine learning by the ADC community may help accelerate development procedures by highlighting the most beneficial conjugation method for a particular disease-target-antibody-drug-linker combination. However, thus far, these have proven inherently difficult to predict and it is unclear if machine learning technologies will be able to do so in the near future.

**Table 1** Brief summary of the benefits and limitations of the various technologies used for site-selective modification in antibody–drug conjugates

| Technology                | Benefits  | Limitations   |
|---------------------------|---|---|
| Engineered cysteines      | <ul style="list-style-type: none"> <li>Homogeneity</li> <li>Tunable reactivity/stability through site of modification alteration</li> </ul> | <ul style="list-style-type: none"> <li>Genetic engineering required</li> <li>Typically limited to DAR 2</li> </ul>                      |
| Disulfide rebridging      | <ul style="list-style-type: none"> <li>Homogeneity</li> <li>Native amino acid sequence and glycosylation</li> </ul>                         | <ul style="list-style-type: none"> <li>Intrachain misbridging</li> <li>Typically limited to DAR 4</li> </ul>                            |
| Non-canonical amino acids | <ul style="list-style-type: none"> <li>Homogeneity</li> <li>Tunable reactivity/stability through site of modification alteration</li> </ul> | <ul style="list-style-type: none"> <li>Genetic engineering required</li> <li>Lower antibody expression yields often observed</li> </ul> |
| Terminus modification     | <ul style="list-style-type: none"> <li>Homogeneity</li> <li>DAR alteration possible</li> </ul>  | <ul style="list-style-type: none"> <li>Genetic engineering required</li> <li>Modification may affect binding interactions</li> </ul>    |
| Transglutaminase          | <ul style="list-style-type: none"> <li>Homogeneity</li> <li>DAR alteration possible</li> </ul>  | <ul style="list-style-type: none"> <li>Often requires aglycosylated/deglycosylated antibodies or genetic engineering</li> </ul>         |
| Other enzymatic methods   | <ul style="list-style-type: none"> <li>Homogeneity</li> <li>DAR alteration possible</li> </ul>  | <ul style="list-style-type: none"> <li>Typically require genetic engineering to install recognition sequence</li> </ul>                 |
| Glycan modification       | <ul style="list-style-type: none"> <li>Homogeneity</li> <li>No alteration of amino acid sequence</li> </ul>                                 | <ul style="list-style-type: none"> <li>Glycosylation profile is important in immune recognition</li> </ul>                              |



Ultimately, widespread further use of many of the methods described here will rely on the clinical success of themselves or analogous counterparts. It is possible that a single method will emerge as the most suitable for widespread ADC development. However, it is equally possible that this will not occur or that a single method will become prevalent for specific payloads, antibodies or indications.

## Conflicts of interest

There are no conflicts to declare.

## Acknowledgements

J. D. B. acknowledges an iCASE studentship from GlaxoSmithKline and the EPSRC. F. M. D. acknowledges the BBSRC and AstraZeneca for funding. A. H. acknowledges the EPSRC and Cambridge Trusts for funding. H. S. A. J. C. and X. O. acknowledges Trinity College Cambridge for a Geoffrey Moorehouse Gibson Scholarship, a Krishnan-Ang Studentship and a Trinity Henry-Barlow Scholarship, respectively. Y. T. acknowledges financial support from The Uehara Memorial Foundation and the JSPS for a Research Fellowship for Young Scientists. The Spring lab acknowledges general lab support from the EPSRC, BBSRC, MRC and Royal Society.

## References

- 1 P. J. Kennedy, C. Oliveira, P. L. Granja and B. Sarmento, *Pharmacol. Ther.*, 2017, **177**, 129–145.
- 2 J. R. Adair, P. W. Howard, J. A. Hartley, D. G. Williams and K. A. Chester, *Expert Opin. Biol. Ther.*, 2012, **12**, 1191–1206.
- 3 N. Jain, S. W. Smith, S. Ghone and B. Tomczuk, *Pharm. Res.*, 2015, **32**, 3526–3540.
- 4 L. Gauzy-Lazo, I. Sassoon and M.-P. P. Brun, *SLAS Discovery*, 2020, 1–26.
- 5 M. Nejadmojhaddam, A. Minai-tehrani and R. Ghahremanzadeh, *Avicenna J. Med. Biotechnol.*, 2019, **11**, 3–23.
- 6 P. F. Bross, J. Beitz, G. Chen, X. H. Chen, E. Duffy, L. Kieffer, S. Roy, R. Sridhara, A. Rahman, G. Williams and R. Pazdur, *Clin. Cancer Res.*, 2001, **7**, 1490–1496.
- 7 Y. N. Lamb, *Drugs*, 2017, **77**, 1603–1610.
- 8 A. Ballantyne and S. Dhillon, *Drugs*, 2013, **73**, 755–765.
- 9 N. C. Richardson, Y. L. Kasamon, H. Chen, R. A. de Claro, J. Ye, G. M. Blumenthal, A. T. Farrell and R. Pazdur, *Oncologist*, 2019, **24**, e180–e187.
- 10 E. D. Deeks, *Drugs*, 2019, **79**, 1467–1475.
- 11 K. S. Hanna, *Drugs*, 2020, **80**, 1–7.
- 12 S. J. Keam, *Drugs*, 2020, **80**, 501–508.
- 13 Y. Y. Syed, *Drugs*, 2020, **80**, 1019–1025.
- 14 H. K. Erickson, W. C. Widdison, M. F. Mayo, K. Whiteman, C. Audette, S. D. Wilhelm and R. Singh, *Bioconjugate Chem.*, 2010, **21**, 84–92.
- 15 R. M. DeVay, K. Delaria, G. Zhu, C. Holz, D. Foletti, J. Sutton, G. Bolton, R. G. Dushin, C. Bee, J. Pons, A. Rajpal, H. Liang, D. Shelton, S.-H. Liu and P. Strop, *Bioconjugate Chem.*, 2017, **28**, 1102–1114.
- 16 B. Nolting, *Methods Mol. Biol.*, 2013, **1045**, 71–100.
- 17 P. R. Hamann, L. M. Hinman, I. Hollander, C. F. Beyer, D. Lindh, R. Holcomb, W. Hallett, H. R. Tsou, J. Upeslacis, D. Shochat, A. Mountain, D. A. Flowers and I. Bernstein, *Bioconjugate Chem.*, 2002, **13**, 47–58.
- 18 G. D. Lewis Phillips, G. Li, D. L. Dugger, L. M. Crocker, K. L. Parsons, E. Mai, W. A. Blättler, J. M. Lambert, R. V. J. Chari, R. J. Lutz, W. L. T. Wong, F. S. Jacobson, H. Koeppen, R. H. Schwall, S. R. Kenkare-Mitra, S. D. Spencer and M. X. Sliwkowski, *Cancer Res.*, 2008, **68**, 9280–9290.
- 19 T. H. Pillow, J. D. Sadowsky, D. Zhang, S. F. Yu, G. Del Rosario, K. Xu, J. He, S. Bhakta, R. Ohri, K. R. Kozak, E. Ha, J. R. Junutula and J. A. Flygare, *Chem. Sci.*, 2016, **8**, 366–370.
- 20 S. O. Doronina, B. E. Toki, M. Y. Torgov, B. A. Mendelsohn, C. G. Cerveny, D. F. Chace, R. L. DeBlanc, R. P. Gearing, T. D. Bovee, C. B. Siegall, J. A. Franciseo, A. F. Wahl, D. L. Meyer and P. D. Senter, *Nat. Biotechnol.*, 2003, **21**, 778–784.
- 21 J. C. Kern, D. Dooney, R. Zhang, L. Liang, P. E. Brandish, M. Cheng, G. Feng, A. Beck, D. Bresson, J. Firdos, D. Gately, N. Knudsen, A. Manibusan, Y. Sun and R. M. Garbaccio, *Bioconjugate Chem.*, 2016, **27**, 2081–2088.
- 22 J. C. Kern, M. Cancilla, D. Dooney, K. Kwasnjuk, R. Zhang, M. Beaumont, I. Figueroa, S. C. Hsieh, L. Liang, D. Tomazela, J. Zhang, P. E. Brandish, A. Palmieri, P. Stivers, M. Cheng, G. Feng, P. Geda, S. Shah, A. Beck, D. Bresson, J. Firdos, D. Gately, N. Knudsen, A. Manibusan, P. G. Schultz, Y. Sun and R. M. Garbaccio, *J. Am. Chem. Soc.*, 2016, **138**, 1430–1445.
- 23 S. C. Jeffrey, J. B. Andreyka, S. X. Bernhardt, K. M. Kissler, T. Kline, J. S. Lenox, R. F. Moser, M. T. Nguyen, N. M. Okeye, I. J. Stone, X. Zhang and P. D. Senter, *Bioconjugate Chem.*, 2006, **17**, 831–840.
- 24 S. Kolodych, C. Michel, S. Delacroix, O. Koniev, A. Ehkirch, J. Eberova, S. Cianfréani, B. Renoux, W. Krezel, P. Poinot, C. D. Muller, S. Papot and A. Wagner, *Eur. J. Med. Chem.*, 2017, **142**, 376–382.
- 25 J. D. Bargh, S. J. Walsh, A. Isidro-Llobet, S. Omarjee, J. S. Carroll and D. R. Spring, *Chem. Sci.*, 2020, **11**, 2375–2380.
- 26 J. D. Bargh, A. Isidro-Llobet, J. S. Parker and D. R. Spring, *Chem. Soc. Rev.*, 2019, **48**, 4361–4374.
- 27 G. Vidarsson, G. Dekkers and T. Rispens, *Front. Immunol.*, 2014, **5**, 520.
- 28 R. M. Hoffmann, B. G. T. Coumbe, D. H. Josephs, S. Mele, K. M. Ilieva, A. Cheung, A. N. Tutt, J. F. Spicer, D. E. Thurston, S. Crescioli and S. N. Karagiannis, *Oncoimmunology*, 2018, **7**, e1395127.
- 29 H. Liu and K. May, *mAbs*, 2012, **4**, 17–23.
- 30 P. Herbener, K. Schönfeld, M. König, M. Germer, J. M. Przyborski, K. Bernöster and J. Schüttrumpf, *PLOS One*, 2018, **13**, e0195823.
- 31 A. F. Labrijn, A. O. Buijsse, E. T. J. Van Den Bremer, A. Y. W. Verwilligen, W. K. Bleeker, S. J. Thorpe, J. Killestein, C. H. Polman, R. C. Aalberse, J. Schuurman, J. G. J. Van De Winkel and P. W. H. I. Parren, *Nat. Biotechnol.*, 2009, **27**, 767–771.
- 32 A. Beck, L. Goetsch, C. Dumontet and N. Corvaia, *Nat. Rev. Drug Discovery*, 2017, **16**, 315–337.



33 K. T. Xenaki, S. Oliveira and P. M. P. van Bergen en Henegouwen, *Front. Immunol.*, 2017, **8**, 1287.

34 K. C. Nicolaou and S. Rigol, *Angew. Chem., Int. Ed.*, 2019, **58**, 11206–11241.

35 S. Yaghoubi, M. H. Karimi, M. Lotfinia, T. Gharibi, M. Mahi-Birjand, E. Kavi, F. Hosseini, K. Sineh Sepehr, M. Khatami, N. Bagheri and M. Abdollahpour-Alitappeh, *J. Cell. Physiol.*, 2020, **235**, 31–64.

36 D. J. Newman, *Mar. Drugs*, 2019, **17**, 324.

37 P. Khongorzul, C. J. Ling, F. U. Khan, A. U. Ihsan and J. Zhang, *Mol. Cancer Res.*, 2020, **18**, 3–19.

38 P. Strop, S.-H. Liu, M. Dorywalska, K. Delaria, R. G. Dushin, T.-T. Tran, W.-H. Ho, S. Farias, M. G. Casas, Y. Abdiche, D. Zhou, R. Chandrasekaran, C. Samain, C. Loo, A. Rossi, M. Rickert, S. Krimm, T. Wong, S. M. Chin, J. Yu, J. Dilley, J. Chaparro-Riggers, G. F. Filzen, C. J. O'Donnell, F. Wang, J. S. Myers, J. Pons, D. L. Shelton and A. Rajpal, *Chem. Biol.*, 2013, **20**, 161–167.

39 M. Dorywalska, P. Strop, J. A. Melton-Witt, A. Hasa-Moreno, S. E. Farias, M. Galindo Casas, K. Delaria, V. Lui, K. Poulsen, C. Loo, S. Krimm, G. Bolton, L. Moine, R. Dushin, T.-T. Tran, S.-H. Liu, M. Rickert, D. Foletti, D. L. Shelton, J. Pons and A. Rajpal, *Bioconjugate Chem.*, 2015, **26**, 650–659.

40 K. J. Hamblett, P. D. Senter, D. F. Chace, M. M. C. Sun, J. Lenox, C. G. Cerveny, K. M. Kissler, S. X. Bernhardt, A. K. Kopcha, R. F. Zabinski, D. L. Meyer and J. A. Francisco, *Clin. Cancer Res.*, 2004, **10**, 7063–7070.

41 J. R. Junutula, H. Raab, S. Clark, S. Bhakta, D. D. Leipold, S. Weir, Y. Chen, M. Simpson, S. P. Tsai, M. S. Dennis, Y. Lu, Y. G. Meng, C. Ng, J. Yang, C. C. Lee, E. Duenas, J. Gorrell, V. Katta, A. Kim, K. McDorman, K. Flagella, R. Venook, S. Ross, S. D. Spencer, W. Lee Wong, H. B. Lowman, R. Vandlen, M. X. Sliwkowski, R. H. Scheller, P. Polakis and W. Mallet, *Nat. Biotechnol.*, 2008, **26**, 925–932.

42 R. P. Lyon, T. D. Bovee, S. O. Doronina, P. J. Burke, J. H. Hunter, H. D. Neff-LaFord, M. Jonas, M. E. Anderson, J. R. Setter and P. D. Senter, *Nat. Biotechnol.*, 2015, **33**, 733–735.

43 X. Sun, J. F. Ponte, N. C. Yoder, R. Laleau, J. Coccia, L. Lanieri, Q. Qiu, R. Wu, E. Hong, M. Bogalhas, L. Wang, L. Dong, Y. Setiady, E. K. Maloney, O. Ab, X. Zhang, J. Pinkas, T. A. Keating, R. Chari, H. K. Erickson and J. M. Lambert, *Bioconjugate Chem.*, 2017, **28**, 1371–1381.

44 A. Bardia, I. A. Mayer, L. T. Vahdat, S. M. Tolaney, S. J. Isakoff, J. R. Diamond, J. O'Shaughnessy, R. L. Moroos, A. D. Santin, V. G. Abramson, N. C. Shah, H. S. Rugo, D. M. Goldenberg, A. M. Sweidan, R. Iannone, S. Washkowitz, R. M. Sharkey, W. A. Wegener and K. Kalinsky, *N. Engl. J. Med.*, 2019, **380**, 741–751.

45 T. Satomaa, H. Pynnönen, A. Vilkman, T. Kotiranta, V. Pitkänen, A. Heiskanen, B. Herpers, L. Price, J. Helin, J. Saarinen, T. Satomaa, H. Pynnönen, A. Vilkman, T. Kotiranta, V. Pitkänen, A. Heiskanen, B. Herpers, L. S. Price, J. Helin and J. Saarinen, *Antibodies*, 2018, **7**, 15.

46 W. Viricel, G. Fournet, S. Beaumel, E. Perrial, S. Papot, C. Dumontet and B. Joseph, *Chem. Sci.*, 2019, **10**, 4048–4053.

47 F. Lhospice, D. Brégeon, C. Belmant, P. Dennler, A. Chiotellis, E. Fischer, L. Gauthier, A. Boëdec, H. Rispaud, S. Savard-Chambard, A. Represa, N. Schneider, C. Paturel, M. Sapet, C. Delcambre, S. Ingoure, N. Viaud, C. Bonnafous, R. Schibli and F. Romagné, *Mol. Pharm.*, 2015, **12**, 1863–1871.

48 P. Agarwal and C. R. Bertozzi, *Bioconjugate Chem.*, 2015, **26**, 176–192.

49 C. D. Spicer and B. G. Davis, *Nat. Commun.*, 2014, **5**, 4740.

50 E. A. Hoyt, P. M. S. D. Cal, B. L. Oliveira and G. J. L. Bernardes, *Nat. Rev. Chem.*, 2019, **3**, 147–171.

51 T. Tamura and I. Hamachi, *J. Am. Chem. Soc.*, 2019, **141**, 2782–2799.

52 O. Boutureira and G. J. L. Bernardes, *Chem. Rev.*, 2015, **115**, 2174–2195.

53 G. T. Hermanson, *Bioconjugate Techniques*, Elsevier Inc., 3rd edn, 2013.

54 B. L. Oliveira, Z. Guo and G. J. L. Bernardes, *Chem. Soc. Rev.*, 2017, **46**, 4895–4950.

55 K. Lang and J. W. Chin, *ACS Chem. Biol.*, 2014, **9**, 16–20.

56 E. M. Sletten and C. R. Bertozzi, *Angew. Chem., Int. Ed.*, 2009, **48**, 6974–6998.

57 F. Searle, C. Bier, R. G. Buckley, S. Newman, R. B. Pedley, K. D. Bagshawe, R. G. Melton, S. M. Alwan and R. F. Sherwood, *Br. J. Cancer*, 1986, **53**, 377–384.

58 R. G. Melton, *Adv. Drug Delivery Rev.*, 1996, **22**, 289–301.

59 S. E. Winston, S. A. Fuller, M. J. Evelegh and J. G. R. Hurrell, *Curr. Protoc. Mol. Biol.*, 2000, **50**, 11.1.1–11.1.7.

60 T. E. Witzig, *Cancer Chemother. Pharmacol.*, 2001, **48**, S91–S95.

61 L. Wang, G. Amphlett, W. A. Blättler, J. M. Lambert and W. Zhang, *Protein Sci.*, 2005, **14**, 2436–2446.

62 A. Wakankar, Y. Chen, Y. Gokarn and F. S. Jacobson, *mAbs*, 2011, **3**, 164–175.

63 H.-W. Chih, B. Gikanga, Y. Yang and B. Zhang, *J. Pharm. Sci.*, 2011, **100**, 2518–2525.

64 S. Kalkhof and A. Sinz, *Anal. Bioanal. Chem.*, 2008, **392**, 305–312.

65 S. Mädler, C. Bich, D. Touboul and R. Zenobi, *J. Mass Spectrom.*, 2009, **44**, 694–706.

66 O. Koniev and A. Wagner, *Chem. Soc. Rev.*, 2015, **44**, 5495.

67 D. S. Wilbur, M. K. Chyan, H. Nakamae, Y. Chen, D. K. Hamlin, E. B. Santos, B. T. Kornblit and B. M. Sandmaier, *Bioconjugate Chem.*, 2012, **23**, 409–420.

68 M. Hayakawa, N. Toda, N. Carrillo, N. J. Thornburg, J. E. Crowe and C. F. Barbas, *ChemBioChem*, 2012, **13**, 2191–2195.

69 I. Dovgan, S. Ursuegui, S. Erb, C. Michel, S. Kolodych, S. Cianferani and A. Wagner, *Bioconjugate Chem.*, 2017, **28**, 1452–1457.

70 M. Moreau, O. Raguin, J. M. Vrigneaud, B. Collin, C. Bernhard, X. Tizon, F. Boschetti, O. Duchamp, F. Brunotte and F. Denat, *Bioconjugate Chem.*, 2012, **23**, 1181–1188.

71 M. M. C. Sun, K. S. Beam, C. G. Cerveny, K. J. Hamblett, R. S. Blackmore, M. Y. Torgov, F. G. M. Handley, N. C. Ihle, P. D. Senter and S. C. Alley, *Bioconjugate Chem.*, 2005, **16**, 1282–1290.

72 P. L. Ross and J. L. Wolfe, *J. Pharm. Sci.*, 2016, **105**, 391–397.

73 H. Liu, C. Chumsae, G. Gaza-Bulseco, K. Hurkmans and C. H. Radziejewski, *Anal. Chem.*, 2010, **82**, 5219–5226.

74 P. A. Szijj, C. Bahou and V. Chudasama, *Drug Discovery Today Technol.*, 2018, **30**, 27–34.

75 B. Q. Shen, K. Xu, L. Liu, H. Raab, S. Bhakta, M. Kenrick, K. L. Parsons-Reponte, J. Tien, S. F. Yu, E. Mai, D. Li, J. Tibbitts, J. Baudys, O. M. Saad, S. J. Scales, P. J. McDonald, P. E. Hass, C. Eigenbrot, T. Nguyen, W. A. Solis, R. N. Fuji, K. M. Flagella, D. Patel, S. D. Spencer, L. A. Khawli, A. Ebens, W. L. Wong, R. Vandlen, S. Kaur, M. X. Sliwkowski, R. H. Scheller, P. Polakis and J. R. Junutula, *Nat. Biotechnol.*, 2012, **30**, 184–189.

76 L. N. Tumey, M. Charati, T. He, E. Sousa, D. Ma, X. Han, T. Clark, J. Casavant, F. Loganzo, F. Barletta, J. Lucas and E. I. Graziani, *Bioconjugate Chem.*, 2014, **25**, 1871–1880.

77 R. J. Christie, R. Fleming, B. Bezabeh, R. Woods, S. Mao, J. Harper, A. Joseph, Q. Wang, Z. Q. Xu, H. Wu, C. Gao and N. Dimasi, *J. Controlled Release*, 2015, **220**, 660–670.

78 S. D. Fontaine, R. Reid, L. Robinson, G. W. Ashley and D. V. Santi, *Bioconjugate Chem.*, 2015, **26**, 145–152.

79 R. P. Lyon, J. R. Setter, T. D. Bovee, S. O. Doronina, J. H. Hunter, M. E. Anderson, C. L. Balasubramanian, S. M. Duniho, C. I. Leiske, F. Li and P. D. Senter, *Nat. Biotechnol.*, 2014, **32**, 1059–1062.

80 S. C. Alley, D. R. Benjamin, S. C. Jeffrey, N. M. Okeley, D. L. Meyer, R. J. Sanderson and P. D. Senter, *Bioconjugate Chem.*, 2008, **19**, 759–765.

81 E. V. Vinogradova, C. Zhang, A. M. Spokoyny, B. L. Pentelute and S. L. Buchwald, *Nature*, 2015, **526**, 687–691.

82 M.-A. Kasper, M. Glanz, A. Stengl, M. Penkert, S. Klenk, T. Sauer, D. Schumacher, J. Helma, E. Krause, M. C. Cardoso, H. Leonhardt and C. P. R. Hackenberger, *Angew. Chem., Int. Ed.*, 2019, **58**, 11625–11630.

83 M. Kasper, A. Stengl, P. Ochtrup, M. Gerlach, T. Stoschek, D. Schumacher, J. Helma, M. Penkert, E. Krause, H. Leonhardt and C. P. R. Hackenberger, *Angew. Chem., Int. Ed.*, 2019, **58**, 11631–11636.

84 M. A. Kasper, M. Glanz, A. Oder, P. Schmieder, J. P. Von Kries and C. P. R. Hackenberger, *Chem. Sci.*, 2019, **10**, 6322–6329.

85 R. Tessier, R. K. Nandi, B. G. Dwyer, D. Abegg, C. Sornay, J. Ceballos, S. Erb, S. Cianférani, A. Wagner, G. Chaubet, A. Adibekian and J. Waser, *Angew. Chem., Int. Ed.*, 2020, **59**, 10961–10970.

86 C. F. McDonagh, E. Turcott, L. Westendorf, J. B. Webster, S. C. Alley, K. Kim, J. Andreyka, I. Stone, K. J. Hamblett, J. A. Francisco and P. Carter, *Protein Eng., Des. Sel.*, 2006, **19**, 299–307.

87 S. D. Gillies and J. S. Wesolowski, *Hum. Antibodies*, 1990, **1**, 47–54.

88 L. N. Tumey, F. Li, B. Rago, X. Han, F. Loganzo, S. Musto, E. I. Graziani, S. Putthenveetil, J. Casavant, K. Marquette, T. Clark, J. Bikker, E. M. Bennett, F. Barletta, N. Piché-Nicholas, A. Tam, C. J. O'Donnell, H. P. Gerber and L. Tchistiakova, *AAPS J.*, 2017, **19**, 1123–1135.

89 J. R. Junutula, S. Bhakta, H. Raab, K. E. Ervin, C. Eigenbrot, R. Vandlen, R. H. Scheller and H. B. Lowman, *J. Immunol. Methods*, 2008, **332**, 41–52.

90 R. Ohri, S. Bhakta, A. Fourie-O'Donohue, J. Dela Cruz-Chuh, S. P. Tsai, R. Cook, B. Wei, C. Ng, A. W. Wong, A. B. Bos, F. Farahi, J. Bhakta, T. H. Pillow, H. Raab, R. Vandlen, P. Polakis, Y. Liu, H. Erickson, J. R. Junutula and K. R. Kozak, *Bioconjugate Chem.*, 2018, **29**, 473–485.

91 J. R. Junutula, H. Raab, S. Clark, S. Bhakta, D. D. Leipold, S. Weir, Y. Chen, M. Simpson, S. P. Tsai, M. S. Dennis, Y. Lu, Y. G. Meng, C. Ng, J. Yang, C. C. Lee, E. Duenas, J. Gorrell, V. Katta, A. Kim, K. McDorman, K. Flagella, R. Venook, S. Ross, S. D. Spencer, W. Lee Wong, H. B. Lowman, R. Vandlen, M. X. Sliwkowski, R. H. Scheller, P. Polakis and W. Mallet, *Nat. Biotechnol.*, 2008, **26**, 925–932.

92 D. Shinmi, E. Taguchi, J. Iwano, T. Yamaguchi, K. Masuda, J. Enokizono and Y. Shiraishi, *Bioconjugate Chem.*, 2016, **27**, 1324–1331.

93 D. Sussman, L. Westendorf, D. W. Meyer, C. I. Leiske, M. Anderson, N. M. Okeley, S. C. Alley, R. Lyon, R. J. Sanderson, P. J. Carter and D. R. Benjamin, *Protein Eng., Des. Sel.*, 2018, **31**, 47–54.

94 N. Dimasi, R. Fleming, H. Zhong, B. Bezabeh, K. Kinneer, R. J. Christie, C. Fazenbaker, H. Wu and C. Gao, *Mol. Pharm.*, 2017, **14**, 1501–1516.

95 H. Uppal, E. Doudement, K. Mahapatra, W. C. Darbonne, D. Bumbaca, B. Q. Shen, X. Du, O. Saad, K. Bowles, S. Olsen, G. D. L. Phillips, D. Hartley, M. X. Sliwkowski, S. Girish, D. Dambach and V. Ramakrishnan, *Clin. Cancer Res.*, 2015, **21**, 123–133.

96 G. C. Kemp, A. C. Tiberghien, N. V. Patel, F. D'Hooge, S. M. Nilapwar, L. R. Adams, S. Corbett, D. G. Williams, J. A. Hartley and P. W. Howard, *Bioorganic Med. Chem. Lett.*, 2017, **27**, 1154–1158.

97 J. P. M. Nunes, V. Vassileva, E. Robinson, M. Morais, M. E. B. Smith, R. B. Pedley, S. Caddick, J. R. Baker and V. Chudasama, *RSC Adv.*, 2017, **7**, 24828–24832.

98 B. Bernardim, P. M. S. D. Cal, M. J. Matos, B. L. Oliveira, N. Martínez-Saéz, I. S. Albuquerque, E. Perkins, F. Corzana, A. C. B. Burtoloso, G. Jiménez-Osés and G. J. L. Bernardes, *Nat. Commun.*, 2016, **7**, 13128.

99 B. L. Oliveira, B. J. Stenton, V. B. Unnikrishnan, C. R. De Almeida, J. Conde, M. Negrão, F. S. S. Schneider, C. Cordeiro, M. G. Ferreira, M. G. Ferreira, G. F. Caramori, J. B. Domingos, R. Fior, G. J. L. Bernardes and G. J. L. Bernardes, *J. Am. Chem. Soc.*, 2020, **142**, 10869–10880.

100 M. J. Matos, C. D. Navo, T. Hakala, X. Ferhati, A. Guerreiro, D. Hartmann, B. Bernardim, K. L. Saar, I. Compañón, F. Corzana, T. P. J. Knowles, G. Jiménez-Osés and G. J. L. Bernardes, *Angew. Chem., Int. Ed.*, 2019, **58**, 6640–6644.

101 E. A. Hoyt, P. M. S. D. Cal, B. L. Oliveira and G. J. L. Bernardes, *Nat. Rev. Chem.*, 2019, **3**, 147–171.

102 P. Ochtrup and C. P. R. Hackenberger, *Curr. Opin. Chem. Biol.*, 2020, **58**, 28–36.

103 J. M. J. M. Ravasco, H. Faustino, A. Trindade and P. M. P. Gois, *Chem. – Eur. J.*, 2019, **25**, 43–59.

104 J. D. Sadowsky, T. H. Pillow, J. Chen, F. Fan, C. He, Y. Wang, G. Yan, H. Yao, Z. Xu, S. Martin, D. Zhang, P. Chu, J. Dela Cruz-Chuh, A. O'Donohue, G. Li, G. Del



Rosario, J. He, L. Liu, C. Ng, D. Su, G. D. Lewis Phillips, K. R. Kozak, S. F. Yu, K. Xu, D. Leipold and J. Wai, *Bioconjugate Chem.*, 2017, **28**, 2086–2098.

105 B. S. Vollmar, B. Wei, R. Ohri, J. Zhou, J. He, S. F. Yu, D. Leipold, E. Cosino, S. Yee, A. Fourie-O'Donohue, G. Li, G. L. Phillips, K. R. Kozak, A. Kamath, K. Xu, G. Lee, G. A. Lazar and H. K. Erickson, *Bioconjugate Chem.*, 2017, **28**, 2538–2548.

106 T. H. Pillow, P. Adhikari, R. A. Blake, J. Chen, G. Del Rosario, G. Deshmukh, I. Figueroa, K. E. Gascoigne, A. V. Kamath, S. Kaufman, T. Kleinheinz, K. R. Kozak, B. Latifi, D. D. Leipold, C. Sing Li, R. Li, M. M. Mulvihill, A. O'Donohue, R. K. Rowntree, J. D. Sadowsky, J. Wai, X. Wang, C. Wu, Z. Xu, H. Yao, S. F. Yu, D. Zhang, R. Zang, H. Zhang, H. Zhou, X. Zhu and P. S. Dragovich, *ChemMed-Chem*, 2020, **15**, 17–25.

107 C. S. Neumann, K. C. Olivas, M. E. Anderson, J. H. Cochran, S. Jin, F. Li, L. V. Loftus, D. W. Meyer, J. Neale, J. C. Nix, P. G. Pittman, J. K. Simmons, M. L. Ulrich, A. B. Waight, A. Wong, M. C. Zaval, W. Zeng, R. P. Lyon and P. D. Senter, *Mol. Cancer Ther.*, 2018, **17**, 2633–2642.

108 A. Kumar, K. Kinneer, L. Masterson, E. Ezeadi, P. Howard, H. Wu, C. Gao and N. Dimasi, *Bioorganic Med. Chem. Lett.*, 2018, **28**, 3617–3621.

109 J. Harper, C. Lloyd, N. Dimasi, D. Toader, R. Marwood, L. Lewis, D. Bannister, J. Jovanovic, R. Fleming, F. D'Hooge, S. Mao, A. M. Marrero, M. Korade, P. Strout, L. Xu, C. Chen, L. Wetzel, S. Breen, L. Van Vlerken-Ysla, S. Jalla, M. Rebelatto, H. Zhong, E. M. Hurt, M. J. Hinrichs, K. Huang, P. W. Howard, D. A. Tice, R. E. Hollingsworth, R. Herbst and A. Kamal, *Mol. Cancer Ther.*, 2017, **16**, 1576–1587.

110 F. Li, M. K. Sutherland, C. Yu, R. B. Walter, L. Westendorf, J. Valliere-Douglass, L. Pan, A. Cronkite, D. Sussman, K. Klussman, M. Ulrich, M. E. Anderson, I. J. Stone, W. Zeng, M. Jonas, T. S. Lewis, M. Goswami, S. A. Wang, P. D. Senter, C. L. Law, E. J. Feldman and D. R. Benjamin, *Mol. Cancer Ther.*, 2018, **17**, 554–564.

111 J. R. Junutula, K. M. Flagella, R. A. Graham, K. L. Parsons, E. Ha, H. Raab, S. Bhakta, T. Nguyen, D. L. Dugger, G. Li, E. Mai, G. D. L. Phillips, H. Hiraragi, R. N. Fuji, J. Tibbitts, R. Vandlen, S. D. Spencer, R. H. Scheller, P. Polakis and M. X. Sliwkowski, *Clin. Cancer Res.*, 2010, **16**, 4769–4778.

112 S. Adams, A. Wilhelm, L. Harvey, C. Bai, N. Yoder, Y. Kovtun, T. Chittenden and J. Pinkas, *Blood*, 2016, **128**, 2832.

113 F. Zammarchi, S. Corbett, L. Adams, M. Mellinas-Gomez, P. Tyrer, S. Dissanayake, S. Sims, K. Havenith, S. Chivers, D. G. Willimas, P. W. Howard, J. A. Hartley and P. van Berkel, *Blood*, 2016, **128**, 4176.

114 W. Tang, X. Huang, Z. Ou, H. Yan, J. Gan, Q. Dong, B. Tan, Y. Yang, Y. Guo, S. Li, B. Thomas and J.-C. Yu, *Cancer Res.*, 2019, **79**, P6-20-16.

115 S. M. Lehar, T. Pillow, M. Xu, L. Staben, K. K. Kajihara, R. Vandlen, L. DePalatis, H. Raab, W. L. Hazenbos, J. Hiroshi Morisaki, J. Kim, S. Park, M. Darwish, B. C. Lee, H. Hernandez, K. M. Loyet, P. Lupardus, R. Fong, D. Yan, C. Chalouni, E. Luis, Y. Khalfin, E. Plise, J. Cheong, J. P. Lyssikatos, M. Strandh, K. Koefoed, P. S. Andersen, J. A. Flygare, M. Wah Tan, E. J. Brown and S. Mariathasan, *Nature*, 2015, **527**, 323–328.

116 M. Peck, M. E. Rothenberg, R. Deng, N. Lewin-Koh, G. She, A. V. Kamath, M. Carrasco-Triguero, O. Saad, A. Castro, L. Teufel, D. S. Dickerson, M. Leonardelli and J. A. Tavel, *Antimicrob. Agents Chemother.*, 2019, **63**, e02588.

117 N. Forte, V. Chudasama and J. R. Baker, *Drug Discovery Today Technol.*, 2018, **30**, 11–20.

118 F. A. Liberatore, R. D. Comeau, J. M. McKearin, D. A. Pearson, B. Q. Belonga, S. J. Brocchini, J. Kath, T. Phillips, K. Osswell and R. G. Lawton, *Bioconjugate Chem.*, 1990, **1**, 36–50.

119 R. B. del Rosario, R. L. Wahl, S. J. Brocchini, R. G. Lawton and R. H. Smith, *Bioconjugate Chem.*, 1990, **1**, 51–59.

120 G. Badescu, P. Bryant, M. Bird, K. Henseleit, J. Swierkosz, V. Parekh, R. Tommasi, E. Pawlisz, K. Jurlewicz, M. Farys, N. Camper, X. Sheng, M. Fisher, R. Grygorash, A. Kyle, A. Abhilash, M. Frigerio, J. Edwards and A. Godwin, *Bioconjugate Chem.*, 2014, **25**, 1124–1136.

121 P. Bryant, M. Pabst, G. Badescu, M. Bird, W. McDowell, E. Jamieson, J. Swierkosz, K. Jurlewicz, R. Tommasi, K. Henseleit, X. Sheng, N. Camper, A. Manin, K. Kozakowska, K. Peciak, E. Laurine, R. Grygorash, A. Kyle, D. Morris, V. Parekh, A. Abhilash, J. W. Choi, J. Edwards, M. Frigerio, M. P. Baker and A. Godwin, *Mol. Pharm.*, 2015, **12**, 1872–1879.

122 M. Dorywalska, R. Dushin, L. Moine, S. E. Farias, D. Zhou, T. Navaratnam, V. Lui, A. Hasa-Moreno, M. G. Casas, T. T. Tran, K. Delaria, S. H. Liu, D. Foletti, C. J. O'Donnell, J. Pons, D. L. Shelton, A. Rajpal and P. Strop, *Mol. Cancer Ther.*, 2016, **15**, 958–970.

123 M. Pabst, W. McDowell, A. Manin, A. Kyle, N. Camper, E. De Juan, V. Parekh, F. Rudge, H. Makwana, T. Kantner, H. Parekh, A. Michelet, X. B. Sheng, G. Popa, C. Tucker, F. Khayrzad, D. Pollard, K. Kozakowska, R. Resende, A. Jenkins, F. Simoes, D. Morris, P. Williams, G. Badescu, M. P. Baker, M. Bird, M. Frigerio and A. Godwin, *J. Controlled Release*, 2017, **253**, 160–164.

124 A. Godwin, A. Kyle and N. Evans, *Conjugates and conjugating reagents comprising a linker that includes at least two  $(-\text{CH}_2-\text{CH}_2-\text{O}-)$  units in a ring*, WO2017/178828, 2017.

125 M. N. Chang, J.-S. Lai, W.-F. Li, I.-J. Chen, Y.-C. Tsai and K.-C. Chen, *Conjugated biological molecules, pharmaceutical compositions and methods*, US2018/0193481, 2018.

126 L. Huang, B. Veneziale, M. Frigerio, G. Badescu, X. Li, Q. Zhao, J. Bahn, J. Souratha, R. Osgood, C. Zhao, K. Phan, J. Cowell, S. Rosengren, J. Parise, M. Pabst, M. Bird, W. McDowell, G. Wei, C. Thompson, A. Godwin, M. Shepard and C. Thanos, *Cancer Res.*, 2016, **76**, 1217.

127 M. Bird, J. Nunes and M. Frigerio, *Methods in Molecular Biology*, Humana Press Inc., 2020, vol. 2078, pp. 113–129.

128 M. E. B. Smith, F. F. Schumacher, C. P. Ryan, L. M. Tedaldi, D. Papaioannou, G. Waksman, S. Caddick and J. R. Baker, *J. Am. Chem. Soc.*, 2010, **132**, 1960–1965.

129 F. F. Schumacher, J. P. M. Nunes, A. Maruani, V. Chudasama, M. E. B. Smith, K. A. Chester, J. R. Baker and S. Caddick, *Org. Biomol. Chem.*, 2014, **12**, 7261–7269.

130 J. P. M. Nunes, M. Morais, V. Vassileva, E. Robinson, V. S. Rajkumar, M. E. B. Smith, R. B. Pedley, S. Caddick, J. R. Baker and V. Chudasama, *Chem. Commun.*, 2015, **51**, 10624–10627.

131 E. Robinson, J. P. M. Nunes, V. Vassileva, A. Maruani, J. C. F. Nogueira, M. E. B. Smith, R. B. Pedley, S. Caddick, J. R. Baker and V. Chudasama, *RSC Adv.*, 2017, **7**, 9073–9077.

132 C. R. Behrens, E. H. Ha, L. L. Chinn, S. Bowers, G. Probst, M. Fitch-Bruhns, J. Monteon, A. Valdiosera, A. Bermudez, S. Liao-Chan, T. Wong, J. Melnick, J. W. Theunissen, M. R. Flory, D. Houser, K. Venstrom, Z. Levashova, P. Sauer, T. S. Migone, E. H. Van Der Horst, R. L. Halcomb and D. Y. Jackson, *Mol. Pharm.*, 2015, **12**, 3986–3998.

133 M. Morais, J. P. M. Nunes, K. Karu, N. Forte, I. Benni, M. E. B. Smith, S. Caddick, V. Chudasama and J. R. Baker, *Org. Biomol. Chem.*, 2017, **15**, 2947–2952.

134 F. Bryden, C. Martin, S. Letast, E. Lles, I. Viéitez-Villemin, A. Rousseau, C. Colas, M. Brachet-Botineau, E. Allard-Vannier, C. Larbouret, M. C. Viaud-Massuard and N. Joubert, *Org. Biomol. Chem.*, 2018, **16**, 1882–1889.

135 N. Forte, M. Livanos, E. Miranda, M. Morais, X. Yang, V. S. Rajkumar, K. A. Chester, V. Chudasama and J. R. Baker, *Bioconjugate Chem.*, 2018, **29**, 486–492.

136 O. Feuillâtre, C. Gély, S. Huvelle, C. B. Baltus, L. Juen, N. Joubert, A. Desgranges, M. C. Viaud-Massuard and C. Martin, *ACS Omega*, 2020, **5**, 1557–1565.

137 M. Maneiro, N. Forte, M. M. Shchepinova, C. S. Kounde, V. Chudasama, J. R. Baker and E. W. Tate, *ACS Chem. Biol.*, 2020, **15**, 1306–1312.

138 V. Chudasama, M. E. B. Smith, F. F. Schumacher, D. Papaioannou, G. Waksman, J. R. Baker and S. Caddick, *Chem. Commun.*, 2011, **47**, 8781–8783.

139 A. Maruani, M. E. B. Smith, E. Miranda, K. A. Chester, V. Chudasama and S. Caddick, *Nat. Commun.*, 2015, **6**, 6645.

140 S. Shao, M.-H. Tsai, J. Lu, T. Yu, J. Jin, D. Xiao, H. Jiang, M. Han, M. Wang and J. Wang, *Bioorg. Med. Chem. Lett.*, 2018, **28**, 1363–1370.

141 M. T. W. Lee, A. Maruani, D. A. Richards, J. R. Baker, S. Caddick and V. Chudasama, *Chem. Sci.*, 2017, **8**, 2056–2060.

142 F. Bryden, J. M. M. Rodrigues, H. Savoie, V. Chudasama, A. Beeby, M. H. Y. Cheng, R. W. Boyle and A. Maruani, *Bioconjugate Chem.*, 2017, **29**, 176–181.

143 A. N. Marquard, J. C. T. Carlson and R. Weissleder, *Bioconjugate Chem.*, 2020, **31**, 1616–1623.

144 M. T. W. Lee, A. Maruani, J. R. Baker, S. Caddick and V. Chudasama, *Chem. Sci.*, 2016, **7**, 799–802.

145 C. Bahou, D. A. Richards, A. Maruani, E. A. Love, F. Javaid, S. Caddick, J. R. Baker and V. Chudasama, *Org. Biomol. Chem.*, 2018, **16**, 1359–1366.

146 B. Shi, M. Wu, Z. Li, Z. Xie, X. Wei, J. Fan, Y. Xu, D. Ding, S. H. Akash, S. Chen and S. Cao, *Cancer Med.*, 2019, **8**, 1793–1805.

147 Z. Miao, T. Zhu, K. B. Alisher, G. Chen, Z. Li and S. Cao, *Anti-HER2 antibody-drug conjugate and applications thereof*, US2019/0091345, 2019.

148 Z. Miao, T. Zhu, A. B. Khasanov, S. Cao, Z. Li and M. Wu, *Anti-5T4 antibody-drug conjugate and use thereof*, US2019/0374651, 2019.

149 Q.-Y. Hu and H. Imase, *Methods for making conjugates from disulfide-containing proteins*, WO2014/083505, 2014.

150 Q.-Y. Hu and M. Allan, *Method for making conjugates from disulfide-containing proteins*, US2019/0381126, 2019.

151 N. Gupta, J. Kancharla, S. Kaushik, A. Ansari, S. Hossain, R. Goyal, M. Pandey, J. Sivaccumar, S. Hussain, A. Sarkar, A. Sengupta, S. K. Mandal, M. Roy and S. Sengupta, *Chem. Sci.*, 2017, **8**, 2387–2395.

152 O. Koniev, I. Dovgan, B. Renoux, A. Ehkirch, J. Eberova, S. Cianfréani, S. Kolodych, S. Papot and A. Wagner, *Med. Chem. Commun.*, 2018, **9**, 827–830.

153 S. Kolodych, O. Koniev, Z. Baatarkhuu, J. Y. Bonnefoy, F. Debaene, S. Cianfréani, A. Van Dorsselaer and A. Wagner, *Bioconjugate Chem.*, 2015, **26**, 197–200.

154 S. J. Walsh, S. Omarjee, W. R. J. D. Galloway, T. T.-L. Kwan, H. F. Sore, J. S. Parker, M. Hyvönen, J. S. Carroll and D. R. Spring, *Chem. Sci.*, 2019, **10**, 694–700.

155 J. Charoenpattarapreeda, S. J. Walsh, J. S. Carroll and D. R. Spring, *Angew. Chem., Int. Ed.*, 2020, DOI: 10.1002/anie.202010090.

156 S. J. Walsh, J. Iegre, H. Seki, J. D. Bargh, H. F. Sore, J. S. Parker, J. S. Carroll and D. R. Spring, *Org. Biomol. Chem.*, 2020, **18**, 4224–4230.

157 A. J. Counsell, S. J. Walsh, N. S. Robertson, H. Sore and D. R. Spring, *Org. Biomol. Chem.*, 2020, **18**, 4739–4743.

158 C. Bahou, E. A. Love, S. Leonard, R. J. Spears, A. Maruani, K. Armour, J. R. Baker and V. Chudasama, *Bioconjugate Chem.*, 2019, **30**, 1048–1054.

159 J. W. Chin, *Nature*, 2017, **550**, 53–60.

160 C. C. Liu and P. G. Schultz, *Annu. Rev. Biochem.*, 2010, **79**, 413–444.

161 T. S. Young and P. G. Schultz, *J. Biol. Chem.*, 2010, **285**, 11039–11044.

162 S. M. Hancock, R. Uprety, A. Deiters and J. W. Chin, *J. Am. Chem. Soc.*, 2010, **132**, 14819–14824.

163 P. R. Chen, D. Groff, J. Guo, W. Ou, S. Cellitti, B. H. Geierstanger and P. G. Schultz, *Angew. Chem., Int. Ed.*, 2009, **48**, 4052–4055.

164 O. Vargas-Rodriguez, A. Sevostyanova, D. Söll and A. Crnković, *Curr. Opin. Chem. Biol.*, 2018, **46**, 115–122.

165 H. Neumann, A. L. Slusarczyk and J. W. Chin, *J. Am. Chem. Soc.*, 2010, **132**, 2142–2144.

166 J. Y. Axup, K. M. Bajjuri, M. Ritland, B. M. Hutchins, C. H. Kim, S. A. Kazane, R. Halder, J. S. Forsyth, A. F. Santidrian, K. Stafin, Y. Lu, H. Tran, A. J. Seller, S. L. Biroc, A. Szydlik, J. K. Pinkstaff, F. Tian, S. C. Sinha, B. Felding-Habermann, V. V. Smider and P. G. Schultz, *Proc. Natl. Acad. Sci. U. S. A.*, 2012, **109**, 16101–16106.

167 G. Roy, J. Reier, A. Garcia, T. Martin, M. Rice, J. Wang, M. Prophet, R. Christie, W. Dall'Acqua, S. Ahuja, M. A. Bowen and M. Marelli, *mAbs*, 2020, **12**, 1684749.

168 F. Tian, Y. Lu, A. Manibusan, A. Sellers, H. Tran, Y. Sun, T. Phuong, R. Barnett, B. Hehli, F. Song, M. J. DeGuzman, S. Ensari, J. K. Pinkstaff, L. M. Sullivan, S. L. Biroc, H. Cho, P. G. Schultz, J. DiJoseph, M. Dougher, D. Ma, R. Dushin, M. Leal, L. Tchistiakova, E. Feyfant, H.-P. Gerber and P. Sapra, *Proc. Natl. Acad. Sci. U. S. A.*, 2014, **111**, 1766–1771.

169 A. Molina, N. Shah, A. Y. Krishnan, N. D. Shah, J. M. Burke, J. M. Melear, A. I. Spira, L. L. Popplewell, C. B. Andreadis, S. Chhabra, J. P. Sharman, J. L. Kaufman, J. B. Cohen, R. Niesvizky, T. G. Martin, C. DiLea, J. Kuriakose, S. L. Matheny and J. P. Leonard, *Hematol. Oncol.*, 2019, **37**, 324–325.

170 R. W. Naumann, D. Uyar, J. W. Moroney, F. S. Braiteh, R. J. Schilder, J. P. Diaz, E. Hamilton, L. P. Martin, D. M. O. Malley, R. T. Penson, C. Dilea, M. Palumbo, V. Dealmeida, L. P. Martin, D. M. O. Malley, R. T. Penson, C. Dilea, M. Palumbo, V. Dealmeida, S. Matheny and A. Molina, *Am. Assoc. Cancer Res. Virtual Annu. Meet.*, 2020.

171 G. Yin, E. D. Garces, J. Yang, J. Zhang, C. Tran, A. R. Steiner, C. Roos, S. Bajad, S. Hudak, K. Penta, J. Zawada, S. Pollitt and C. J. Murray, *mAbs*, 2012, **4**, 217–225.

172 S. T. Jung, T. H. Kang, W. Kelton and G. Georgiou, *Curr. Opin. Biotechnol.*, 2011, **22**, 858–867.

173 M. Pott, M. J. Schmidt and D. Summerer, *ACS Chem. Biol.*, 2014, **9**, 2815–2822.

174 G. Yin, H. T. Stephenson, J. Yang, X. Li, S. M. Armstrong, T. H. Heibeck, C. Tran, M. R. Masikat, S. Zhou, R. L. Stafford, A. Y. Yam, J. Lee, A. R. Steiner, A. Gill, K. Penta, S. Pollitt, R. Baliga, C. J. Murray, C. D. Thanos, L. M. McEvoy, A. K. Sato and T. J. Hallam, *Sci. Rep.*, 2017, **7**, 3026.

175 M. P. VanBrunt, K. Shanebeck, Z. Caldwell, J. Johnson, P. Thompson, T. Martin, H. Dong, G. Li, H. Xu, F. D'Hooge, L. Masterson, P. Bariola, A. Tiberghien, E. Ezeadi, D. G. Williams, J. A. Hartley, P. W. Howard, K. H. Grabstein, M. A. Bowen and M. Marelli, *Bioconjugate Chem.*, 2015, **26**, 2249–2260.

176 B. Oller-Salvia, G. Kym and J. W. Chin, *Angew. Chem., Int. Ed.*, 2018, **57**, 2831–2834.

177 A. H. Amant, F. Huang, J. Lin, D. Lemen, C. Chakiath, S. Mao, C. Fazenbaker, H. Zhong, J. Harper, W. Xu, N. Patel, L. Adams, B. Vijayakrishnan, P. W. Howard, M. Marelli, H. Wu, C. Gao, J. Read de Alaniz and R. J. Christie, *Bioconjugate Chem.*, 2019, **30**, 2340–2348.

178 S. A. Kularatne, V. Deshmukh, J. Ma, V. Tardif, R. K. V. Lim, H. M. Pugh, Y. Sun, A. Manibusan, A. J. Sellers, R. S. Barnett, S. Srinagesh, J. S. Forsyth, W. Hassenpflug, F. Tian, T. Javahishvili, B. Felding-Habermann, B. R. Lawson, S. A. Kazane and P. G. Schultz, *Angew. Chem., Int. Ed.*, 2014, **53**, 11863–11867.

179 D. Jackson, J. Atkinson, C. I. Guevara, C. Zhang, V. Kery, S.-J. Moon, C. Virata, P. Yang, C. Lowe, J. Pinkstaff, H. Cho, N. Knudsen, A. Manibusan, F. Tian, Y. Sun, Y. Lu, A. Sellers, X.-C. Jia, I. Joseph, B. Anand, K. Morrison, D. S. Pereira and D. Stover, *PLoS One*, 2014, **9**, e83865.

180 R. K. V. Lim, S. Yu, B. Cheng, S. Li, N.-J. Kim, Y. Cao, V. Chi, J. Y. Kim, A. K. Chatterjee, P. G. Schultz, M. S. Tremblay and S. A. Kazane, *Bioconjugate Chem.*, 2015, **26**, 2216–2222.

181 S. Yu, A. D. Pearson, R. K. V. Lim, D. T. Rodgers, S. Li, H. B. Parker, M. Weglarz, E. N. Hampton, M. J. Bollong, J. Shen, C. Zambaldo, D. Wang, A. K. Woods, T. M. Wright, P. G. Schultz, S. A. Kazane, T. S. Young and M. S. Tremblay, *Mol. Ther.*, 2016, **24**, 2078–2089.

182 V. V. Rostovtsev, L. G. Green, V. V. Fokin and K. B. Sharpless, *Angew. Chem., Int. Ed.*, 2002, **41**, 2596–2599.

183 N. J. Agard, J. A. Prescher and C. R. Bertozzi, *J. Am. Chem. Soc.*, 2004, **126**, 15046–15047.

184 P. E. Brandish, A. Palmieri, S. Antonenko, M. Beaumont, L. Benso, M. Cancilla, M. Cheng, L. Fayadat-Dilman, G. Feng, I. Figueroa, J. Firdos, R. Garbaccio, L. Garvin-Queen, D. Gately, P. Geda, C. Haines, S. Hseih, D. Hodges, J. Kern, N. Knudsen, K. Kwasnjuk, L. Liang, H. Ma, A. Manibusan, P. L. Miller, L. Y. Moy, Y. Qu, S. Shah, J. S. Shin, P. Stivers, Y. Sun, D. Tomazela, H. C. Woo, D. Zaller, S. Zhang, Y. Zhang and M. Zielstorff, *Bioconjugate Chem.*, 2018, **29**, 2357–2369.

185 E. S. Zimmerman, T. H. Heibeck, A. Gill, X. Li, C. J. Murray, M. R. Madlansacay, C. Tran, N. T. Uter, G. Yin, P. J. Rivers, A. Y. Yam, W. D. Wang, A. R. Steiner, S. U. Bajad, K. Penta, W. Yang, T. J. Hallam, C. D. Thanos and A. K. Sato, *Bioconjugate Chem.*, 2014, **25**, 351–361.

186 X. Li, C. Abrahams, S. Zhou, S. Krimm, R. Henningsen, H. Stephenson, J. Hanson, M. R. Masikat, K. Bajjuri, T. Heibeck, C. Tran, G. Yin, J. Zawada, G. Sarma, J. Chen, M. Bruhns, W. Solis, A. Steiner, A. Galan, T. Kline, R. Stafford, A. Yam, V. I. De Almeida, M. Lupher and T. Hallam, *Cancer Res.*, 2018, **78**, 1782.

187 C. L. Abrahams, X. Li, M. Embry, A. Yu, S. Krimm, S. Krueger, N. Y. Greenland, K. W. W. Wen, C. Jones, V. DeAlmeida, W. A. Solis, S. Matheny, T. Kline, A. Y. Yam, R. Stafford, A. P. Wiita, T. Hallam, M. Lupher and A. Molina, *Oncotarget*, 2018, **9**, 37700–37714.

188 S. H. Ahn, B. A. Vaughn, W. A. Solis, M. L. Lupher, T. J. Hallam and E. Boros, *Bioconjugate Chem.*, 2020, **31**, 1177–1187.

189 Y. Wu, H. Zhu, B. Zhang, F. Liu, J. Chen, Y. Wang, Y. Wang, Z. Zhang, L. Wu, L. Si, H. Xu, T. Yao, S. Xiao, Q. Xia, L. Zhang, Z. Yang and D. Zhou, *Bioconjugate Chem.*, 2016, **27**, 2460–2468.

190 C. Koehler, P. F. Sauter, M. Wawryszyn, G. E. Girona, K. Gupta, J. J. M. Landry, M. H.-Y. Fritz, K. Radic, J.-E. Hoffmann, Z. A. Chen, J. Zou, P. S. Tan, B. Galik, S. Junntila, P. Stolt-Bergner, G. Pruner, A. Gynesei, C. Schultz, M. B. Biskup, H. Besir, V. Benes, J. Rappsilber, M. Jechlinger, J. O. Korbel, I. Berger, S. Braese and E. A. Lemke, *Nat. Methods*, 2016, **13**, 997–1000.

191 A. H. St. Amant, F. Huang, J. Lin, K. Rickert, V. Oganesyan, D. Lemen, S. Mao, J. Harper, M. Marelli, H. Wu, C. Gao,

J. Read de Alaniz and R. J. Christie, *Angew. Chem., Int. Ed.*, 2019, **58**, 8489–8493.

192 T. Hofer, L. R. Skeffington, C. M. Chapman and C. Rader, *Biochemistry*, 2009, **48**, 12047–12057.

193 T. Hofer, J. D. Thomas, T. R. Burke and C. Rader, *Proc. Natl. Acad. Sci. U. S. A.*, 2008, **105**, 12451–12456.

194 D. L. Hatfield and V. N. Gladyshev, *Mol. Cell. Biol.*, 2002, **22**, 3565–3576.

195 X. Li, J. Yang and C. Rader, *Methods*, 2014, **65**, 133–138.

196 X. Li, C. G. Nelson, R. R. Nair, L. Hazlehurst, T. Moroni, P. Martinez-Acedo, A. R. Nanna, D. Hymel, T. R. Burke and C. Rader, *Cell Chem. Biol.*, 2017, **24**, 433–442.

197 Y. Zheng, P. S. Addy, R. Mukherjee and A. Chatterjee, *Chem. Sci.*, 2017, **8**, 7211–7217.

198 D. L. Dunkelmann, J. C. W. Willis, A. T. Beattie and J. W. Chin, *Nat. Chem.*, 2020, **12**, 535–544.

199 H. Xiao, A. Chatterjee, S. Choi, K. M. Bajjuri, S. C. Sinha and P. G. Schultz, *Angew. Chem., Int. Ed.*, 2013, **52**, 14080–14083.

200 N. Nilchan, X. Li, L. Pedzisa, A. R. Nanna, W. R. Roush and C. Rader, *Antib. Ther.*, 2019, **2**, 71–78.

201 X. Li, J. T. Patterson, M. Sarkar, L. Pedzisa, T. Kodadek, W. R. Roush and C. Rader, *Bioconjugate Chem.*, 2015, **26**, 2243–2248.

202 M. Barok, V. Le Joncour, A. Martins, J. Isola, M. Salmikangas, P. Laakkonen and H. Joensuu, *Cancer Lett.*, 2020, **473**, 156–163.

203 J. T. Snyder, M.-C. Malinao, J. Dugal-Tessier, J. E. Atkinson, B. S. Anand, A. Okada and B. A. Mendelsohn, *Mol. Pharm.*, 2018, **15**, 2384–2390.

204 N. Rudra-Ganguly, P. M. Challita-Eid, C. Lowe, M. Mattie, S.-J. Moon, B. A. Mendelsohn, M. Leavitt, C. Virata, A. Verlinsky, L. Capo, M. S. Chang, D. L. Russell, B. Randhawa, G. Liu, R. Hubert, M. Brodey, H. Aviña, C. Zhang, J. D. Abad, B. Anand, S. Karki, Z. An, R. Luethy, F. Doñate, D. S. Pereira, K. Morrison, I. B. J. Joseph and D. R. Stover, *Cancer Res.*, 2016, **76**, 574.

205 C. B. Rosen and M. B. Francis, *Nat. Chem. Biol.*, 2017, **13**, 697–705.

206 L. S. Witus, C. Netirojanakul, K. S. Palla, E. M. Muehl, C.-H. Weng, A. T. Iavarone and M. B. Francis, *J. Am. Chem. Soc.*, 2013, **135**, 17223–17229.

207 G. Casi, N. Huguenin-Dezot, K. Zuberbühler, J. Scheuermann and D. Neri, *J. Am. Chem. Soc.*, 2012, **134**, 5887–5892.

208 L. Harris, D. Tavares, L. Rui, E. Maloney, A. Wilhelm, J. Costoplus, K. Archer, M. Bogalhas, L. Harvey, R. Wu, X. Chen, X. Xu, S. Connaughton, L. Wang, K. Whiteman, O. Ab, E. Hong, W. Widdison, M. Shizuka, M. Miller, J. Pinkas, T. Keating, R. Chari and N. Fishkin, *Cancer Res.*, 2015, **75**, 647.

209 D. Vitharana, A. Wilhelm, L. Harris, K. Archer, M. Shizuka, E. Maloney, O. Ab, R. Laleau, X. Sun, J. Pinkas, M. Miller, R. Chari, T. Keating and N. Fishkin, *Cancer Res.*, 2016, **76**, 2965.

210 P. Thompson, B. Bezabeh, R. Fleming, M. Pruitt, S. Mao, P. Strout, C. Chen, S. Cho, H. Zhong, H. Wu, C. Gao and N. Dimasi, *Bioconjugate Chem.*, 2015, **26**, 2085–2096.

211 C. Zhang, M. Welborn, T. Zhu, N. J. Yang, M. S. Santos, T. Van Voorhis and B. L. Pentelute, *Nat. Chem.*, 2016, **8**, 120–128.

212 C. Zhang, P. Dai, A. A. Vinogradov, Z. P. Gates and B. L. Pentelute, *Angew. Chem., Int. Ed.*, 2018, **57**, 6459–6463.

213 Z. Dai, X. N. Zhang, F. Nasertorabi, Q. Cheng, J. Li, B. B. Katz, G. Smbatyan, H. Pei, S. G. Louie, H. J. Lenz, R. C. Stevens, Y. Zhang, Y. Zhang, Y. Zhang and Y. Zhang, *Sci. Adv.*, 2020, **6**, eaba6752.

214 M. J. Matos, B. L. Oliveira, N. Martínez-Sáez, A. Guerreiro, P. M. S. D. Cal, J. Bertoldo, M. Maneiro, E. Perkins, J. Howard, M. J. Deery, J. M. Chalker, F. Corzana, G. Jiménez-Osés and G. J. L. Bernardes, *J. Am. Chem. Soc.*, 2018, **140**, 4004–4017.

215 M. Chilamari, N. Kalra, S. Shukla and V. Rai, *Chem. Commun.*, 2018, **54**, 7302–7305.

216 C. Rader, S. C. Sinha, M. Popkov, R. A. Lerner and C. F. Barbas, *Proc. Natl. Acad. Sci. U. S. A.*, 2003, **100**, 5396–5400.

217 A. R. Nanna, X. Li, E. Walseng, L. Pedzisa, R. S. Goydel, D. Hymel, T. R. Burke, W. R. Roush and C. Rader, *Nat. Commun.*, 2017, **8**, 1112.

218 A. R. Nanna, A. V. Kel'in, C. Theile, J. M. Pierson, Z. X. Voo, A. Garg, J. K. Nair, M. A. Maier, K. Fitzgerald and C. Rader, *Nucleic Acids Res.*, 2020, **48**, 5281–5293.

219 D. Hwang, K. Tsuji, H. Park, T. R. Burke and C. Rader, *Bioconjugate Chem.*, 2019, **30**, 2889–2896.

220 D. Hwang and C. Rader, *Biomolecules*, 2020, **10**, 764.

221 M. R. Mortensen, M. B. Skovsgaard, A. H. Okholm, C. Scavenius, D. M. Dupont, C. B. Rosen, J. J. Enghild, J. Kjems and K. V. Gothelf, *Bioconjugate Chem.*, 2018, **29**, 3016–3025.

222 M. B. Skovsgaard, T. E. Jeppesen, M. R. Mortensen, C. H. Nielsen, J. Madsen, A. Kjaer and K. V. Gothelf, *Bioconjugate Chem.*, 2019, **30**, 881–887.

223 S. R. Adusumalli, D. G. Rawale, U. Singh, P. Tripathi, R. Paul, N. Kalra, R. K. Mishra, S. Shukla and V. Rai, *J. Am. Chem. Soc.*, 2018, **140**, 15114–15123.

224 S. R. Adusumalli, D. G. Rawale, K. Thakur, L. Purushottam, N. C. Reddy, N. Kalra, S. Shukla and V. Rai, *Angew. Chem., Int. Ed.*, 2020, **59**, 10332–10336.

225 I. Dovgan, S. Erb, S. Hessmann, S. Ursuegui, C. Michel, C. Muller, G. Chaubet, S. Cianfréani and A. Wagner, *Org. Biomol. Chem.*, 2018, **16**, 1305–1311.

226 D. Hwang, N. Nilchan, A. R. Nanna, X. Li, M. D. Cameron, W. R. Roush, H. J. Park and C. Rader, *Cell Chem. Biol.*, 2019, **26**, 1229.

227 C. Sornay, S. Hessmann, S. Erb, I. Dovgan, A. Ehrkirch, T. Botzanowski, S. Cianfréani, A. Wagner and G. Chaubet, *Chem. – Eur. J.*, 2020, **26**, 13797–13805, DOI: 10.1002/chem.202002432.

228 B. Nilsson, T. Moks, B. Jansson, L. Abrahmsén, A. Elmlöd, E. Holmgren, C. Henrichson, T. A. Jones and M. Uhlén, *Protein Eng.*, 1987, **1**, 107–113.

229 Y. Mazor, I. Barnea, I. Keydar and I. Benhar, *J. Immunol. Methods*, 2007, **321**, 41–59.

230 Y. Mazor, R. Noy, W. S. Wels and I. Benhar, *Cancer Lett.*, 2007, **257**, 124–135.

231 S. Shapira, A. Shapira, A. Starr, D. Kazanov, S. Kraus, I. Benhar and N. Arber, *Gastroenterology*, 2011, **140**, 935–946.

232 I. Barnea, R. Ben-Yosef, V. Karaush, I. Benhar and A. Vexler, *Head Neck*, 2013, **35**, 1171–1177.

233 J. Park, Y. Lee, B. J. Ko and T. H. Yoo, *Bioconjugate Chem.*, 2018, **29**, 3240–3244.

234 N. Vance, N. Zacharias, M. Ultsch, G. Li, A. Fourie, P. Liu, J. LaFrance-Vanassee, J. A. Ernst, W. Sandoval, K. R. Kozak, G. Phillips, W. Wang and J. Sadowsky, *Bioconjugate Chem.*, 2019, **30**, 148–160.

235 S. Kishimoto, Y. Nakashimada, R. Yokota, T. Hatanaka, M. Adachi and Y. Ito, *Bioconjugate Chem.*, 2019, **30**, 698–702.

236 C. Yu, J. Tang, A. Loredo, Y. Chen, S. Y. Jung, A. Jain, A. Gordon and H. Xiao, *Bioconjugate Chem.*, 2018, **29**, 3522–3526.

237 J. Ohata and Z. T. Ball, *J. Am. Chem. Soc.*, 2017, **139**, 12617–12622.

238 B. V. Popp and Z. T. Ball, *Chem. Sci.*, 2011, **2**, 690–695.

239 K. Yamada, N. Shikida, K. Shimbo, Y. Ito, Z. Khedri, Y. Matsuda and B. A. Mendelsohn, *Angew. Chem., Int. Ed.*, 2019, **58**, 5592–5597.

240 Y. Matsuda, V. Robles, M. C. Malinao, J. Song and B. A. Mendelsohn, *Anal. Chem.*, 2019, **91**, 12724–12732.

241 Y. Matsuda, C. Clancy, Z. Tawfiq, V. Robles and B. A. Mendelsohn, *ACS Omega*, 2019, **4**, 20564–20570.

242 Y. Matsuda, K. Yamada, T. Okuzumi and B. A. Mendelsohn, *Org. Process Res. Dev.*, 2019, **23**, 2647–2654.

243 Y. Matsuda, M. Leung, T. Okuzumi and B. Mendelsohn, *Antibodies*, 2020, **9**, 16.

244 Y. Matsuda, M. C. Malinao, V. Robles, J. Song, K. Yamada and B. A. Mendelsohn, *J. Chromatogr. B: Anal. Technol. Biomed. Life Sci.*, 2020, **1140**, 121981.

245 N. Gupta, A. Ansari, G. V. Dhoke, M. Chilamari, J. Sivaccumar, S. Kumari, S. Chatterjee, R. Goyal, P. K. Dutta, M. Samarla, M. Mukherjee, A. Sarkar, S. K. Mandal, V. Rai, G. Biswas, A. Sengupta, S. Roy, M. Roy and S. Sengupta, *Nat. Biomed. Eng.*, 2019, **3**, 917–929.

246 L. N. Lund, P. E. Gustavsson, R. Michael, J. Lindgren, L. Nørskov-Lauritsen, M. Lund, G. Houen, A. Staby and P. M. Hilaire, *J. Chromatogr. A*, 2012, **1225**, 158–167.

247 D. Q. Lin, H. F. Tong, H. Y. Wang and S. J. Yao, *J. Phys. Chem. B*, 2012, **116**, 1393–1400.

248 M. Farràs, J. Miret, M. Camps, R. Román, Ó. Martínez, X. Pujol, S. Erb, A. Ehkirch, S. Cianferani, A. Casablancas and J. J. Cairó, *mAbs*, 2020, **12**, 1702262.

249 H. Schneider, L. Deweid, O. Avrutina and H. Kolmar, *Anal. Biochem.*, 2020, **595**, 113615.

250 M. Griffin, R. Casadio and C. M. Bergamini, *Biochem. J.*, 2002, **368**, 377–396.

251 H. Ando, M. Adachi, K. Umeda, A. Matsuura, M. Nonaka, R. Uchio, H. Tanaka and M. Motoki, *Agric. Biol. Chem.*, 1989, **53**, 2613–2617.

252 H. S. Mostafa, *Biocatal. Biotransformation*, 2020, **38**, 161–177.

253 P. Strop, *Bioconjugate Chem.*, 2014, **25**, 855–862.

254 A. Josten, L. Haalck, F. Spener and M. Meusel, *J. Immunol. Methods*, 2000, **240**, 47–54.

255 A. Josten, M. Meusel and F. Spener, *Anal. Biochem.*, 1998, **258**, 202–208.

256 T. L. Mindt, V. Jungi, S. Wyss, A. Friedli, G. Pla, I. Novak-Hofer, J. Grünberg and R. Schibli, *Bioconjugate Chem.*, 2008, **19**, 271–278.

257 S. Jeger, K. Zimmermann, A. Blanc, J. Grünberg, M. Honer, P. Hunziker, H. Struthers and R. Schibli, *Angew. Chem., Int. Ed.*, 2010, **49**, 9995–9997.

258 S. Matsumiya, Y. Yamaguchi, J. ichi Saito, M. Nagano, H. Sasakawa, S. Otaki, M. Satoh, K. Shitara and K. Kato, *J. Mol. Biol.*, 2007, **368**, 767–779.

259 M. J. Feige, S. Nath, S. R. Catharino, D. Weinfurtner, S. Steinbacher and J. Buchner, *J. Mol. Biol.*, 2009, **391**, 599–608.

260 S. Krapp, Y. Mimura, R. Jefferis, R. Huber and P. Sondermann, *J. Mol. Biol.*, 2003, **325**, 979–989.

261 J. Grünberg, S. Jeger, D. Sarko, P. Dennler, K. Zimmermann, W. Mier and R. Schibli, *PLoS One*, 2013, **8**, e60350.

262 P. Dennler, A. Chiotellis, E. Fischer, D. Brégeon, C. Belmant, L. Gauthier, F. Lhospice, F. Romagne and R. Schibli, *Bioconjugate Chem.*, 2014, **25**, 569–578.

263 P. Dennler, R. Schibli and E. Fischer, *Methods Mol. Biol.*, 2013, **1045**, 205–215.

264 N. Bodyak and A. V. Yurkovetskiy, *Innovations for Next-Generation Antibody-Drug Conjugates*, 2018, pp. 215–240.

265 Y. Anami, W. Xiong, X. Gui, M. Deng, C. C. Zhang, N. Zhang, Z. An and K. Tsuchikama, *Org. Biomol. Chem.*, 2017, **15**, 5635–5642.

266 Y. Anami, C. M. Yamazaki, W. Xiong, X. Gui, N. Zhang, Z. An and K. Tsuchikama, *Nat. Commun.*, 2018, **9**, 2512.

267 M. J. Costa, J. Kudaravalli, J. T. Ma, W. H. Ho, K. Delaria, C. Holz, A. Stauffer, A. G. Chunyk, Q. Zong, E. Blasi, B. Buetow, T. T. Tran, K. Lindquist, M. Dorywalska, A. Rajpal, D. L. Shelton, P. Strop and S. H. Liu, *Sci. Rep.*, 2019, **9**, 2443.

268 D. N. Thornlow, E. C. Cox, J. A. Walker, M. Sorkin, J. B. Plesset, M. P. Delisa and C. A. Alabi, *Bioconjugate Chem.*, 2019, **30**, 1702–1710.

269 J. A. Walker, J. J. Bohn, F. Ledesma, M. R. Sorkin, S. R. Kabaria, D. N. Thornlow and C. A. Alabi, *Bioconjugate Chem.*, 2019, **30**, 2452–2457.

270 S. Puthenveetil, S. Musto, F. Loganzo, L. N. Tumey, C. J. O'Donnell and E. Graziani, *Bioconjugate Chem.*, 2016, **27**, 1030–1039.

271 S. Beck, J. Schultze, H. J. Räder, R. Holm, M. Schinnerer, M. Barz, K. Koynov and R. Zentel, *Polymers*, 2018, **10**, 141.

272 A. Sadiki, E. M. Kercher, H. Lu, R. T. Lang, B. Q. Spring and Z. S. Zhou, *Photochem. Photobiol.*, 2020, **96**, 596–603.

273 J. Park, P. L. Chariou and N. F. Steinmetz, *Bioconjugate Chem.*, 2020, **31**, 1408–1416.

274 C. Marculescu, A. Lakshminarayanan, J. Gault, J. C. Knight, L. K. Folkes, T. Spink, C. V. Robinson, K. Vallis, B. G. Davis and B. Cornelissen, *Chem. Commun.*, 2019, **55**, 11342–11345.

275 E. B. Irvine and G. Alter, *Glycobiology*, 2020, **30**, 241–253.

276 D. Reusch and M. L. Tejada, *Glycobiology*, 2015, **25**, 1325–1334.

277 K. Zheng, C. Bantog and R. Bayer, *mAbs*, 2011, **3**, 568–576.

278 S. Dickgiesser, M. Rieker, D. Mueller-Pompalla, C. Schröter, J. Tonillo, S. Warszawski, S. Raab-Westphal, S. Kühn, T. Knehans, D. Könning, J. Dotterweich, U. A. K. Betz, J. Anderl, S. Hecht and N. Rasche, *Bioconjugate Chem.*, 2020, **31**, 1070–1076.

279 S. E. Farias, P. Strop, K. Delaria, M. Galindo Casas, M. Dorywalska, D. L. Shelton, J. Pons and A. Rajpal, *Bioconjugate Chem.*, 2014, **25**, 240–250.

280 I. J. Huggins, C. A. Medina, A. D. Springer, A. Van Den Berg, S. Jadhav, X. Cui and S. F. Dowdy, *Molecules*, 2019, **24**, 3287.

281 P. Strop, K. Delaria, D. Foletti, J. M. Witt, A. Hasa-Moreno, K. Poulsen, M. G. Casas, M. Dorywalska, S. Farias, A. Pios, V. Lui, R. Dushin, D. Zhou, T. Navaratnam, T.-T. Tran, J. Sutton, K. C. Lindquist, B. Han, S.-H. Liu, D. L. Shelton, J. Pons and A. Rajpal, *Nat. Biotechnol.*, 2015, **33**, 694–696.

282 H. Schneider, L. Deweid, T. Pirzer, D. Yanakieva, S. Englert, B. Becker, O. Avrutina and H. Kolmar, *ChemistryOpen*, 2019, **8**, 354–357.

283 M. Dorywalska, P. Strop, J. A. Melton-Witt, A. Hasa-Moreno, S. E. Farias, M. Galindo Casas, K. Delaria, V. Lui, K. Poulsen, J. Sutton, G. Bolton, D. Zhou, L. Moine, R. Dushin, T.-T. Tran, S.-H. Liu, M. Rickert, D. Foletti, D. L. Shelton, J. Pons and A. Rajpal, *PLoS One*, 2015, **10**, e0132282.

284 O. K. Wong, T. T. Tran, W. H. Ho, M. G. Casas, M. Au, M. Bateman, K. C. Lindquist, A. Rajpal, D. L. Shelton, P. Strop and S. H. Liu, *Oncotarget*, 2018, **9**, 33446–33458.

285 P. Strop, T.-T. Tran, M. Dorywalska, K. Delaria, R. Dushin, O. K. Wong, W.-H. Ho, D. Zhou, A. Wu, E. Kraynov, L. Aschenbrenner, B. Han, C. J. O'Donnell, J. Pons, A. Rajpal, D. L. Shelton and S.-H. Liu, *Mol. Cancer Ther.*, 2016, **15**, 2698–2708.

286 G. T. King, K. D. Eaton, B. R. Beagle, C. J. Zopf, G. Y. Wong, H. I. Krupka, S. Y. Hua, W. A. Messersmith and A. B. El-Khoueiry, *Invest. New Drugs*, 2018, **36**, 836–847.

287 A. S. Ratnayake, L. P. Chang, L. N. Tumey, F. Loganzo, J. A. Chemler, M. Wagenaar, S. Musto, F. Li, J. E. Janso, T. E. Ballard, B. Rago, G. L. Steele, W. Ding, X. Feng, C. Hosselet, V. Buklan, J. Lucas, F. E. Koehn, C. J. O'Donnell and E. I. Graziani, *Bioconjugate Chem.*, 2019, **30**, 200–209.

288 V. Siegmund, S. Schmelz, S. Dickgiesser, J. Beck, A. Ebenig, H. Fittler, H. Frauendorf, B. Piater, U. A. K. Betz, O. Avrutina, A. Scrima, H. L. Fuchsbauer and H. Kolmar, *Angew. Chem., Int. Ed.*, 2015, **54**, 13420–13424.

289 A. Ebenig, N. E. Juettner, L. Deweid, O. Avrutina, H. Fuchsbauer and H. Kolmar, *ChemBioChem*, 2019, **20**, 2411–2419.

290 S. Yamazoe, J. M. Hogan, S. M. West, X. A. Deng, S. Kotapati, X. Shao, P. Holder, V. Lamba, M. Huber, C. Qiang, S. Gangwar, C. Rao, G. Dollinger, A. Rajpal and P. Strop, *Bioconjugate Chem.*, 2020, **31**, 1199–1208.

291 H. Abe, M. Goto and N. Kamiya, *Chem. Commun.*, 2010, **46**, 7160.

292 P. R. Spycher, C. A. Amann, J. E. Wehrmüller, D. R. Hurwitz, O. Kreis, D. Messmer, A. Ritler, A. Küchler, A. Blanc, M. Béhé, P. Walde and R. Schibli, *ChemBioChem*, 2017, **18**, 1923–1927.

293 J. L. Spidel, B. Vaessen, E. F. Albone, X. Cheng, A. Verdi and J. B. Kline, *Bioconjugate Chem.*, 2017, **28**, 2471–2484.

294 J. L. Spidel and E. F. Albone, *Methods in Molecular Biology*, Humana Press Inc., 2019, vol. 2033, pp. 53–65.

295 T. I. Chio, B. R. Demestichas, B. M. Brems, S. L. Bane and L. N. Tumey, *Angew. Chem., Int. Ed.*, 2020, **59**, 13814–13820.

296 S. R. Benjamin, C. P. Jackson, S. Fang, D. P. Carlson, Z. Guo and L. N. Tumey, *Mol. Pharm.*, 2019, **16**, 2795–2807.

297 K. Yokoyama, H. Utsumi, T. Nakamura, D. Ogaya, N. Shimba, E. Suzuki and S. Taguchi, *Appl. Microbiol. Biotechnol.*, 2010, **87**, 2087–2096.

298 L. Deweid, L. Neureiter, S. Englert, H. Schneider, J. Deweid, D. Yanakieva, J. Sturm, S. Bitsch, A. Christmann, O. Avrutina, H. Fuchsbauer and H. Kolmar, *Chem. – Eur. J.*, 2018, **24**, 15195–15200.

299 K. Buettner, T. C. Hertel and M. Pietzsch, *Amino Acids*, 2012, **42**, 987–996.

300 K. Ohtake, T. Mukai, F. Iraha, M. Takahashi, K. I. Haruna, M. Date, K. Yokoyama and K. Sakamoto, *ACS Synth. Biol.*, 2018, **7**, 2170–2176.

301 B. Böhme, B. Moritz, J. Wendler, T. C. Hertel, C. Ihling, W. Brandt and M. Pietzsch, *Amino Acids*, 2020, **52**, 313–326.

302 W. Steffen, F. C. Ko, J. Patel, V. Lyamichev, T. J. Albert, J. Benz, M. G. Rudolph, F. Bergmann, T. Streidl, P. Kratzsch, M. Boenitz-Dulat, T. Oelschlaegel and M. Schraeml, *J. Biol. Chem.*, 2017, **292**, 15622–15635.

303 T. Kashiwagi, K. ichi Yokoyama, K. Ishikawa, K. Ono, D. Ejima, H. Matsui and E. ichiro Suzuki, *J. Biol. Chem.*, 2002, **277**, 44252–44260.

304 D. York, J. Baker, P. G. Holder, L. C. Jones, P. M. Drake, R. M. Barfield, G. T. Bleck and D. Rabuka, *BMC Biotechnol.*, 2016, **16**, 23.

305 P. Agarwal, R. Kudirka, A. E. Albers, R. M. Barfield, G. W. de Hart, P. M. Drake, L. C. Jones and D. Rabuka, *Bioconjugate Chem.*, 2013, **24**, 846–851.

306 P. M. Drake, A. E. Albers, J. Baker, S. Banas, R. M. Barfield, A. S. Bhat, G. W. de Hart, A. W. Garofalo, P. Holder, L. C. Jones, R. Kudirka, J. McFarland, W. Zmolek and D. Rabuka, *Bioconjugate Chem.*, 2014, **25**, 1331–1341.

307 P. M. Drake, A. Carlson, J. M. McFarland, S. Bañas, R. M. Barfield, W. Zmolek, Y. C. Kim, B. C. B. Huang, R. Kudirka and D. Rabuka, *Mol. Cancer Ther.*, 2018, **17**, 161–168.

308 A. P. Maclare, N. Levin and H. Lowman, *Experimental and Molecular Therapeutics*, American Association for Cancer Research, 2018, vol. 78, pp. 835–835.

309 Triphase Accelerator and Catalent Announce Interim Results of a Dose Escalation Phase 1 Clinical Trial of TRPH-222 in Patients with Non-Hodgkin's Lymphoma,

[https://www.prweb.com/releases/triphase\\_accelerator\\_and\\_catalent\\_announce\\_interim\\_results\\_of\\_a\\_dose\\_escalation\\_phase\\_1\\_clinical\\_trial\\_of\\_trph\\_222\\_in\\_patients\\_with\\_non-hodgkins\\_lymphoma/prweb17129205.htm](https://www.prweb.com/releases/triphase_accelerator_and_catalent_announce_interim_results_of_a_dose_escalation_phase_1_clinical_trial_of_trph_222_in_patients_with_non-hodgkins_lymphoma/prweb17129205.htm), accessed 16 July 2020.

310 R. Barfield, Y. C. Kim, S. Chuprakov, F. Zhang, M. Bauzon, A. Ogunkoya, D. Yeo, C. Hickle, M. Pegram, D. Rabuka and P. Drake, *Mol. Cancer Ther.*, 2020, **19**, 1866–1874, DOI: 10.1101/2020.03.13.991448.

311 S. Pomplun, M. Y. H. Mohamed, T. Oelschlaegel, C. Wellner and F. Bergmann, *Angew. Chem., Int. Ed.*, 2019, **58**, 3542–3547.

312 R. Kudirka, R. M. Barfield, J. McFarland, A. E. Albers, G. W. de Hart, P. M. Drake, P. G. Holder, S. Banas, L. C. Jones, A. W. Garofalo and D. Rabuka, *Chem. Biol.*, 2015, **22**, 293–298.

313 R. A. Kudirka, R. M. Barfield, J. M. McFarland, P. M. Drake, A. Carlson, S. Bañas, W. Zmolek, A. W. Garofalo and D. Rabuka, *ACS Med. Chem. Lett.*, 2016, **7**, 994–998.

314 M. Rashidian, J. M. Song, R. E. Pricer and M. D. Distefano, *J. Am. Chem. Soc.*, 2012, **134**, 8455–8467.

315 Y. Zhang, M. J. Blanden, C. Sudheer, S. A. Gangopadhyay, M. Rashidian, J. L. Hougland and M. D. Distefano, *Bioconjugate Chem.*, 2015, **26**, 2542–2553.

316 J. Lee, H.-J. Choi, M. Yun, Y. Kang, J.-E. Jung, Y. Ryu, T. Y. Kim, Y. Cha, H.-S. Cho, J.-J. Min, C.-W. Chung and H.-S. Kim, *Angew. Chem., Int. Ed.*, 2015, **54**, 12020–12024.

317 Y. Kim, T. Park, S. Woo, H. Lee, S. Kim, J. Cho, D. Jung, Y. Kim, H. Kwon, K. Oh, Y. Chung and Y. Park, *Antibody-active agent conjugates and methods of use*, US20150105541A1, USA, 2015.

318 B. ill Lee, M.-H. Park, J.-J. Byeon, S.-H. Shin, J. Choi, Y. Park, Y.-H. Park, J. Chae and Y. G. Shin, *Molecules*, 2020, **25**, 1515.

319 R. R. Beerli, T. Hell, A. S. Merkel and U. Grawunder, *PLoS One*, 2015, **10**, e0131177.

320 N. Stefan, R. Gébleux, L. Waldmeier, T. Hell, M. Escher, F. I. Wolter, U. Grawunder and R. R. Beerli, *Mol. Cancer Ther.*, 2017, **16**, 879–892.

321 L. D'Amico, U. Menzel, M. Prummer, P. Müller, M. Buchi, A. Kashyap, U. Haessler, A. Yermanos, R. Gébleux, M. Briendl, T. Hell, F. I. Wolter, R. R. Beerli, I. Truxova, Š. Radek, T. Vlajnic, U. Grawunder, S. Reddy and A. Zippelius, *J. Immunother. Cancer*, 2019, **7**, 16.

322 T. J. Harmand, D. Bousbaine, A. Chan, X. Zhang, D. R. Liu, J. P. Tam and H. L. Ploegh, *Bioconjugate Chem.*, 2018, **29**, 3245–3249.

323 M. D. Lee, W. Y. Tong, T. Nebl, L. A. Pearce, T. M. Pham, A. Golbaz-Hagh, S. Puttick, S. Rose, T. E. Adams and C. C. Williams, *Bioconjugate Chem.*, 2019, **30**, 2539–2543.

324 T. Pirzer, K.-S. Becher, M. Rieker, T. Meckel, H. D. Mootz and H. Kolmar, *ACS Chem. Biol.*, 2018, **13**, 2058–2066.

325 V. Siegmund, B. Piater, B. Zakeri, T. Eichhorn, F. Fischer, C. Deutsch, S. Becker, L. Toleikis, B. Hock, U. A. K. Betz and H. Kolmar, *Sci. Rep.*, 2016, **6**, 39291.

326 J. J. Bruins, A. H. Westphal, B. Albada, K. Wagner, L. Bartels, H. Spits, W. J. H. van Berkel and F. L. van Delft, *Bioconjugate Chem.*, 2017, **28**, 1189–1193.

327 S. Sato, M. Matsumura, T. Kadonosono, S. Abe, T. Ueno, H. Ueda and H. Nakamura, *Bioconjugate Chem.*, 2020, **31**, 1417–1424.

328 J. Grünewald, H. E. Klock, S. E. Cellitti, B. Bursulaya, D. McMullan, D. H. Jones, H. P. Chiu, X. Wang, P. Patterson, H. Zhou, J. Vance, E. Nigoghossian, H. Tong, D. Daniel, W. Mallet, W. Ou, T. Uno, A. Brock, S. A. Lesley and B. H. Geierstanger, *Bioconjugate Chem.*, 2015, **26**, 2554–2562.

329 J. Grünewald, Y. Jin, J. Vance, J. Read, X. Wang, Y. Wan, H. Zhou, W. Ou, H. E. Klock, E. C. Peters, T. Uno, A. Brock and B. H. Geierstanger, *Bioconjugate Chem.*, 2017, **28**, 1906–1915.

330 M. Pučić, A. Knežević, J. Vidič, B. Adamczyk, M. Novokmet, O. Polašek, O. Gornik, S. Šupraha-Goreta, M. R. Wormald, I. Redžić, H. Campbell, A. Wright, N. D. Hastie, J. F. Wilson, I. Rudan, M. Wuhrer, P. M. Rudd, D. Josić and G. Lauc, *Mol. Cell. Proteomics*, 2011, **10**, 1–15.

331 M. Wuhrer, J. C. Stam, F. E. Van De Geijn, C. A. M. Koeleman, C. T. Verrips, R. J. E. M. Dolhain, C. H. Hokke and A. M. Deelder, *Proteomics*, 2007, **7**, 4070–4081.

332 L.-X. Wang, X. Tong, C. Li, J. P. Giddens and T. Li, *Annu. Rev. Biochem.*, 2019, **88**, 433–459.

333 A. Morell, G. Ashwell, A. Irvine, I. Sternlieb and I. H. Cheinberg, *J. Biol. Chem.*, 1968, **243**, 155–159.

334 D. J. O'Shannessy, M. J. Doberen and R. H. Quarles, *Immunol. Lett.*, 1984, **8**, 273–277.

335 M.-M. Chua, S.-T. Fan and F. Karush, *BBA, Biochim. Biophys. Acta, Gen. Subj.*, 1984, **800**, 291–300.

336 B. C. Laguzza, J. J. Starling, A. L. Baker, T. F. Bumol, J. R. F. Corvalan, C. L. Nichols, S. L. Briggs, G. J. Cullinan and D. A. Johnson, *J. Med. Chem.*, 1989, **32**, 548–555.

337 L. M. Hinman, P. R. Hamann, R. Wallace, A. T. Menendez, F. E. Durr and J. Upeslacis, *Cancer Res.*, 1993, **53**, 3336–3342.

338 A. C. Stan, D. L. Radu, S. Casares, C. A. Bona and T. D. Brumeanu, *Cancer Res.*, 1999, **59**, 115–121.

339 K. Zuberbühler, G. Casi, G. J. L. Bernardes and D. Neri, *Chem. Commun.*, 2012, **48**, 7100–7102.

340 C. Vaccaro, J. Zhou, R. J. Ober and E. S. Ward, *Nat. Biotechnol.*, 2005, **23**, 1283–1288.

341 W. Wang, J. Vlasak, Y. Li, P. Pristatsky, Y. Fang, T. Pittman, J. Roman, Y. Wang, T. Prueksaritanont and R. Ionescu, *Mol. Immunol.*, 2011, **48**, 860–866.

342 Q. Zhou, J. E. Stefano, C. Manning, J. Kyazike, B. Chen, D. A. Gianolio, A. Park, M. Busch, J. Bird, X. Zheng, H. Simonds-Mannes, J. Kim, R. C. Gregory, R. J. Miller, W. H. Brondyke, P. K. Dhal and C. Q. Pan, *Bioconjugate Chem.*, 2014, **25**, 510–520.

343 Faridoon, W. Shi, K. Qin, Y. Tang, M. Li, D. Guan, X. Tian, B. Jiang, J. Dong, F. Tang and W. Huang, *Org. Chem. Front.*, 2019, **6**, 3144–3149.

344 J. Garbe and M. Collin, *J. Innate Immun.*, 2012, **4**, 121–131.

345 P. W. Robbins, R. B. Trimble, D. F. Wirth, C. Hering, F. Maley, G. F. Maley, R. Das, B. W. Gibson, N. Royal and K. Biemann, *J. Biol. Chem.*, 1984, **259**, 7577–7583.



346 N. Takahashi, *Biochem. Biophys. Res. Commun.*, 1977, **76**, 1194–1201.

347 J. Sjögren, R. Lood and A. Nägeli, *Glycobiology*, 2019, **30**, 254–267.

348 Y. Wei, C. Li, W. Huang, B. Li, S. Strome and L. X. Wang, *Biochemistry*, 2008, **47**, 10294–10304.

349 J. J. Goodfellow, K. Baruah, K. Yamamoto, C. Bonomelli, B. Krishna, D. J. Harvey, M. Crispin, C. N. Scanlan and B. G. Davis, *J. Am. Chem. Soc.*, 2012, **134**, 8030–8033.

350 W. Huang, J. Giddens, S. Q. Fan, C. Toonstra and L. X. Wang, *J. Am. Chem. Soc.*, 2012, **134**, 12308–12318.

351 M. Kurogochi, M. Mori, K. Osumi, M. Tojino, S. Sugawara, S. Takashima, Y. Hirose, W. Tsukimura, M. Mizuno, J. Amano, A. Matsuda, M. Tomita, A. Takayanagi, S.-I. Shoda and T. Shirai, *PLoS One*, 2015, **10**, e0132848.

352 C. W. Lin, M. H. Tsai, S. T. Li, T. I. Tsai, K. C. Chu, Y. C. Liu, M. Y. Lai, C. Y. Wu, Y. C. Tseng, S. S. Shivatare, C. H. Wang, P. Chao, S. Y. Wang, H. W. Shih, Y. F. Zeng, T. H. You, J. Y. Liao, Y. C. Tu, Y. S. Lin, H. Y. Chuang, C. L. Chen, C. S. Tsai, C. C. Huang, N. H. Lin, C. Ma, C. Y. Wu and C. H. Wong, *Proc. Natl. Acad. Sci. U. S. A.*, 2015, **112**, 10611–10616.

353 T. B. Parsons, W. B. Struwe, J. Gault, K. Yamamoto, T. A. Taylor, R. Raj, K. Wals, S. Mohammed, C. V. Robinson, J. L. P. Benesch and B. G. Davis, *Angew. Chem., Int. Ed.*, 2016, **55**, 2361–2367.

354 S. Manabe, Y. Yamaguchi, K. Matsumoto, H. Fuchigami, T. Kawase, K. Hirose, A. Mitani, W. Sumiyoshi, T. Kinoshita, J. Abe, M. Yasunaga, Y. Matsumura and Y. Ito, *Bioconjugate Chem.*, 2019, **30**, 1343–1355.

355 J. Sjögren, W. B. Struwe, E. F. J. Cosgrave, P. M. Rudd, M. Stervander, M. Allhorn, A. Hollands, V. Nizet and M. Collin, *Biochem. J.*, 2013, **455**, 107–118.

356 T. Li, X. Tong, Q. Yang, J. P. Giddens and L. X. Wang, *J. Biol. Chem.*, 2016, **291**, 16508–16518.

357 S. S. Shivatare, L. Y. Huang, Y. F. Zeng, J. Y. Liao, T. H. You, S. Y. Wang, T. Cheng, C. W. Chiu, P. Chao, L. T. Chen, T. I. Tsai, C. C. Huang, C. Y. Wu, N. H. Lin and C. H. Wong, *Chem. Commun.*, 2018, **54**, 6161–6164.

358 J. P. Giddens, J. V. Lomino, M. N. Amin and L. X. Wang, *J. Biol. Chem.*, 2016, **291**, 9356–9370.

359 C. P. Liu, T. I. Tsai, T. Cheng, V. S. Shivatare, C. Y. Wu, C. Y. Wu and C. H. Wong, *Proc. Natl. Acad. Sci. U. S. A.*, 2018, **115**, 720–725.

360 S. Manabe, Y. Yamaguchi, J. Abe, K. Matsumoto and Y. Ito, *R. Soc. Open Sci.*, 2018, **5**, 171521.

361 M. Iwamoto, Y. Sekiguchi, K. Nakamura, Y. Kawaguchi, T. Honda and J. Hasegawa, *PLoS One*, 2018, **13**, e0193534.

362 F. Tang, Y. Yang, Y. Tang, S. Tang, L. Yang, B. Sun, B. Jiang, J. Dong, H. Liu, M. Huang, M. Y. Geng and W. Huang, *Org. Biomol. Chem.*, 2016, **14**, 9501–9518.

363 B. Ramakrishnan and P. K. Qasba, *J. Biol. Chem.*, 2002, **277**, 20833–20839.

364 B. Ramakrishnan, P. S. Shah and P. K. Qasba, *J. Biol. Chem.*, 2001, **276**, 37665–37671.

365 E. Boeggeman, B. Ramakrishnan, M. Pasek, M. Manzoni, A. Puri, K. H. Loomis, T. J. Waybright and P. K. Qasba, *Bioconjugate Chem.*, 2009, **20**, 1228–1236.

366 Z. Zhu, B. Ramakrishnan, J. Li, Y. Wang, Y. Feng, P. Prabakaran, S. Colantonio, M. A. Dyba, P. K. Qasba and D. S. Dimitrov, *mAbs*, 2014, **6**, 1190–1200.

367 P. Thompson, E. Ezeadi, I. Hutchinson, R. Fleming, B. Bezabeh, J. Lin, S. Mao, C. Chen, L. Masterson, H. Zhong, D. Toader, P. Howard, H. Wu, C. Gao and N. Dimasi, *ACS Med. Chem. Lett.*, 2016, **7**, 1005–1008.

368 R. van Geel, M. A. Wijdeven, R. Heesbeen, J. M. M. Verkade, A. A. Wasie, S. S. van Berk and F. L. van Delft, *Bioconjugate Chem.*, 2015, **26**, 2233–2242.

369 B. M. Zeglis, C. B. Davis, R. Aggeler, H. C. Kang, A. Chen, B. J. Agnew and J. S. Lewis, *Bioconjugate Chem.*, 2013, **24**, 1057–1067.

370 B. M. Zeglis, C. B. Davis, D. Abdel-Atti, S. D. Carlin, A. Chen, R. Aggeler, B. J. Agnew and J. S. Lewis, *Bioconjugate Chem.*, 2014, **25**, 2123–2128.

371 P. Adumeau, D. Vivier, S. K. Sharma, J. Wang, T. Zhang, A. Chen, B. J. Agnew and B. M. Zeglis, *Mol. Pharm.*, 2018, **15**, 892–898.

372 N. M. Okeley, B. E. Toki, X. Zhang, S. C. Je, P. J. Burke, S. C. Alley and P. D. Senter, *Bioconjugate Chem.*, 2013, **24**, 1650–1655.

373 R. Neupane and J. Bergquist, *Eur. J. Mass Spectrom.*, 2017, **23**, 417–426.

